PALEOMAGNETISM OF THE ORDOVICIAN REDBEDS OF BELL ISLAND, NEWFOUNDLAND

KUNDURI. V. RAO, M.Sc. (TECH.) (ANDHRA)

15666


MEMORIAL UNIVERSITY
LIBRARY
APR 20 1971
OF NEWFOUNDLAND

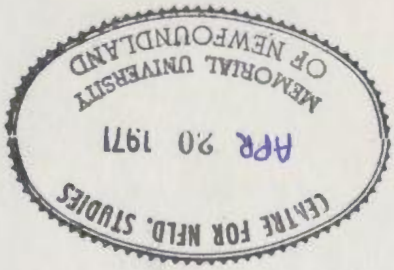
MEMORIAL UNIVERSITY
OF NEWFOUNDLAND
APR 20 1971
CENTRE FOR NFLD. STUDIES

PALEOMAGNETISM OF THE ORDOVICIAN REDBEDS OF BELL ISLAND, NEWFOUNDLAND

by

© KUNDURI. V. RAO, M.Sc. (TECH.) (ANDHRA)

"Submitted in partial fulfilment of the
requirements for the degree of Master of Science,
Memorial University of Newfoundland

August, 1970"

CONTENTS

ABSTRACT

A thermomagnetic study of oölitic hematite sandstone from the gently dipping Lower Ordovician Bell Island and Wabana groups near St. John's revealed three to four superposed magnetic components. The rocks were collected from a 150-meter section at 24 sites up to 6 km apart, plus one site 180 m below that section.

The natural remanence (NRM) directions occur in two nearly antiparallel groupings (A, B) close to published late Paleozoic directions. Two or more specimens each from 116 samples were stepwise thermally demagnetized in air, with field-nulling carefully controlled to $\leq 25\ \gamma$. Two new vector groupings (C, D), diverging sharply from the NRM, appeared after the 600°C and 685°C steps.

Up to 600°C the intensity (J) increased, sometimes by factors of 2 or more, compared with the NRM (10^{-5} - 10^{-4} emu/cm^3), before dropping sharply to a minimum at 685°C. Powder measurements in a magnetic balance to 750°C showed this to be mainly due to formation of a new, strongly magnetic component with Curie point 610 - 620°C, which x-ray diffraction tests suggest is γ-Fe_2O_3. This process had no observable effect on the high-temperature groupings (C, D), probably associated with α-Fe_2O_3.

Mean directions of the thermally discrete group D (685°C) component were significantly better aligned (k = 160) than expected from the present secular variation. Assuming reversed polarity, a possibly Ordovician pole calculated from this direction is in the

central Pacific (27.8°N, 168.2°W, dp = 1.8°, dm = 3.6°, N = 11 vertical zones) and constitutes the first paleomagnetic result from laboratory-treated Ordovician rocks in North America. The published evidence is still inadequate to interpret this result in terms of Lower Paleozoic paleogeography around the North Atlantic.

CHAPTER 1

PALEOMAGNETISM IN THE APPALACHIAN REGION

1.1. Introduction

Paleomagnetism is the study of the record of remanent magnetization of rocks. Its usefulness rests upon two fundamental assumptions, (i) (the "stability assumption"): that the direction of the geomagnetic field in which the rock became magnetized has been preserved, assuming further that the time of magnetization is known; (ii) (the "axial dipole assumption"): that during the geological past the field, when averaged over a suitable time span, was that of a dipole aligned with the Earth's spin axis. The minimum time span for averaging is of the order of the secular variation ($\sim 10^3$ years) or may be as much as 10^5 - 10^6 years (Hide, 1967).

1.1.1. Applications of paleomagnetism

Paleomagnetism is relevant to three broad fields of geophysical and physical research.

(1) It provides evidence relating to planetary evolution, being applicable to geophysical hypotheses such as continental drift, sea-floor spreading, polar wander and expansion of the Earth (Section 1.1.2). More generally, this includes applications of rock magnetism to problems of geological structure (Hospers and Van Andel, 1969) or their extension

to extraterrestrial material such as meteorites and rocks brought from nearby planets (Irving, 1964; Stacey, 1967).

(2) Secondly, paleomagnetism is a study of the Earth's magnetic field itself, extending its history to the time preceding direct observations. This concerns the nature of the main field and its secular variation, and the changes of field intensity and reversals of polarity during geological history (Smith, 1967).

(3) Thirdly, paleomagnetism involves a solid state study of magnetic minerals responsible for the record preserved in the rocks (Néel, 1955; Nicholls, 1955; Stacey, 1963; Nagata, 1964). Particularly important for geological interpretations are studies concerning the mode of acquisition of remanence components in rocks, their relative stability and certain mechanisms for self-reversal of polarity (Néel, 1955; Uyeda, 1958). Recent interest has centered on mineralogical studies of oxidation and exsolution phenomena in iron-titanium oxides and their effect on magnetic parameters and stability in volcanic rocks (Wilson and Watkins, 1967; Wilson et al., 1968; Larson et al., 1969). Ferromagnetic properties of sedimentary rocks, particularly red sandstones, have also been investigated in detail and will be discussed in Section 1.3.

1.1.2. Paleomagnetism and global tectonics

(i) Theory, procedures and results of paleomagnetic studies have been discussed by several authors, notably Cox and Doell (1960), Nagata (1961) and Irving (1964). Instrumentation and methods of paleomagnetism are summarized in Collinson, Creer and Runcorn (1967). Possibilities of

using rock magnetism as a tool for studying continental drift and polar wandering has a long history (Mercanton, 1926; Graham, 1954). The first application of this method which yielded significant results seems to have been the work of Clegg, Almond and Stubbs (1954) on the British Triassic red sandstones.

(ii) The practice of expressing rock magnetic results in terms of ancient pole positions was introduced by Creer, Irving and Runcorn (1954), who published the earliest polar wandering paths for Europe, and by Runcorn (1956) for North America. These earlier studies, followed by further investigations led to fairly consistent "polar wandering" curves which, relative to a particular land mass, tend to move away from the present pole progressively with increasing age; moreover the curves for different land masses tend to be separated, often by significant distances.

(iii) Various interpretations of (ii) are possible and these have been extensively discussed in various symposium volumes, in the context of polar wandering and continental drift, edited by Carey (1956), Runcorn (1962), Blackett et al., (1965), Garland (1966), and Markowitz and Guinot (1968).

(iv) The divergence of the paleomagnetic polar wandering paths for different continents can be interpreted in terms of an expanding Earth (Hospers and Van Andel, 1967). The possibility of an expanding Earth was first studied on various geophysical grounds by Egyed (1956), who estimated a mean increase in the circumference by 0.2 - 0.5 cm/year. Possible expansion can be tested paleomagnetically by comparing

contemporaneous rocks at widely separated sites in a single land mass. Cox and Doell (1961) and Ward (1963) concluded from such tests that expansion at Egyed's moderate rates could not be ruled out, but that larger rates (Carey, 1956; Heezen, 1960) are incompatible with the evidence.

(v) Paleomagnetic results also seem to be often compatible with specific drift reconstructions, as long proposed for (a) Gondwanaland (Du Toit, 1937) and (b) the opening of the North Atlantic (Wegener, 1929). Paleomagnetic data from the Gondwanic continents has been discussed by Creer (1965) and McElhinny (1967). The case of the North Atlantic is especially pertinent in the present study, in view of the critical position of Newfoundland in the paleogeography of land masses around the Atlantic (Section 1.2.1).

(vi) For Cretaceous and later times, independent evidence may be increasingly obtained from the geometry of sea-floor spreading (Hess, 1962; Dietz, 1966) and the associated magnetic anomaly patterns (Vine and Matthews, 1963; Morley and Larochelle, 1964), along with the paleomagnetic study of ocean cores (Opdyke et al., 1966, and many later authors).

(vii) The evidence that the geomagnetic field reverses, which relates to the second aspect of paleomagnetism (Section 1.1.1) has been firmly established for the past 4 to 5 million years, for which time span a comparison of paleomagnetic and radiogenic measurements made on young lava flows from many parts of the world has led to a geomagnetic polarity time scale (Cox et al., 1967). This has received striking

confirmation from the paleomagnetic study of deep-sea sediment cores and by the regular patterns of magnetic field anomalies "taped" onto the mobile ocean floor (Heirtzler et al., 1968; Isacks et al., 1968).

(viii) The paleomagnetic data is also often in accordance with the findings of paleoclimatology, reviewed in Nairn (1961, 1964).

1.2. Paleozoic paleomagnetic studies in eastern Canada

1.2.1. The Northeastern Appalachians and continental drift

The Appalachian region of Canada comprises parts of the four Atlantic provinces and that part of Quebec lying southeast of the Logan fault (Fig. 1.1). This is underlain chiefly by Paleozoic rocks, though both older and younger formations are present. The region underwent extensive deformation during the Paleozoic, first during the Taconic orogeny at the close of the Ordovician and again during the Acadian orogeny in Devonian time; both of these disturbances developed structures with a dominant northeasterly trend. The Appalachian revolution at the close of the Paleozoic, which folded and faulted the strata to the south, thereby producing the Appalachian mountains, had only local effects in the northern region, and these effects are most strongly shown in Newfoundland and eastern Nova Scotia.

Increasing attention is being given to comparative features between the Appalachians of Canada and the British Caledonides (Wilson, 1962; Kay, 1967) bearing on the structural-stratigraphic fit of the two orogenic belts (Phinney, 1968). The interpretation of drift in the

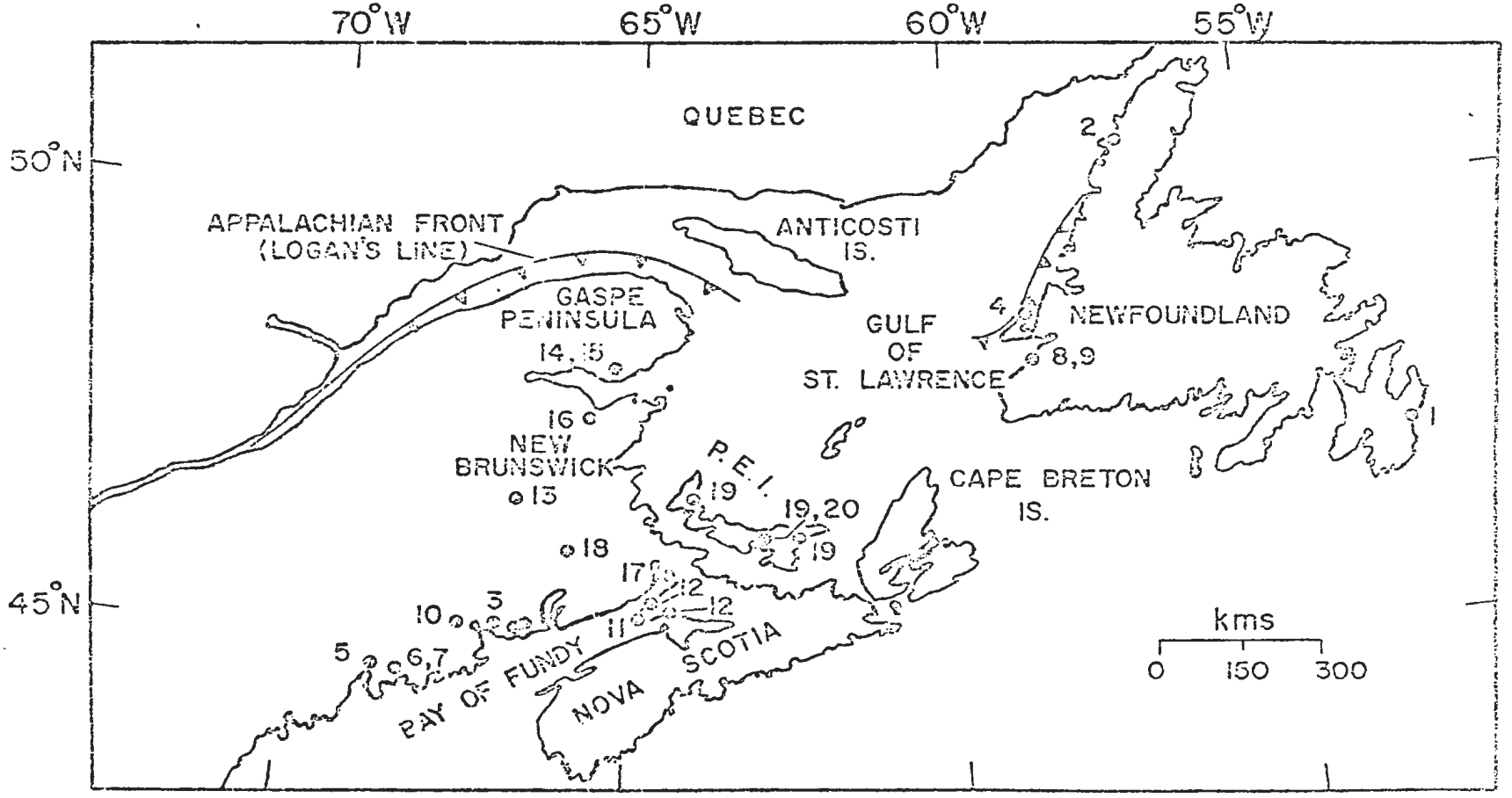

Fig. 1.1 Pre-Mesozoic paleomagnetic sampling areas in the Canadian Appalachian region

(Numbers are as in Table 1.1.)

North Atlantic based on bathymetric reconstructions (Bullard et al., 1965) is compatible with those based on tectonic belts (Kay, 1967), and both approaches give a fit resembling that made long ago by Taylor (1916). Paleomagnetic results also are consistent with the fit by Bullard et al., as discussed by Wells and Verhoogen (1967) and Hospers and Van Andel (1968).

The most significant result to emerge from the studies of Late Paleozoic and Mesozoic Paleomagnetism of the land masses bordering the North Atlantic is the systematic displacement between the Upper Paleozoic to Triassic poles for North America compared to Europe, which clearly favours the concept of continental drift in terms of the opening of the North Atlantic. Two prominent features observed by Runcorn (1956), Irving (1957), Collinson and Runcorn (1960) and others, have been discussed by Deutsch (1969): (1) for the Carboniferous-Triassic interval a westward displacement of the North American polar path from the European path and (2) a northward component of the polar shift in both these curves. Because of the statistical uncertainties in some of the inferred pole positions and the lack of adequate Triassic data from both continents, and of Cretaceous data from Europe, a precise paleomagnetic estimate of the beginning of the opening of the North Atlantic ocean cannot yet be made, other than the statement that it occurred in Late Permian or Mesozoic times.

Several continental drift reconstructions (e.g. Du Toit, 1937) place Paleozoic Newfoundland in the vicinity of Western Ireland. Some papers in the recent Gander Symposium volume (Kay, 1969) give strong

support to the occurrence of continental drift across the North Atlantic since the Late Paleozoic.

Wilson (1966) proposed the existence of a "Proto-Atlantic" during the early Paleozoic which gradually closed during the Paleozoic and then reopened. In the process, certain crustal portions that had been on opposite sides of the Atlantic during the Lower Paleozoic (among them western and eastern Newfoundland) were welded together. While the paleomagnetism of Late Paleozoic and younger rocks is relevant to the problem of the opening of the present Atlantic, a test of Wilson's hypothesis would require voluminous paleomagnetic data from Middle Paleozoic and older rocks.

Thus the problems concerned in Newfoundland are largely tectonic or structural. Deutsch (1966) mentions a number of inter-related problems amenable to paleomagnetic study in the Atlantic region, where the existing data are still sparse compared with those from other land masses. These problems include (i) correlation of structures across the North Atlantic, (ii) the rotation of Newfoundland (Wegener, Transl. 1966) and (iii) the unbending of oroclines (Carey, 1955).

1.2.2. Previous paleomagnetic work

Paleozoic paleomagnetic work in eastern Canada started with a study by Nairn et al. (1959) of the Carboniferous Codroy group sediments in western Newfoundland (Table 1.1, no. 8). The same authors studied the Precambrian Signal Hill and Blackhead red sediments of eastern

TABLE 1.1

Paleomagnetic directions obtained from studies of Precambrian and Paleozoic rocks in eastern Canada

No. and Area[1]	Rock Formation[2]	Age[3]	D[4]	I[5]	α_{95}[6]	Treatment[7]	Reference
1*(a)	Signal Hill and Blackhead Seds	Pree	262	+39	14	nt	Nairn et al. (1959)
2(a)	Bradore Seds	L.ε	151	+45	9	af	Black (1964)
3(b)	Ratcliff Brook Seds	L.ε	168	+53	15	af	Black (1964)
4(a)	Clam Bank group Seds	L.D	338	-20	11	af	Black (1964)
5(b)	Perry Volcs	U.D	184	+34	15	af	Black (1964)
6(b)	Perry Seds	U.D	174	+20	9	af	Black (1964)
7(b)	Perry Volcs and Seds	U.D	175	+23	15	th	Robertson et al (1968)
8(a)	Codroy Seds	M	166	+ 8	8	nt	Nairn et al. (1959)
9(a)	Codroy Seds	M	175	+23	10	af	Black (1964)
10(b)	Kennebecassis Seds	M	161	+33	10	th	Du Bois (1959)
11(b)	Maringouin formation redbeds	U.M	179	+21	8	th	Roy and Robertson (1968)
12(b)	Hopewell Group redbeds	U.M to L.P	358	-20	7	th	Roy and Park (1969)
13(b)	Prepictou Seds	M or P	162	+31	15	af	Black (1964)
14(e)	Bonaventure Seds	M or P	166	+13	7	nt	Du Bois (1959)

TABLE 1.1, continued

No. and Area[1]	Rock Formation[2]	Age[3]	D[4]	I[5]	α_{95}[6]	Treatment[7]	Reference
15(b)	Pictou and Bonaventure formation Seds	M or P	167	+ 3	4	th	Roy (1966)
16(b)	Bathrust beds	P	162	+16	9	nt	Du Bois (1959)
17(d)	Cumberland group red Seds	P	172	+16	5	th	Roy (1969)
18(b)	Hurleycreek formation redbeds	U.P	171	+ 9	10	th	Roy et al. (1968)
19**(c)	Eastern, central and NW P.E.I. redbeds	PC	173	+ 6	6	af	Black (1964)
20(c)	P.E.I. redbeds	PC	168	0	6	th	Roy (1966)

[1]Area of site: (a) Newfoundland; (b) New Brunswick; (c) Prince Edward Island (P.E.I.); (d) Nova Scotia; (e) Gaspé.

[2]Rock type: (e.g. "sediments", "redbeds", "volcanics") are as denoted in original papers.

[3]Geological age: L = Lower; U = Upper; Preε = Precambrian; ε = Cambrian; D = Devonian; C = Carboniferous; M = Mississippian; P = Pennsylvanian; PC = Permo-Carboniferous.

[4]Mean declination (deg) of remanent magnetization.

[5]Mean inclination (deg), north pole positive, downward.

[6]Radius (deg) of 95% confidence circle (Fisher, 1953).

[7]Laboratory treatment: af, alternating field demagnetization; th, thermal demagnetization; nt, no treatment.

*Mean taken from Irving (1964).

**Mean was obtained giving equal weight to the three area means.

Newfoundland (No. 1). The only other pre-Carboniferous paleomagnetic results for the Atlantic provinces are from the Lower Cambrian Bradore sediments in western Newfoundland (No. 2) and Ratcliffe Brook sediments in New Brunswick (No. 3), both by Black (1964), and the Lower Devonian Clam Bank group sediments in western Newfoundland (No. 4; Black, 1964) and Upper Devonian Perry volcanics and sediments in New Brunswick (Nos. 5, 6: Black, 1964; No. 7: Robertson et al., 1968). All other results in Table 1.1 (i.e. nos. 8 - 20) are from paleomagnetic studies of Late Paleozoic rocks.

From the paleomagnetic results relative to eastern Canada, Roy (1969) infers a systematic trend with time, not only between pole positions derived from Lower and Upper Paleozoic data, but also within the Upper Paleozoic. Although the ellipses of confidence of some of the Upper Paleozoic pole positions overlap, the poles derived from the younger formations tend to be more easterly. The overall displacement of Upper Paleozoic poles, 27°, is in good agreement with contemporaneous Paleozoic European data obtained by Storetvedt (1968), and Roy (1969) considers a 25° - 30° polar change relative to both continents during Upper Paleozoic times to be possible. An apparent polar change at approximately the same time, though of greater magnitude, was also observed in Australia (Irving, 1966) and Africa (McElhinny and Opdyke, 1968). The paleomagnetic data for the Atlantic provinces are consistent with a low-latitude position of that region during the Upper Paleozoic.

1.2.3. Rotation of Newfoundland

Though some positive evidence is claimed by Briden (1967) for possible continental drift before the Late Paleozoic, paleomagnetism has yet to establish this possibility in the case of the North Atlantic. In this connection, the Bell Island study may be capable of contributing important evidence, since the rocks concerned are of Lower Ordovician age, and such evidence must come from Middle Paleozoic and older rocks on both sides of the Atlantic.

Paleomagnetic data from eastern North America, including Newfoundland, are capable of providing evidence on the proposed (Wegener, 1966 Transl.) 30^{0} anticlockwise rotation of Newfoundland. A positive test would yield a significant difference in magnetic declination between contemporaneous rock formations in Newfoundland and in some nearby region such as the Maritime provinces, the Newfoundland declinations being smaller; one assumes here that the sampling sites in the Maritimes belonged to a tectonically stable part of North America during the Lower Paleozoic. Nairn et al. (1959) inferred a 20^{0} anticlockwise rotation of Newfoundland since the Carboniferous from a comparison between their Mississippian results for Newfoundland (Table 1.1, no. 8) and data from the United States. However, the significance of this was disputed by DuBois (1959), whose Carboniferous data from New Brunswick and Gaspé (Nos. 10, 14, 16), along with data by later authors for the Atlantic provinces (Nos. 9, 11 - 13, 15, 17 - 20), indicate that there is no significant difference in Upper Paleozoic paleomagnetic directions between Newfoundland and the adjoining Atlantic provinces.

Nor should the directions differ since the rotation of Newfoundland, even if it did occur, would have been associated with the Middle to Late Devonian Acadian orogeny (Poole, 1967) and would have been completed by the Carboniferous. Therefore, as in the case of Wilson's hypothesis (1966), the evidence concerning the rotation of Newfoundland must come from Middle Paleozoic or older rocks.

Black (1964) deduced a 30^{0} anticlockwise rotation of Western Newfoundland from a paleomagnetic comparison between (i) Cambrian (Table 1.1, nos. 2, 3) and (ii) Devonian (Nos. 4, 6) sedimentary formations in Newfoundland and New Brunswick. However, Robertson et al. (1968) argue that Black's results are inconclusive for two reasons: (1) The Cambrian mainland and Newfoundland directions are not significantly different at the 95% confidence level (compare α_{95} Values in Table 1.1); (2) the corresponding "Devonian" directions may not be contemporaneous, as the magnetization of the Upper Devonian Perry formation in New Brunswick, which Black had compared with the Lower Devonian Clam Bank group sediments in Newfoundland, may be of Mississippian age (Robertson et al., 1968). (3) A third objection (Deutsch, 1969) is that, even assuming conclusive paleomagnetic results, these would not have constituted unambiguous evidence for the rotation of Newfoundland since they could equally well be interpreted as supporting Wilson's (1966) model. Unambiguous evidence would have had to include data from mainland sites in the stable interior of North America.

The above paleomagnetic observations which suggest that, from Lower Cambrian to Lower Devonian time, Newfoundland remained fixed with

respect to mainland Canada, are supported by the findings of Sheridan and Drake (1968), from seismic evidence in the Gulf of St. Lawrence, suggesting that the Gulf was open during the relevant times.

1.2.4. The "orocline" concept applied to the Appalachians

According to Carey (1955) an orocline is the impressed strain in an originally linear orogenic system "flexed in plan to a horse-shoe or elbow shape" by stresses postdating its main period of genesis; this process he considers to be an essential aspect of continental drift.

Orocline tectonics can be tested paleomagnetically by comparison of declinations in different parts of the presumed orocline, similar to the rotation test in Section 1.2.3. As an example of an orocline test, Irving and Opdyke (1965) studied paleomagnetically the Upper Silurian Bloomsburg redbeds of Pennsylvania at various sites along a 40^{o}-bend in the central Appalachian geosyncline, comparing them with the nearby Middle Silurian Rosehill and Clinton beds. They were able to explain the results on the supposition that the geosyncline was straight in Silurian time. Subsequently, Roy et al. (1967) confirmed the earlier findings by a further investigation, but further paleomagnetic work is needed to confirm the proposed oroclinal nature of the Appalachian Mountains (Knowles and Opdyke, 1968).

1.3. Magnetism of red sediments

The terms "red sandstone", "red sediment", "redbed", etc., are

used by authors in the widest sense to include sandstones, siltstones, mudstones and limestones ranging in colour from purple through red to brown (Collinson, 1965). Red sediments have been widely used in paleomagnetism because a stable component of measurable intensity is often present in their natural remanent magnetization (NRM) or may be isolated by suitable demagnetization techniques; moreover, these rocks often occur in well-bedded and relatively undisturbed strata. Much of the present data on which continental reconstructions and polar wandering curves are based derives from measurements of red sediments, particularly those of Europe and North America. Neither the mode of acquisition of primary magnetization nor the ferromagnetic mineralogy of red sediments is yet fully understood, and it is now believed that such rocks are not formed by a unique process (Van Houten, 1968). However, the extensive use of red sandstones in paleomagnetism has resulted in an interest in their magnetic properties leading to investigations into processes by which they acquire their natural remanent magnetization (NRM) (Collinson, 1969).

1.3.1. Magnetic constituents of red sediments

Red sediments are now thought to originate under a variety of geological and climatic conditions affecting both the source rock and the site of deposition. Van Houten (1961) states that the red pigment, believed to be finely divided anhydrous or hydrous ferric oxide, is generally developed in soils under humid conditions, these soils being later deposited as a sediment in an oxidizing environment. The magnetic

constituents of the red pigment include goethite (α-FeOOH), lepidocrocite (γ-FeOOH) and maghemite (γ-Fe_2O_3), as well as hematite (α-Fe_2O_3) and magnetite (Fe_3O_4); the hematite probably originated through dehydration of goethite (Creer, 1961; Strangway et al., 1968).

Besides red pigment, hematite also occurs in red sediments in the form of black multi-crystalline grains of "specularite". X-ray and chemical analyses have shown that the hematite occurring as specularite may be associated with ilmenite ($TiFeO_3$) and ilmenite-hematite solid solutions or intergrowths, though there is little evidence that these ilmenite forms are important in the magnetism of redbeds (Van Houten, 1968).

In view of the differences in history and petrology between different redbed formations, as well as the difficulty of separating the pigment from the specularite, it is not easy to determine whether the origin of the NRM lies predominantly in the red pigment which gives the rock its distinctive colour, or in the black iron-oxide particles (mainly specularite). However, there is evidence (Collinson, 1966) that hematite in both forms can carry remanence; the pigment appears to have a high coercivity of remanence relative to specularite, whereas the saturated isothermal remanence (IRM) of each is about the same. It is probable that the properties depend extensively on grain size, and if this is sufficiently small, superparamagnetic particles may be present, particularly in the pigment (Creer, 1961; Collinson, 1969); such particles would not contribute significantly to the NRM.

The available evidence strongly suggests that the stable primary remanence of red sediments is carried by hematite (α-Fe_2O_3); this is shown by chemical and x-ray analyses, and by the results of thermal demagnetization of the NRM; which vanished at about 680°C (Collinson, 1969) close to the Curie point of natural and synthetic hematites. In the majority of the formations studied so far, neither magnetite nor maghemite appears to be an important magnetic constituent. Collinson (1968) found evidence that ferrous and ferric iron in minerals such as clays, siderite and biotite contribute to some magnetic properties of sedimentary rocks, but these minerals being paramagnetic in pure form, cannot contribute to the remanence.

1.3.2. Acquisition of remanence by red sediments

Sedimentary rocks can acquire their magnetism by one of two processes: (i) Depositional (or "detrital") remanent magnetization (DRM) by which ferromagnetic grains derived from a source rock are being aligned in the Earth's field while settling, generally in water; (ii) Chemical remanent magnetization (CRM) by which the rock acquires a ferromagnetic component either through precipitation from a circulating iron-bearing solution or through chemical change of an existing component, e.g. oxidation of magnetite to maghemite. In redbeds, it is most likely (Collinson, 1966) that DRM is associated with specularite, whereas CRM might be associated with either specularite or the pigment, in the former case through diagenetic alteration of magnetite to hematite, in the latter case if the pigment had been precipitated from solution.

Certain magnetic and geological criteria can be helpful in judging the likelihood of alternative DRM and CRM mechanisms being operative in particular redbeds (Collinson, 1965). These include (1) the occurrence of an "inclination error" (Griffiths et al., 1962; Van Andel and Hospers, 1966; Irving, 1967), applying to DRM but not CRM; (2) differences in the intensity of magnetization (generally 10^{-7} to 10^{-4} gauss); and (3) the scatter of directions of magnetizations, (i) within samples and (ii) between samples from a given site; usually (i) is less than (ii). According to Irving (1957), intensity and directional scatter are linked critically by the dependence of both properties on grain size, the coarser samples reflecting deposition in turbulent conditions, leading to a reduced intensity of the DRM compared with the ideal case of a perfect particle alignment. Collinson (1969) did not observe such a correlation and considers it unlikely to exist if the NRM is carried only by a small proportion of the hematite present, the grain size of which might be unrepresentative of the rock. However, assuming the CRM process to be less turbulent than the DRM, one would expect the NRM intensity of the latter to be less than in a CRM involving the same amount of hematite.

Although within-sample and between-sample scatter in redbeds is often random, systematic disturbing factors can occur, such as the well-known "streaking" of directions of magnetization towards the present field direction due to the presence of secondary components of magnetization (Irving et al., 1961). Existence of inhomogeneity in redbeds is postulated by Irving (1964), though the extent of the phenomenon has not been definitely established.

1.4. Objective

The objective of the investigation described here was the study and interpretation of some magnetic properties and the paleomagnetism of Lower Paleozoic red sandstones in the easternmost part of the Canadian maritime Appalachians. A 500-meter vertical section of the gently dipping ($\sim 10^0$) Lower Ordovician Bell Island and Wabana groups from Bell Island near St. John's was sampled, but the present study is confined mainly to measurements of 116 hand samples of oölitic hematite sandstone from the upper third of this section, including the Airfield and Wabana formations; these were subjected to systematic thermal demagnetization studies. The rocks were collected from these formations over a 150 m vertical section at 24 sites situated up to 6 km apart. A possibly primary (Ordovician) geomagnetic pole relative to eastern Newfoundland, obtained in the present study, will be compared with other Lower Paleozoic paleomagnetic data from North America and Europe; this result will be discussed in terms of Lower Paleozoic paleogeography.

CHAPTER 2

GEOLOGY AND SAMPLING

2.1. Geologic setting, age and stratigraphy

Conception Bay of the Avalon peninsula is surrounded by tightly folded and faulted Precambrian volcanic and sedimentary rocks, except for a narrow strip around its south shore between Topsail and Brigus (Fig. 2.1). This strip has exposures of sediments ranging in age from Lower to Upper Cambrian overlying unconformably the Precambrian rocks; the dip changes progressively from 8^{o}NW near Topsail to 50^{o}E in the Brigus area on the west side of the Bay where open folds are developed.

Lower Ordovician sediments are exposed in eastern Conception Bay, on Little Bell, Kelly and Great Bell Islands[1], striking northeasterly and dipping in general 10^{o}NW; they appear to be conformable with the Upper Cambrian beds to the south, though the contact is not exposed. The present collection was confined to the Clinton-type iron ore-bearing section (Gross, 1965) in Conception Bay, which out-crops only on Bell Island. The geology is described mainly by Hayes (1915), Rose (1952), Lyons (1957), Nautiyal (1967) and Gross (1967).

The Lower Ordovician age of the Bell Island rocks has been established from fossils (Van Ingen, 1914). The stratigraphy of the

[1]Conforming to common usage, "Bell Island" will henceforth be used to denote Great Bell Island.

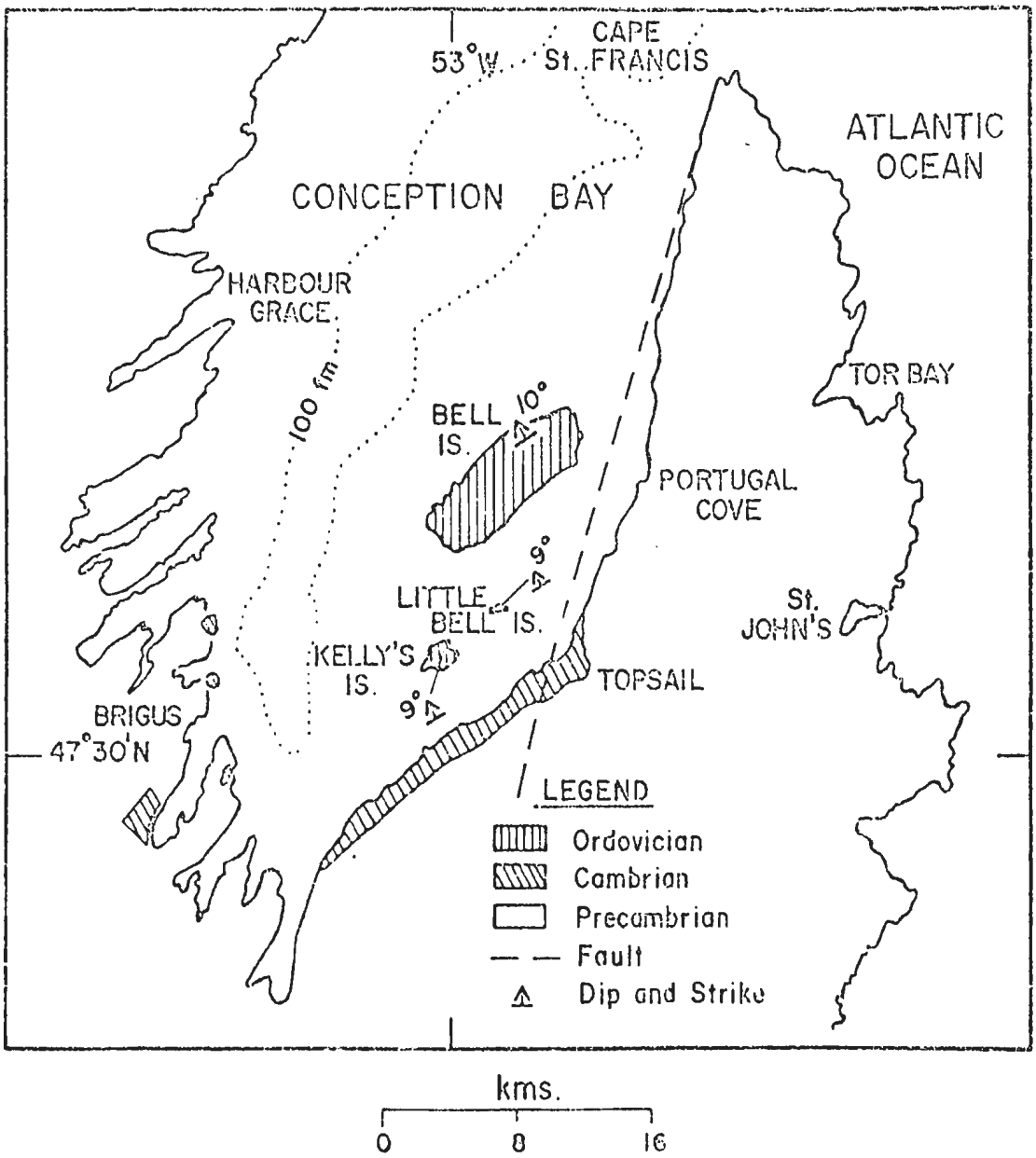

Fig. 2.1 Generalized geological map of Conception Bay (Modified after Hayes, 1915)

rocks has been worked out according to the occurrence of ferruginous rocks (Hayes, 1915) on petrological (Rose, 1952) and paleontological (Nautiyal, 1967) grounds. The stratigraphy due to different workers and the stratigraphic coverage of paleomagnetic sampling is summarized in Fig. 2.2.

Bell Island covers an area of 41 km^2 and in general consists of varying grey sandstones and shales, either separately or intercalated with beds of red-brown hematitic oölite, greenish-black sandstone and moderately to highly ferruginous sandstone and shale. The strata are present in the form of interbeds, intercalations and broad lenticulations of varying thickness.

According to the stratigraphy of Van Ingen (1914) and Rose (1952), these Lower Ordovician sediments are divisible into two major rock units, the Bell Island and Wabana Groups. The former comprises thick formations of grey, grey-brown, greenish and whitish sandstones and black shales, along with beds of red oölitic hematite and ferruginous sandstone and shale. The Wabana Group overlies the Bell Island Group and, except for more abundant black shale, is lithologically similar to the latter.

Hayes (1915) divided the stratigraphic succession into six zones based on the occurrence of oölitic iron ore and ferruginous rocks on Bell Island, three of the zones being mineable. According to Rose (1952) and Lyons (1957), the Clinton-type iron formations occur in three beds, the (i) Dominion or Lower, (ii) Scotia or Middle, and (iii) Upper beds, separated respectively by about 70 m and 18 m of shale and sandstone.

Nautiyal (1967) found it useful to revise the rock stratigraphy units proposed by Van Ingen (1914) and Rose (1952). In his classification (Fig. 2.2), the Wabana Group (93 m) of Rose has been lowered to formational rank, with a Lower (3 m), Middle (60 m) and Upper (30 m) member. The Bell Island Group is subdivided into three mappable stratigraphic formations from the oldest to the youngest, namely the Polls Head (120 m), Townsquare (180 m) and Airfield (60 m) formations, going upward. The Lower member of Nautiyal's Wabana formation is a conglomerate bed containing oölitic pyrite, making discomformable contact with the underlying Airfield formation at the Dominion bed of Rose. The disconformity therefore separates the Bell Island Group from the Wabana formation. Neither the base of the former nor the top of the latter is exposed.

2.2. Structural geology of Conception Bay

One of the main structural features of Conception Bay is the contrast between the gently deformed Lower Paleozoic sedimentary basin and the underlying, tightly folded and eroded Precambrian rocks. Although the same general fold and fault pattern seems to apply throughout the Precambrian to Ordovician section, the uniform low dip of the Cambrian and Lower Ordovician strata is evidence that they have been only moderately deformed since their deposition and consolidation (Rose, 1952).

Among several periods of earth movements, some took place before and others after the deposition of the Cambro-Ordovician iron

Fig. 2.2 Generalized stratigraphy of Bell Island

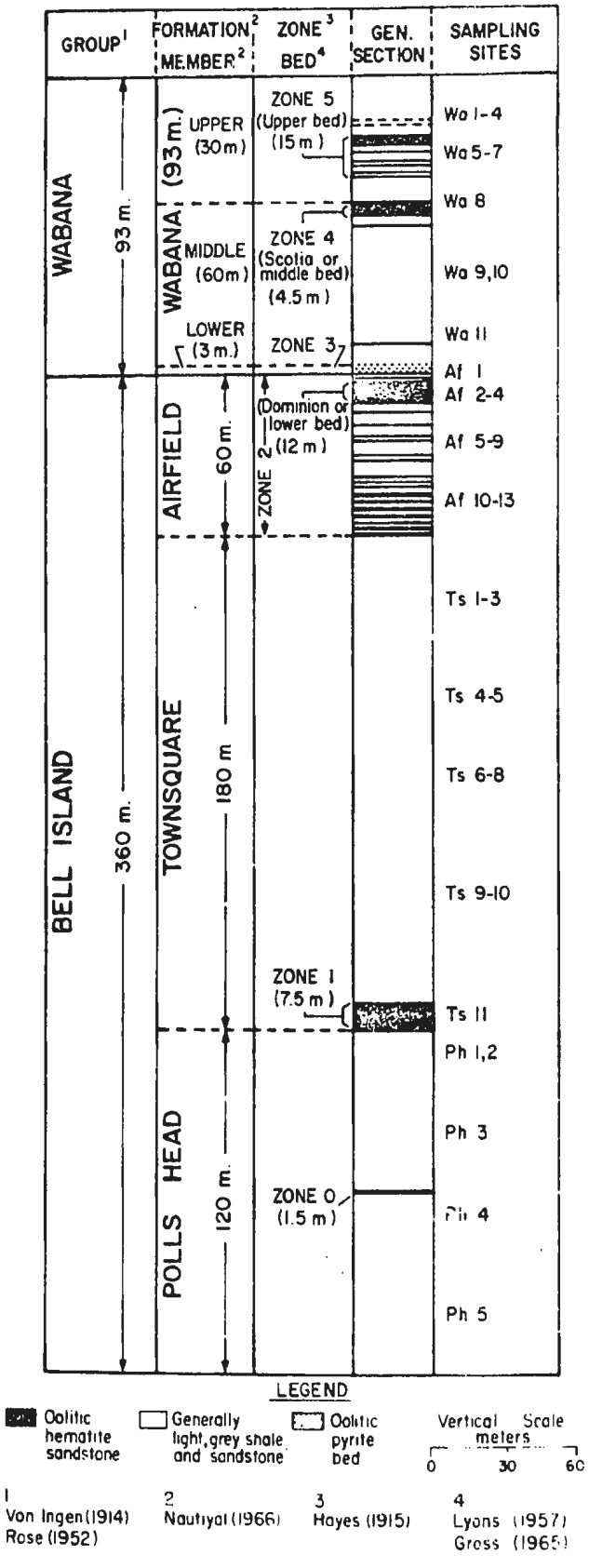

ore-bearing series. It is probably (Hayes, 1915) that these Precambrian movements, which had prepared the sea-floor for the accummulation of the Lower Paleozoic deposits, resulted in lines of weakness, along which or parallel to which Post-Cambrian dislocations or faults originated.

The Precambrian rocks are cut by thrust faults predominantly trending northeast. One of the most conspicuous features is the Topsail fault zone (Fig. 2.1), exposed between Topsail and Cape St. Francis, which terminates the Cambrian beds lying southeast. The attitudes of these beds suggest that Conception Bay is underlain by an asymmetric synclinal trough plunging north-northeast at low angle; this trough may be due to broad folding of the strata in Post-Cambrian time. As the Lower Ordovician beds form the youngest known consolidated rocks of the area, it is not possible to assess accurately the effect of later tectonic events upon them, nor is there direct evidence to indicate that rocks younger than Ordovician were ever deposited.

2.3. Composition and mode of formation of beds

Iron ore has been mined from the Lower (or Dominion), Middle (or Scotia) and Upper beds (Fig. 2.2) of Rose (1952) which are comparable in their general characteristics but differ from one another in both thickness and mineral distribution.

The Lower bed is 4 - 12 m thick and is the major source of the Wabana ore, which occurs here in several large lenses of hematite. The 70 m of shale and sandstone lying between the Lower and Middle beds contains an average of 6.9% Fe and 50.4 % SiO_2. The Middle bed is 1.5 - 4.5 m

thick and represents a much more sharply defined zone of deposition than either the Lower or Upper bed. The latter is located 12 - 27 m above the Middle bed and is characterized by erratic distribution of thin ore zones and lenses and by relatively much siderite ($FeCO_3$). In the three beds, the composition of the "clean ore", which is relatively free of clastic material, ranges from 59.6 to 45.0% Fe and 6.4 to 20.0% SiO_2.

These three beds of the Airfield and Wabana formations are typically deep red to purple, and massive, and are composed of oölites, i.e. spherules consisting of hematite (Fe_2O_3), chamosite (a green, hydrous silicate) and siderite (Fig. 2.3). A typical analysis is given in Table 2.1. The composition of the ore mostly varies within the following limits (Hayes, 1915): Hematite, 50 - 70%; chamosite, 15 - 25%; siderite, 0 - 50%; calcium phosphate, 4 - 5%; calcite, 0 - 1%; quartz, 0 - 10%.

The Bell Island rocks commonly contain ripple marks, cross-bedding and other evidence of shallow-water deposition characteristic of Clinton-type iron formations, and tend to occur in lenticular beds of varying thickness, usually 3 to 5 m, but not exceeding 12 m. Other prominent occurrences of early Paleozoic oölitic iron ores are (Petranek, 1966) in Thuringia, Morocco (Ait Amar), northern Portugal, France (Normandy), Bohemia, north Wales and the U.S.A. (Silurian Clinton Group). Hematitic oölite beds occur in all formal rock units found on Bell Island, except for the Lower member of the Wabana formation. The following are some main conclusions from a comprehensive study of the Wabana deposits (Hayes, 1915):

TABLE 2.1

Mineral composition of the Bell Island ore beds

(from ore mined in 1927, Lyons, 1957)

Mineral	Chemical composition	Bed average	
		"Lower" bed (%)	"Middle-Upper" bed (%)
Chamosite	25.64% SiO_2 19.75% AlO_3 39.74% FeO 2.98% MgO_2 11.89% H_2O	23.2	22.7
Hematite	Fe_2O_3	61.5	54.8
Siderite	$FeCO_3$	2.8	13.3
Quartz (sand grains)	SiO_2	6.1	3.6
Calcium phosphate (shell fragments)	$Ca_3(PO_4)_2$	4.7	4.4
Calcite (in joints, faults)	$CaCO_3$	0.8	1.2
Manganese oxide	MnO_2	0.3	0.3
Titanic acid	TiO_2	0.3	0.4
Pyrite	FeS_2	0.1	0.1
	Total:	99.8	100.8

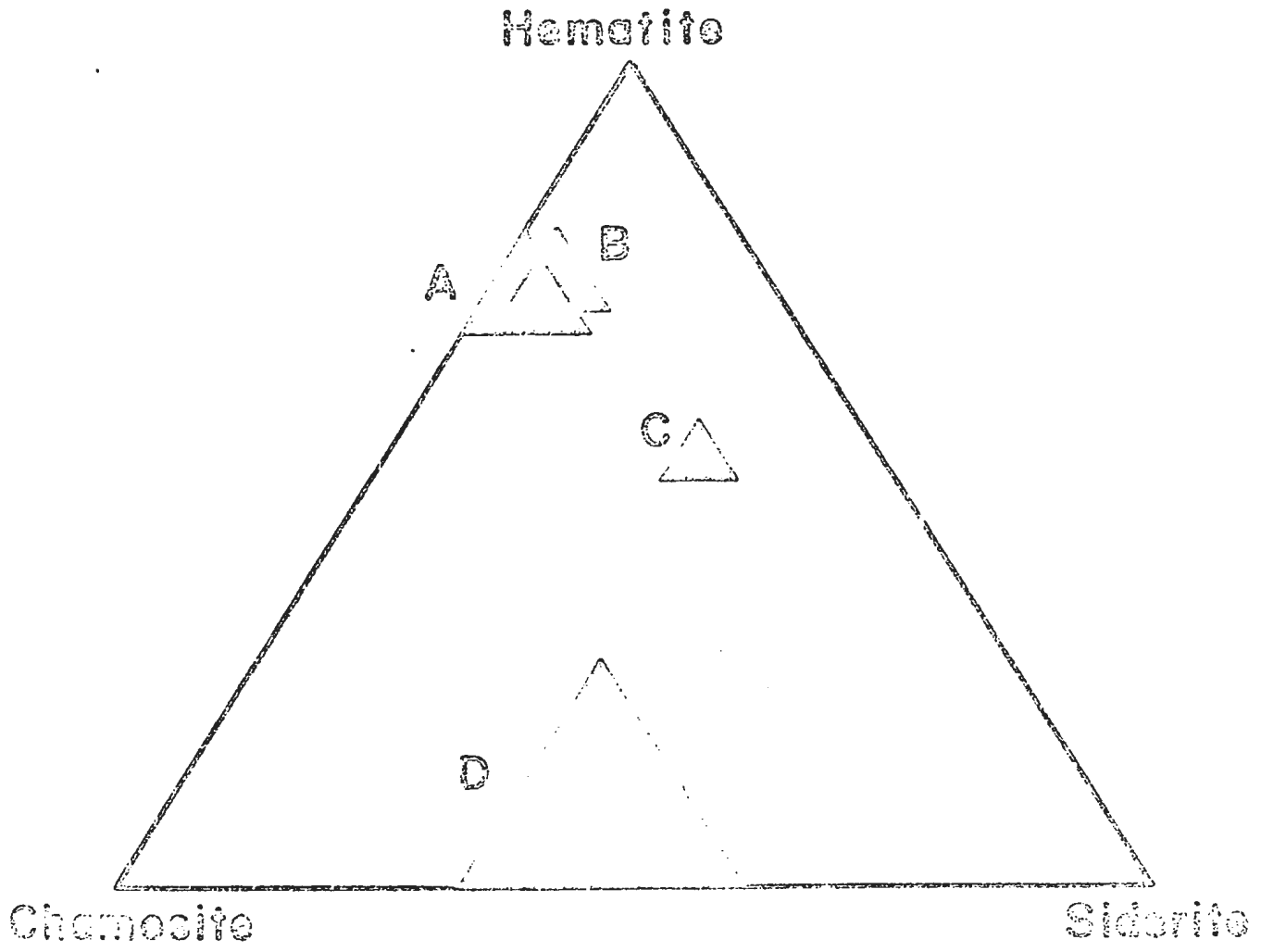

Fig. 2.3. Mineral composition of red sediments, Bell Island (from Pettijohn, 1957)

A, B, C: Lower, Middle and Upper beds
D: A ferruginous sandstone from another level

(1) Deposition of the ore beds under shallow marine conditions is probable, as they contain marine fossils (brachiopods, triolobites, worm tubes, algae, etc.) that are known to have lived in the littoral zone.

(2) The reddish-brown colour of the ore is typical of amorphous hematite. The weathered surfaces exhibit a fine, granular appearance due to oölitic structure.

(3) Microscopic studies reveal that the oölites are formed around nuclei of fossil fragments, sand grains or granules that are now siderite and siderite-chamosite mixtures. The oölites vary typically between 0.1 and 0.5 mm in diameter and tend to be disc-shaped (Fig. 2.4), as though flattened by pressure normal to the bedding plane of the ore.

(4) Alternate concentric rings of hematite and chamosite surround the nuclei, and oölites are held in a matrix of hematite or siderite, with one or the other predominant in a given zone or bed. The outer rings are nearly always hematite. The oölites have been little altered since deposition, as indicated by delicate, well-preserved algae borings that cut across some of the oölitic rings.

(5) While direct evidence for the source of the iron is lacking, Hayes, in common with other authors studying iron formations, inferred that the hematite ore was produced by oxidation (possibly through algae action at the sea bottom) of the precipitated hydrates of iron (e.g. goëthite), which in turn were derived from the weathering products of earlier rocks. Since oölitic ores are found associated with argillaceous rocks, the chamosite and other iron silicates probably

Fig. 2.4 Micro-photograph of polished sections from Bell Island rock, showing oölitic structure (enlarged 125x)

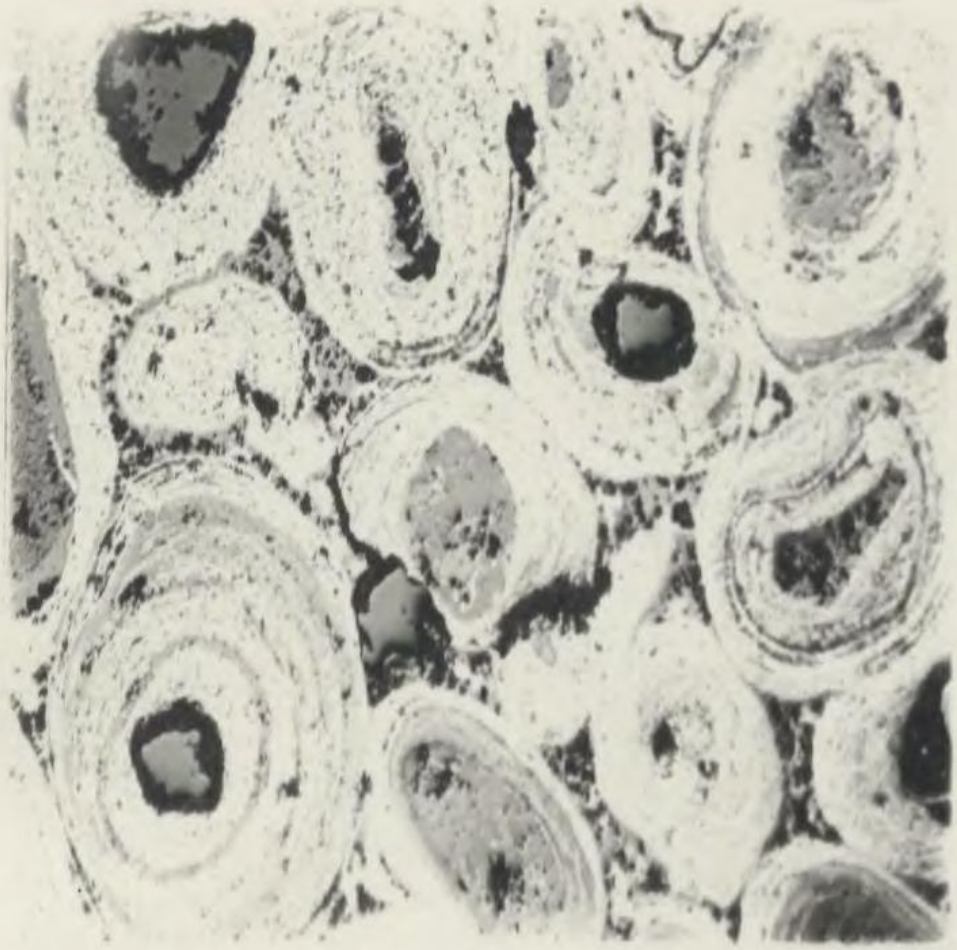

Fresh specimen

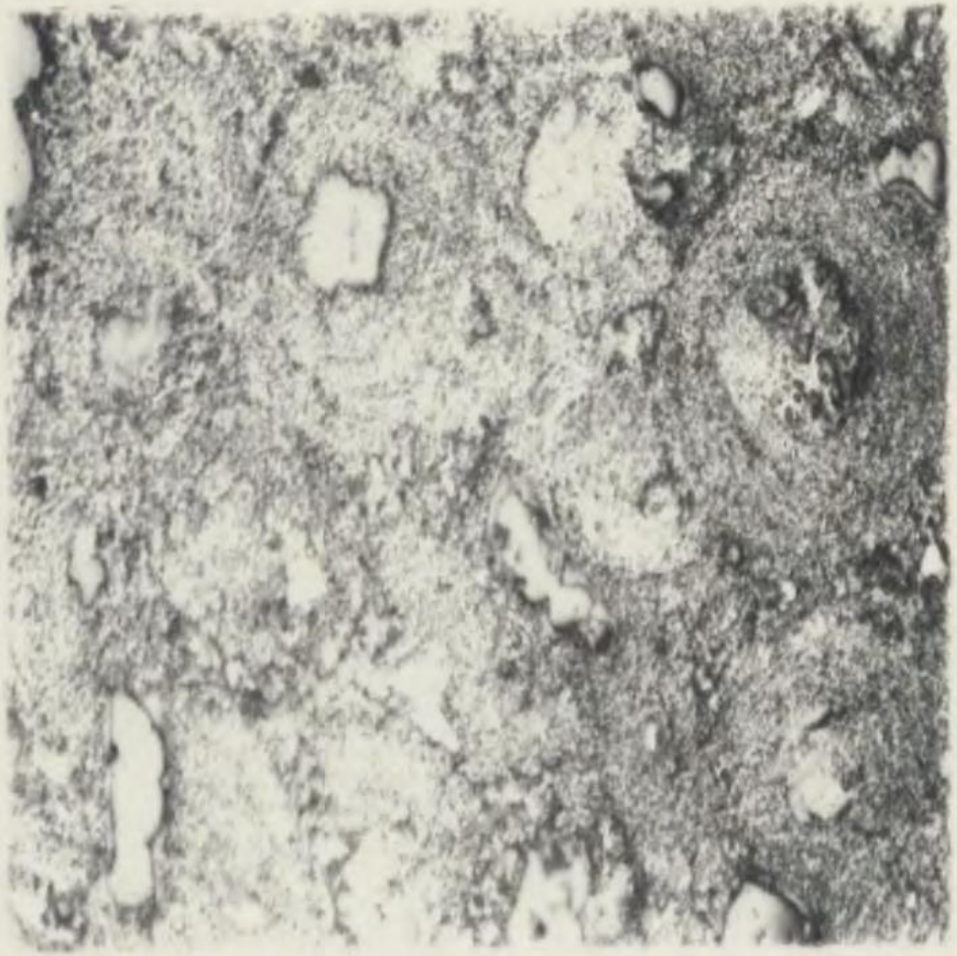

After heating in air to 685°C

originated through a combination of iron and hydrated aluminous silicates at the time when the hematite was also formed.

(6) A considerable deepening of the sea at the close of deposition of Hayes (1915) Zone 2 (Fig. 2.2) is suggested by the presence of graptolites in Zone 3: shallow-water conditions again prevailed at the close of deposition of Zone 4, probably accompanied by vertical oscillations as inferred from the existence of concentric layers of chamosite and hematite on the oölites.

Gross (1967) concludes that the source of iron in the Wabana beds is still uncertain because of the complexity of the conditions under which they were formed, involving a delicate adjustment of depth and Eh and pH conditions of the sea water and distribution of clastic material.

2.4. The paleomagnetic collection

A 16-km drive connects St. John's to the harbour of Portugal Cove on the eastern shore of Conception Bay, from which Bell Island is served by a regular car and passenger ferry. The island has a maximum width (SW - NE) of 10 km and has a well-developed road system from which every point apart from coastal cliffs can be reached on foot with comparative ease (Fig. 2.5).

2.4.1. Distribution of sampling sites

In the summer of 1968, 181 oriented hand samples of red and

Fig. 2.5 Geological formations and paleomagnetic sampling sites at Bell Island

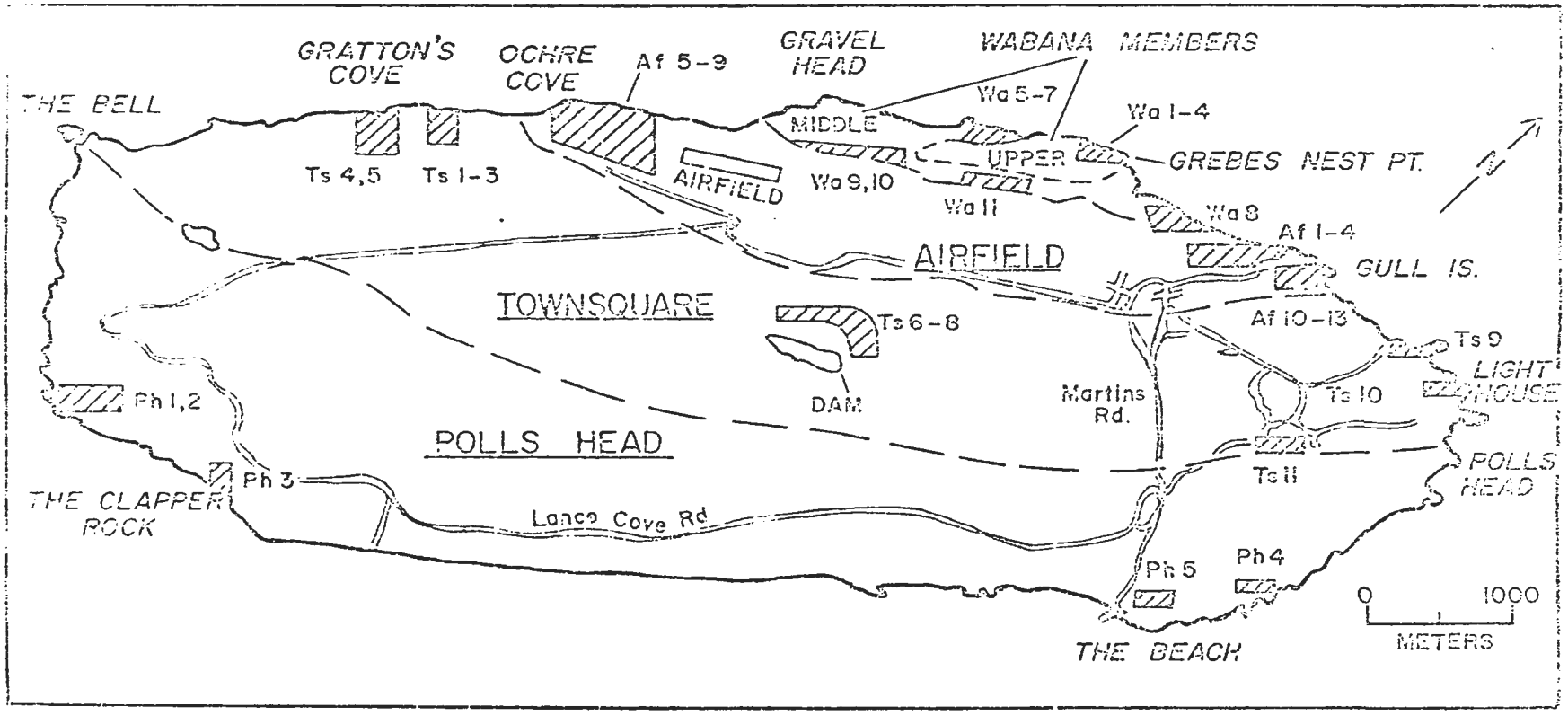

—— —— —— Formation Boundary

– – – – – – – – – Member Boundary

TOWNSQUARE = Formation Name

Wa 9,10 Site, Location & Numbers

grey sandstone and shale were collected by the author and an assistant at 40 sites on Bell Island

To optimize stratigraphic coverage and statistical control, the collection sites were chosen to cover as large a vertical section and area as possible, with an average distance of 6 - 8 m between samples at a site. Stratigraphically, the collection ranged from the lowest exposures of the Polls Head formation on the Beach (SE coast; Fig. 2.5, Site Ph 5) to the Upper bed out-crop of the Wabana formation near Grebes Nest Point (NW coast; Site Wa 1), making a total section of about 450 m (Figs. 2.2, 2.5)

Sites have been numbered according to the following convention: Double letters designating the formation (Wa, Af, Ts, Ph) are followed by numbers which, in ascending order, denote progressively older (i.e. stratigraphically lower) beds; in the case of adjacent sites having stratigraphic overlap, numbers increase from west to east. The stratigraphic and other geologic details of the sites occupied were inferred mainly from Nautiyal (1967).

2.4.2. Sampling procedures

Oriented hand samples were collected from almost all the accessible exposures on Bell Island, though the Laboratory studies to be reported in Chapters 3, 4 and 5 were confined mainly to the Wabana and Airfield samples (Table 2.2). Generally, more than two (but fewer than ten) samples were collected per site to permit adequate within-site comparisons of magnetic properties and detection of any gross orientation errors.

TABLE 2.2

Stratigraphic coverage of paleomagnetic collection

(see Figs. 2.2, 2.3)

Formation (thickness)	Site No.	S[1]	s[2]	Stratigraphic location[3]	Site location, near:
Wabana	1	5	11	Above Zone 5	Grebes Nest Point
(93 m)	2	6	12	Above Zone 5	Grebes Nest Point
	3	5	10	Above Zone 5	Grebes Nest Point
	4	5	10	Above Zone 5	Grebes Nest Point
	5	5	8	Zone 5 (Upper bed)	Gravel Head
	6	3	4	Below Upper bed	Gravel Head
	7	3	8	Below Upper bed	Gravel Head
	8	10	33	Zone 4 (Scotia bed)	Grebes Nest Point
	9	8	17	Below Scotia bed	Gravel Head
	10	6	10	Below Scotia bed	Gravel Head
	11	7	10	Lowest Wabana	Mine House (Surgery)
	Total:	63	133		

[1]S: Oriented samples collected.

[2]s: Specimens used in laboratory studies (3-step procedure).*

[3]Distances in meters denote elevations above base of formation.

*Specimens used in 1-step and 10-step procedures are not included (see Table 4.10.1).

TABLE 2.2, continued

Formation (thickness)	Site No.	S[1]	s[2]	Stratigraphic location[3]	Site location, near:
Airfield (60 m)	1	5	25	Above Dominion bed (Zone 2)	Gull Islands (off North Head)
	2	6	19	Dominion bed	Gull Islands (off North Head)
	3	3	9	Dominion bed	Gull Islands (off North Head)
	4	3	9	Dominion bed	Gull Islands (off North Head)
	5	3	5	Below Dominion bed (Zone 2)	Youngster's Gulch
	6	4	8	Below Dominion bed (Zone 2)	Youngster's Gulch
	7	5	22	Below Dominion bed (Zone 2)	Youngster's Gulch
	8	5	10	Below Dominion bed (Zone 2)	Youngster's Gulch
	9	4	8	Below Dominion bed (Zone 2)	Youngster's Gulch
	10	2	14	Bottom part (Zone 2)	South Head
	11	4	8	Bottom part (Zone 2)	South Head
	12	6	12	Bottom part (Zone 2)	South Head
	13	3	9	Bottom part (Zone 2)	South Head
	Total:	53	158		

[1]S: Oriented samples collected.

[2]s: Specimens used in laboratory studies (3-step procedure).*

[3]Distances in meters denote elevations above base of formation.

*Specimens used in 1-step and 10-step procedures are not included (see Table 4.10.1).

TABLE 2.2, continued

Formation (thickness)	Site No.	S[1]	s[2]	Stratigraphic location[3]	Site location, near:
Townsquare	1	3	—	160 - 180 m	Scott Gulch
(180 m)	2	3	—	160 - 180 m	Scott Gulch
	3	4	—	160 - 180 m	Scott Gulch
	4	6	—	140 - 160 m	Grutton's Cove
	5	9	—	140 - 160 m	Grutton's Cove
	6	3	—	90 m	The Dam
	7	3	—	90 m	V. T. School
	8	4	—	90 m	Mine Road
	9	6	—	60 m	Redman's Head
	10	4	—	Above Zone 1	Lighthouse
	11	6	4	Zone 1	Eastern Head
	Total:	51	4		
Polls Head	1	3	—	Beneath Zone 1	Freshwater Cove
(120 m)	2	2	—	Beneath Zone 1	Freshwater Cove
	3	2	—	Beneath Zone 1	Little Cove
	4	5	—	Beneath Zone 1	Pulpithead
	5	2	—	Bottom part, Polls Head	The Beach
	Total:	14	0		

[1]S: Oriented samples collected.

[2]s: Specimens used in laboratory studies (3-step procedure).*

[3]Distances in meters denote elevations above base of formation.

*Specimens used in 1-step and 10-step procedures are not included (see Table 4.10.1).

The samples were oriented with respect to their in situ attitudes by the standard technique using a Brunton compass and a level. One of the two or more horizontals marked on the sample is a bearing line representing the measured in situ direction relative to true north, allowing for the declination (28^{o}W). Since the presence of excessively magnetic rock, at least within the Airfield and Wabana formations, could not be ruled out, it was possible that the use of the Brunton compass in orienting these rocks might lead to significant bearing errors.

Hence, in the case of 14 out of the 24 Airfield and Wabana sites, a total of 80 samples were also oriented non-magnetically by means of a solar compass. This was a war surplus bomb-sight adapted for orienting, using a design by Larochelle (1964). The comparisons, being based on a representative sampling of the two formations, indicated no significant difference between readings obtained by the two compasses, the maximum difference in any pair of readings being 4^{o}; the arithmetic mean difference for the 80 comparisons was 0.2^{o} with a standard deviation of $\pm 2.5^{o}$.

2.4.3. Orientation errors

In the Laboratory, each sample was set in plaster of Paris in a preferred position related to its field orientation. Cores were drilled with a drill press using a water-cooled, stainless steel diamond drill bit of 2.2 cm inner diameter. One or more cylinders of average height 2.2 cm were cut from each core and will be denoted "specimens".

The estimated orientation error due to setting in plaster and transfer of the orientation marks from sample to core and core to specimen surfaces is $\pm 1^{0}$, each relative to the horizontal plane and relative to north. When comparable field orientation errors are added to this (i.e. $\pm 1^{0}$ due to levelling and $\pm 1^{0}$ compass reading), one obtains a maximum estimated specimen orientation error of $\pm 2 - 3^{0}$. The non-systematic part of this error tended to be reduced when two or more specimens from the same core, or cores from the same sample, were separately oriented. Similarly, the orientation error affecting a site mean direction of magnetization tended to be reduced when two or more samples were averaged at a site, which was always the case (Table 2.2).

CHAPTER 3

REMANENT MAGNETISM OF THE BELL ISLAND FORMATIONS

3.1. Measurement of the natural remanent magnetization (NRM)

The natural remanent magnetization (NRM) of rocks is measured, in general, with either an astatic magnetometer (Blackett, 1952) or a spinner-type magnetometer (Gough, 1967). The spinner, being less sensitive to stray magnetic fields and tending to be faster to operate than an astatic magnetometer, is better suited to the present purpose, which required a large number of measurements, to be carried out in the magnetically noisy environment of the Chemistry-Physics building. Except for some supplementary experiments in which the astatic magnetometer described by Murthy (1966) was used, the magnetization of the specimens was measured with a PAR Model SM-1 spinner magnetometer made by Princeton Applied Research Corporation.

This instrument provides direct and simultaneous measurement of any two orthogonal components of the specimen's remanent magnetic moment in a plane perpendicular to the spin axis. A plastic cup containing the specimen in a preferred orientation is spun at 105 Hz, with the spin axis perpendicular to the common axis of two pick-up coils connected in series. The signal from these coils is amplified and synchronously detected with respect to the signals generated by two photo-choppers mounted orthogonally relative to the specimen cup.

The demodulated detector output represents the magnitude and direction of the magnetic moment vector in the plane perpendicular to the spin axis. In the six-spin procedure adopted here, the measurement is repeated five times, with the cup containing the specimen re-positioned in a different preferred orientation before each spin. In this way any error due to asymmetric centering of the specimen in the cup can be virtually eliminated. An orthogonally mounted set of 1-meter diameter helmholtz coils have been added to the PAR spinner at Memorial University to reduce possible systematic measurement errors arising from the presence of direct laboratory fields.

The manufacturers of the PAR spinner list the minimum detectable magnetization of a specimen as 7×10^{-9} emu/cm^3, for which value they claim accuracies to 1% and $\pm 0.5^{o}$ in magnitude and phase calibration, respectively. In practice many factors contribute to the noise level of the magnetometer, making it difficult even to approach these quoted specifications. However, the great majority of the magnetizations encountered in the present study were in the range $J = 2 \times 10^{-5}$ to 1×10^{-2} emu/cm^3, so that highly reproducible results could be routinely obtained.

An estimate of the measurement error was made from a reproducibility test in which the intensity and direction of magnetization of one specimen each from the Airfield and Wabana formations were obtained from ten consecutive sets of spinner observations. Before each new six-spin set of measurements, the specimen was reoriented in its holder. From the results (Table 3.1), the maximum errors in any quoted value of

TABLE 3.1

Results of 10 consecutive measurements of two specimens with the PAR spinner

	Specimen Af 12-2			Specimen Wa 8-6		
No.	D	I	J x 10^{-5} emu/cm^3	D	I	J x 10^{-5} emu/cm^3
1.	24.6	+14.8	4.80	189.8	-10.4	6.64
2.	23.9	+13.8	4.76	189.6	-10.8	6.64
3.	24.4	+14.4	4.77	189.5	-10.9	6.60
4.	24.8	+14.9	4.82	189.9	-11.0	6.58
5.	24.7	+14.7	4.81	191.0	-11.1	6.62
6.	24.5	+14.5	4.79	190.1	-10.8	6.63
7.	24.8	+14.3	4.77	189.8	-10.6	6.63
8.	23.9	+13.9	4.80	190.4	-11.0	6.65
9.	24.4	+14.4	4.76	188.9	-10.6	6.60
10.	24.5	+14.2	4.81	189.4	-10.6	6.65
Mean	24.5 ±0.3	+14.4 ±0.4	4.79 ±0.02	189.8 ±0.6	-10.8 ±0.2	6.62 ±0.03

± Values quoted are standard deviations.

intensity or direction of magnetization were estimated to be ± ½% and less than 1^0, respectively, for specimens whose intensity falls into the general range of values encountered in this study.

Directions and intensities of magnetization and Fisher (1953) statistics were obtained from the spinner data with the aid of an IBM 360-40 Computer and a Hewlett-Packard Model 9100-A Desk Calculator.

3.2. Results of the NRM measurements

In this investigation, only the red sandstones were studied, as the grey ones (Fig. 2.2) did not appear to possess a significant remanence. The NRM of two specimens from each sample was measured relative to the *in situ* position of the rock, and a sample mean direction was obtained as the resultant of the two specimen directions, giving each unit weight (Table A1.1). The site mean direction is similarly the resultant of the sample mean directions, giving each unit weight. The sample and site mean intensities of magnetization (J) were taken as the arithmetic mean values of the specimen and sample intensities respectively. Values of J (in emu/cm^3) were in the ranges 3.5 to 10×10^{-5} for the Wabana formation, 3.7 to 7.3×10^{-5} for the Airfield formation and 2.4 to 3.2×10^{-5} for the single site of the Townsquare formation.

The sample mean directions of magnetization are plotted in Figs. 3.1 - 3.4. The NRM magnetization directions in specimens from the same sample and in different samples at a site generally agree well, as shown also by the fact that the values of Fisher's (1953) precision

Fig. 3.1 Equal-area plot of sample mean directions of magnetization at different sites, for NRM and after 600 and 685°C stepwise demagnetization (Wabana, sites 1-6)

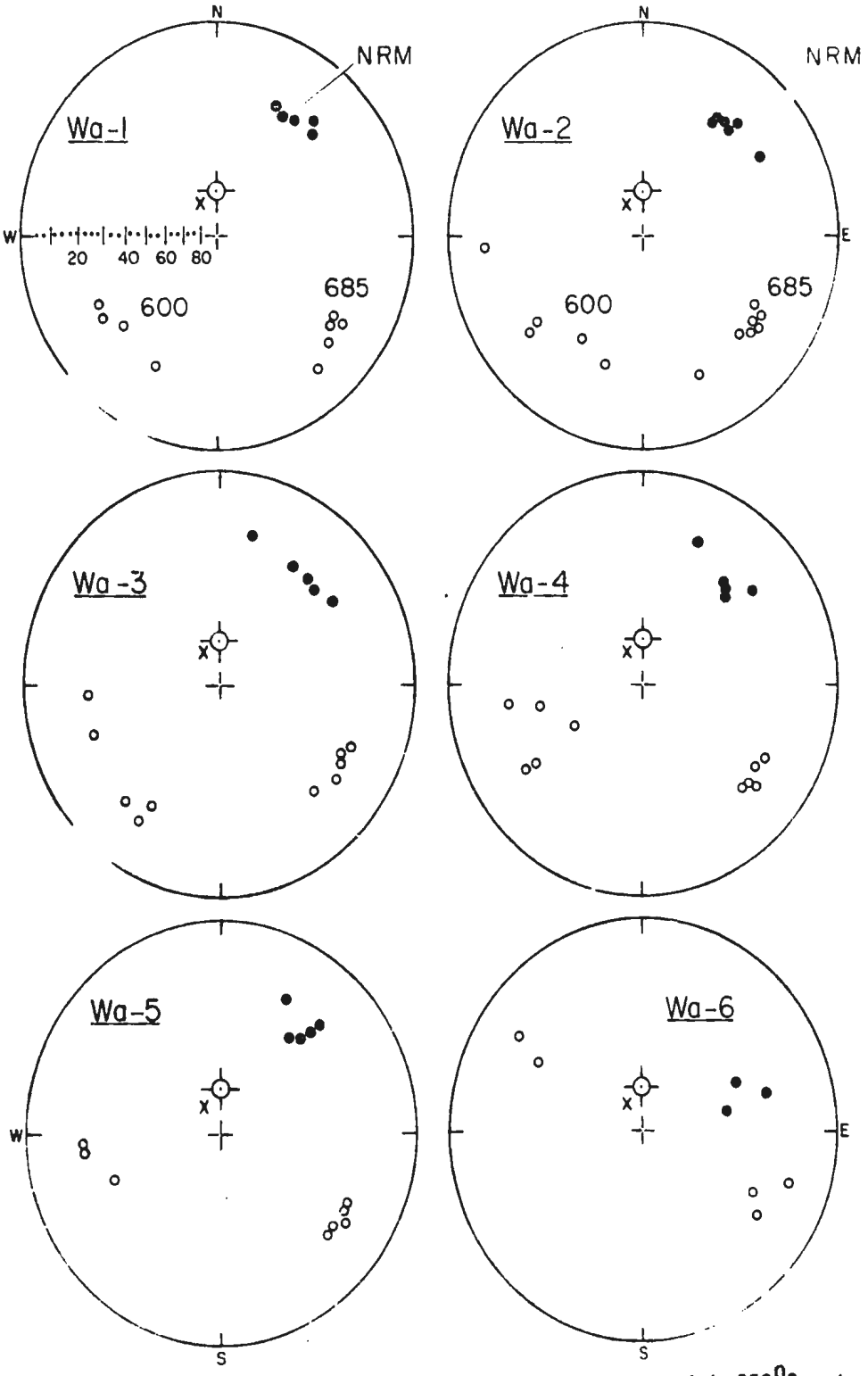

Two specimens averaged per sample based on 3-step procedure, with 350°C not shown; steps are not always denoted (NRM, 600, 685).

North pole: ● down, ○ up, ⊕ axial dipole field, X 1968 field.

Fig. 3.2 Sample mean directions of magnetization, for Wabana sites 7-11
(See caption in Fig. 3.1)

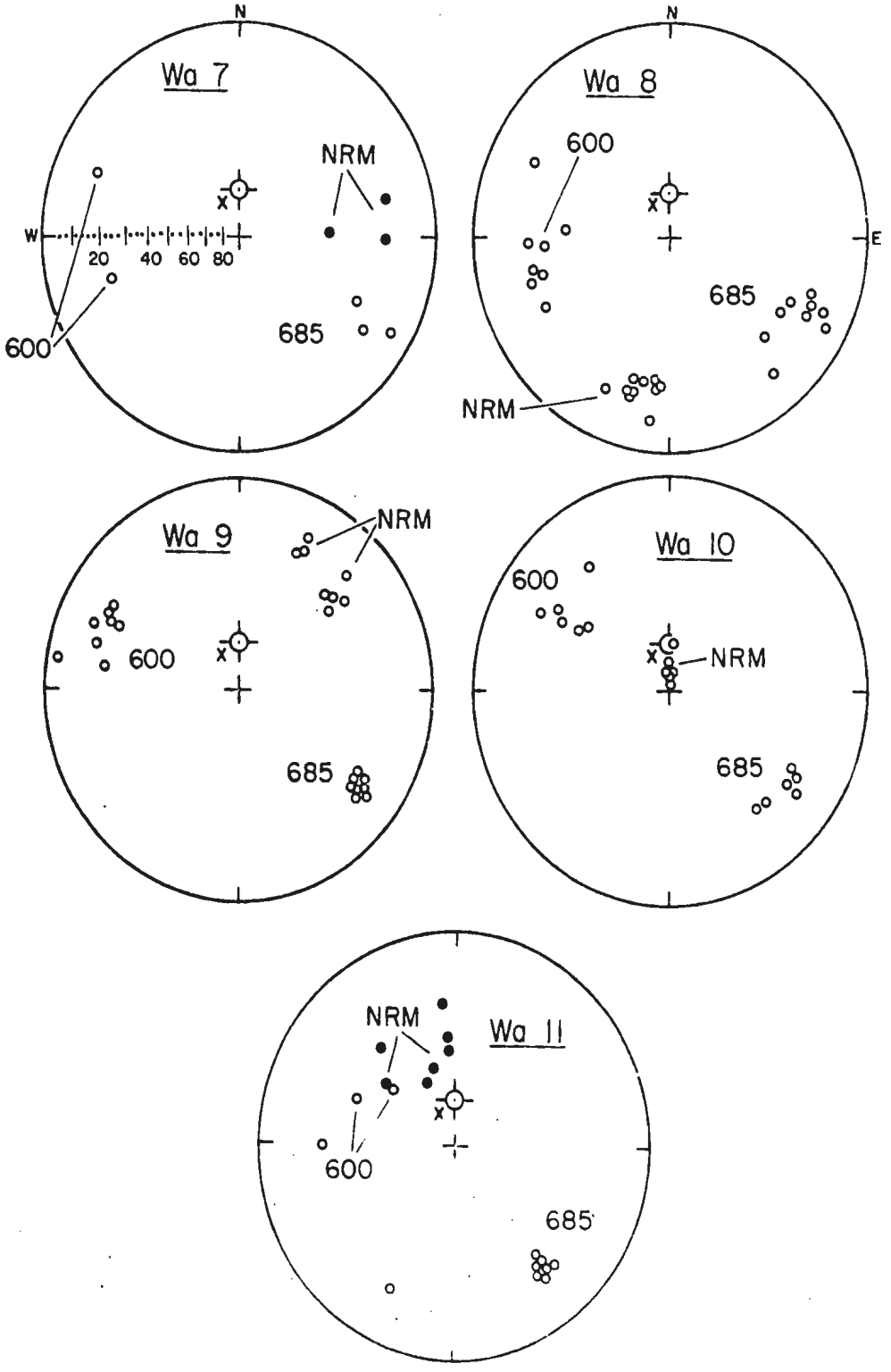

Fig. 3.3 Sample mean directions of magnetization, for Airfield sites 1-6

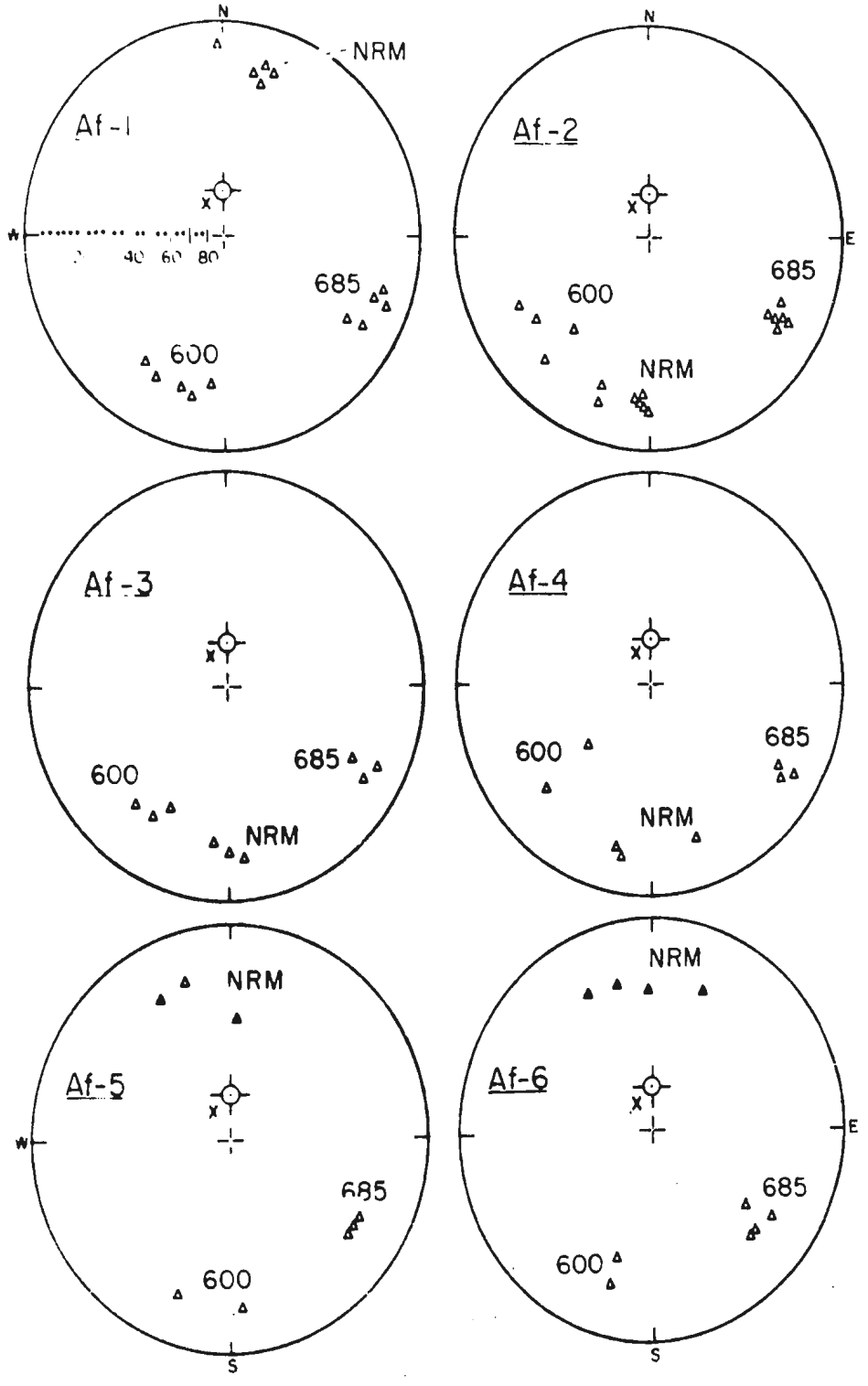

North pole: ▲ down, △ up. Remaining symbols as in Fig. 3.1.

Fig. 3.4 Sample mean directions of magnetization, for Airfield sites 7-13 and Townsquare site 11

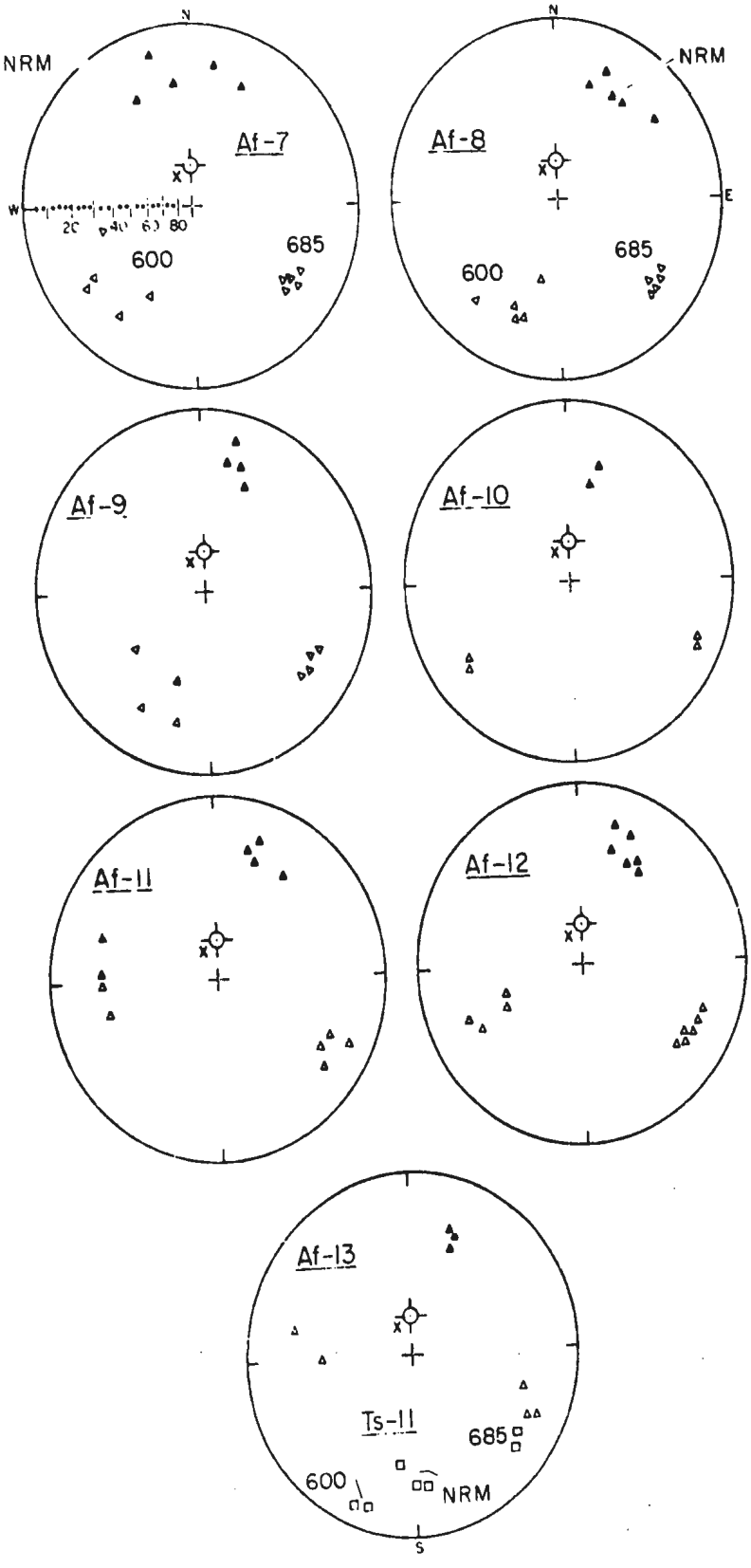

Townsquare: North pole up. Other symbols as in Figs. 3.1 and 3.3.

parameter, k, associated with the NRM site mean statistics tend to be large (Tables 3.2 and 3.3); in fifteen cases where a large number of specimens from the same sample were measured, the sample mean directions also had fairly large k values, reflecting good specimen vector grouping; four examples are given in Table 3.4.

The NRM directions for both the Airfield and Wabana formations fall into a "northerly" and a "southerly" group; the two groups will be called "A" and "B", respectively (Tables 3.2 and 3.3). The group A inclinations range from I = - 12^{0} to + 30^{0} for the Airfield formation and I = - 80^{0} to + 40^{0} for the Wabana formation, where the steep negative inclinations (- 80^{0}) in the latter case are due to the samples from a single site (Wa 10) only; these directions are intermediate between groups A and B, but they were included in group A, as demagnetization to 300^{0}C (Section 3.4.1.4) moved the remanence vectors close to directions for other group A sites. The group A site mean directions show a fairly wide range from NE to NW, the Wabana declinations tending to be more easterly than the Airfield declinations. For both formations the "within-site" scatter (i.e. the directional scatter between samples for the same site) in general is significantly less than the "between-site" scatter (comparing sites of the same formation) (Chapter 4). The group B NRM directions are close to southward (D = 180^{0} to 192^{0}), with low upward inclinations (I = - 15^{0} to - 20^{0}) and are found in the samples from three of the 13 Airfield sites, from one of the 11 Wabana sites and from the single Townsquare site, with excellent grouping of the five site mean directions (Tables 3.5 and A1.1).

TABLE 3.2

Site mean directions of natural remanent magnetization (NRM)

Wabana formation

Group	Site No.	N	D	I	J x 10^{-5}	R	k	α_{95}
A	1	5	37.1	+21.5	5.0	4.963	110	7.4
	2	6	42.6	+21.8	4.4	5.949	98	6.8
	3	5	38.5	+21.7	4.6	4.866	30	14.2
	4	5	41.1	+23.5	4.4	4.921	51	10.8
	5	5	39.9	+22.9	3.9	4.964	110	7.3
	6	3	71.2	+33.4	4.4	2.963	54	16.9
	7	3	84.1	+25.4	4.2	2.926	27	24.2
	9	8	41.1	-21.9	7.0	7.849	47	8.2
	10	6	1.9	-78.6	7.6	5.958	120	6.2
	11	7	339.6	+40.1	5.2	6.720	22	13.3
B	8	10	191.9	-19.5	8.0	9.933	130	4.2

N = Number of samples per each site.

D = Mean declination (deg) of remanent magnetization.

I = Mean inclination (deg), north pole positive, downward.

J = Mean intensity of magnetization (emu/cm^3).

R = Resultant of N unit vectors.

k = Estimate of Fisher's precision parameter (Fisher, 1953). 3-digit values are rounded off in the second digit.

α_{95} = Radius (deg) of 95% confidence circle.

TABLE 3.3

Site mean directions of natural remanent magnetization (NRM)

Airfield formation

Group	Site No.	N	D	I	J x 10^{-5}	R	k	α_{95}
A	1	5	10.5	-12.4	6.4	4.959	97	7.8
	5	3	344.1	+21.7	4.5	2.913	23	26.3
	6	4	354.6	+21.9	4.8	3.833	18	22.3
	7	5	356.9	+19.0	4.5	4.736	15	20.3
	8	5	33.3	+20.5	4.9	4.895	38	12.6
	9	4	18.4	+18.8	5.2	3.968	94	9.5
	10	2	16.5	+28.0	4.7	—	—	—
	11	4	22.6	+19.0	4.8	3.959	74	10.8
	12	6	25.5	+21.5	4.9	5.938	81	7.5
	13	3	21.2	+21.0	4.7	2.996	460	5.7
B	2	6	183.0	-15.3	6.5	5.992	650	2.6
	3	3	180.0	-15.4	5.9	2.987	150	10.0
	4	3	181.7	-14.9	6.7	2.917	24	25.7

Symbols as in Table 3.2.

TABLE 3.4

Within-sample directions of NRM

(Four representative examples)[1]

	Sample Af 10-1			Sample Af 12-7		
Specimen No.	D	I	J x 10^{-5}	D	I	J x 10^{-5}
1	14.2	+27.6	4.6	25.3	+23.2	4.1
2	14.8	+28.9	4.6	26.2	+21.4	4.4
3	14.8	+29.8	4.7	21.4	+20.3	4.2
4	14.3	+28.1	4.7	25.8	+20.3	4.1
5	15.6	+29.2	4.6	24.3	+21.4	4.1
6	16.1	+28.1	4.6	23.6	+20.1	4.2
7	12.3	+24.3	4.7	22.4	+19.6	4.0
8	15.6	+21.2	4.8	21.3	+21.8	4.2
Mean	14.7	+27.2	4.7	23.8	+21.0	4.1
R		7.9897			7.9951	
k		680			1400	
α_{95}		2.1			1.5	

[1]Symbols are as in Table 3.2.

TABLE 3.4, continued

Specimen No.	Sample Wa 8-6 D	I	J x 10^{-5}	Sample Wa 9-1 D	I	J x 10^{-5}
1	191.8	-10.2	6.6	48.0	-18.2	10.4
2	192.6	-21.8	6.8	49.0	-13.3	9.6
3	190.2	-18.6	7.1	46.2	-21.8	8.8
4	183.2	-21.4	6.6	48.8	-21.2	9.2
5	200.1	-18.3	6.4	50.2	-18.3	9.1
6	192.3	-19.4	6.8	52.6	-16.8	9.2
7	183.8	-21.8	6.5	51.4	-17.1	8.2
8	191.4	-22.6	6.6	49.7	-19.6	9.0
Mean	190.7	-19.3	6.7	49.5	-18.3	9.2
R		7.9560			7.9885	
k		160			600	
α_{95}		4.4			2.3	

TABLE 3.5

Group and formation mean directions of natural remanent magnetization (NRM)

Airfield and Wabana formations

Group	Formation	N	D	I	J x 10^{-5}	R	k	α_{95}
A	Airfield	10	12.5	+18.6	4.9	9.544	20	11.1
	Wabana	10	42.1	+16.2	5.1	7.761	4	27.6
	[1]Airfield and Wabana	20	25.8	+18.1	5.0			
B	Airfield	3	181.6	-15.2	6.4	2.9993	3000	2.2
	Wabana	1	191.9	-19.5	8.0	—	—	—
	Airfield and Wabana	4	184.1	-16.3	7.0	3.986	220	6.3

N = Number of sites in each formation.

Other symbols as in Table 3.4.

3-digit and 4-digit values of k are rounded off in the second digit.

[1]The group A mean direction is based on a smeared distribution of site mean vectors, and Fisher statistics are not quoted.

At 24 of the 25 sites, the NRM directions are notably misaligned with both the present axial dipole field direction and with the 1968 field direction at Bell Island (Fig. 3.5). At the remaining site (Wa 10), while the directions are nearly aligned with the dipole and 1968 fields, the polarity is negative. These results indicate at least partial stability of the natural remanent magnetization.

3.3. Primary and secondary components

The NRM of sedimentary rocks usually consists of two or more components, including a "primary" one which is of major importance. Conclusions from paleomagnetic studies require the assumption that the magnetization component of interest - usually the primary component - was acquired in the direction of the earth's field at the (known) time of formation of the rock, and is either revealed in the NRM or can be isolated by suitable latoratory tests. However, processes resulting in the possible complete destruction of a primary component have been described (Krs, 1967; Storetvedt, 1968). Secondary magnetizations may be aligned during the post-depositional history of the rock in several possible ways.

Viscous magnetizations (VRM) may be associated with a wide range of time constants including "soft" (low-coercivity) components acquired late in geologic history, sometimes even in the laboratory. Such VRM's generally can be removed with relative care by alternating-field or thermal demagnetization techniques in the laboratory. Secondary

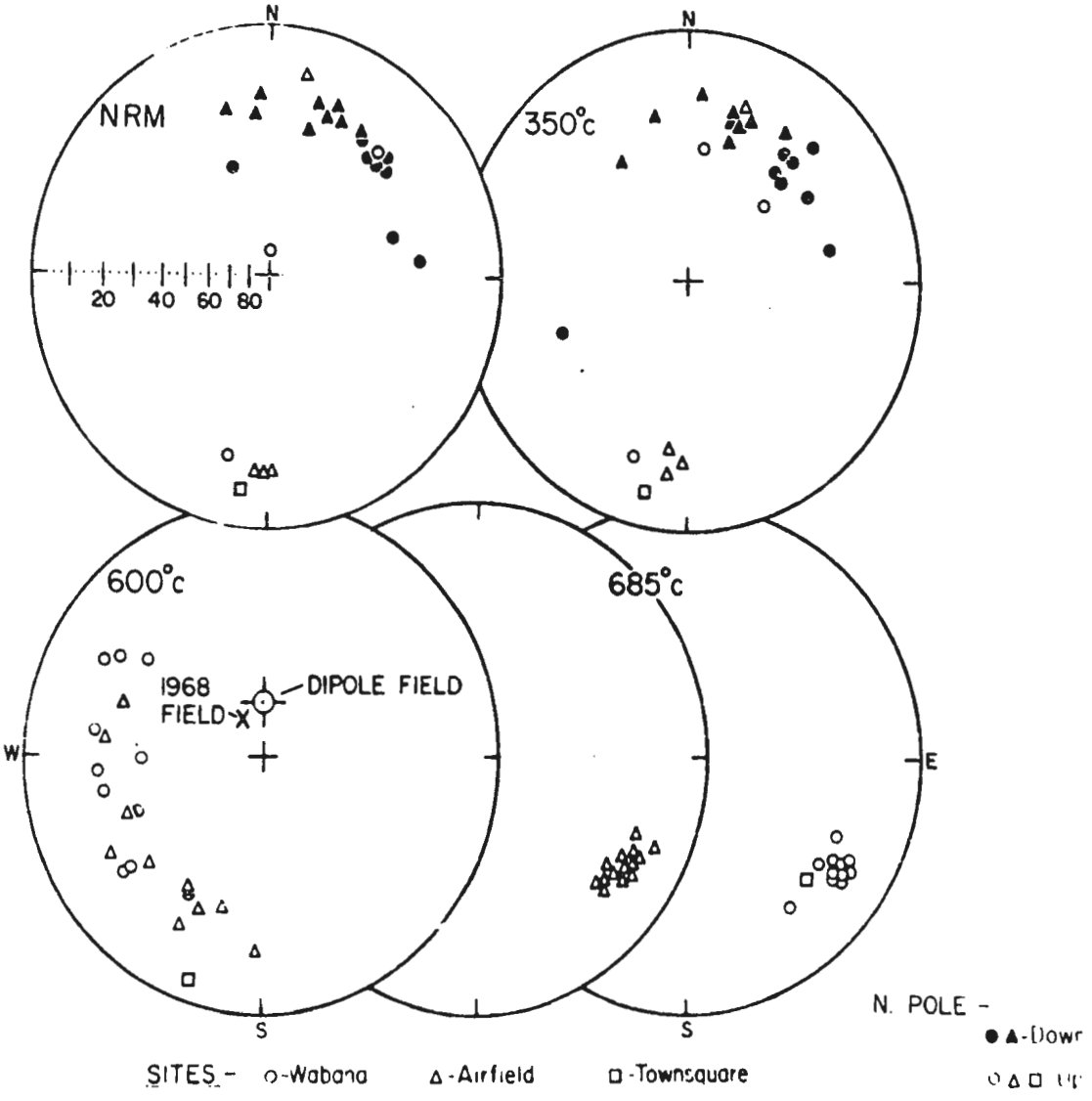

Fig. 3.5 Site-mean directions of magnetization for Wabana, Airfield and Townsquare formations; NRM and after 350, 600 and 685°C demagnetization

magnetizations of chemical origin and some viscous magnetizations (e.g. viscous build-up at moderate temperatures (Briden, 1965; Krs, 1967; Storetvedt, 1968) may be of comparable or greater hardness than the primary component.

3.3.1. Field tests

Two powerful field tests (the "fold test" and the "conglomerate" test (Graham, 1949; Strangway, 1967)) which, however, are only applicable under certain geological conditions, may be used to set a minimum age to the origin of the observed magnetization. In the fold test, one compares the grouping of magnetization directions (either NRM or isolated by laboratory "cleaning") for samples from different parts of a folded structure: if the grouping improves significantly after "unfolding" the structure, the magnetization may be said to have been acquired prior to folding. However, where field tests are inapplicable, the laboratory procedures, used for the determination of stability in general, may also result in the isolation and/or detection of the primary component itself. This was necessary in the case of Bell Island where the entire redbed sequence is uniformly flat-lying and where suitable conglomerate beds are absent.

3.3.2. Demagnetization of red sediments

Creer (1957) and Collinson and Runcorn (1960) showed that the observations on red sandstones fall into the broad groups: (1) with the

directions of magnetization symmetrically distributed about their mean allowing direct application of statistical methods (Fisher, 1953) and (2) with the directions of magnetization scattered along a great circle [called by Khramov (1958) the 'circle of remagnetization'] through the direction of the axial dipole field. These results have been verified by several workers (Irving, 1964). The simplest hypothesis to explain them (Collinson and Runcorn, 1960) is to suppose that the directions of group 1 (assuming that they depart significantly from a recent geomagnetic field direction) have been unaffected by the changing field since their original magnetization; hence they may be termed 'stable'. On the other hand, in group 2 the magnetizations appear to be the vector resultants of an original, stable component and one or more less stable components that were acquired (probably as VRM's) in subsequent geological times; such rocks are therefore termed 'partially stable'. However, the secondary magnetization causing the planar distribution in group 2 must also be comparatively stable (Irving et al., 1961), since the superposition of low-coercivity components upon a stable group 1 type magnetization would give rise to a close vector grouping rather than a planar distribution.

In the laboratory, samples from red sediments are generally subjected to demagnetization treatment by alternating magnetic fields (AF demagnetization) or heating. Although the first method applied to red sediments has been shown to be useful for removing unstable VRM imposed by a recent field (Creer, 1959) and for reducing dispersion (Black, 1963; Gough and Opdyke, 1963), the maximum field strengths

available in most paleomagnetic laboratories (∿ 1000 oersteds) are too weak to affect the high stability components (Opdyke, 1961). The reason is that in redbeds these commonly reside in hematite, which is characterized by coercivities of the order of 10^4 oersteds (Roquet, 1954). Therefore thermal demagnetization is often the only known method permitting an analysis of the full range of the stability spectrum, and it is used extensively (Collinson, 1965; Storetvedt et al., 1967).

Schwarz (1969) lists three main types of NRM decay curves resulting from thermal demagnetization of redbed samples: (1) the total NRM is lost in a small temperature interval just below the curie point, (2) the NRM decays more or less continuously between approximately 300° and 700°C and (3) the NRM increases up to a certain temperature and decays during further heating. Examples of such curves and of hybrid curves are given by Irving and Opdyke (1965) and others (Fig. 3.6).

A type-1 curve would be expected in the case of a stable, single component NRM. The cause for occurrence of type-2 is not clear, but Irving and Opdyke (1965) have suggested that these curves may be associated with distributed blocking temperatures of domain walls which implies a wide range in grain size of chemically homogeneous NRM carriers. Several other factors may be operative, such as (a) heterogeneity in chemical composition of NRM carriers resulting in a series of curie points or (b) the occurrence, during treatment, of chemical reactions involving the NRM carriers. Type-3 curves appear to be the resultant of preferential demagnetization of NRM components of roughly opposed direction and different thermal stability in a sample as

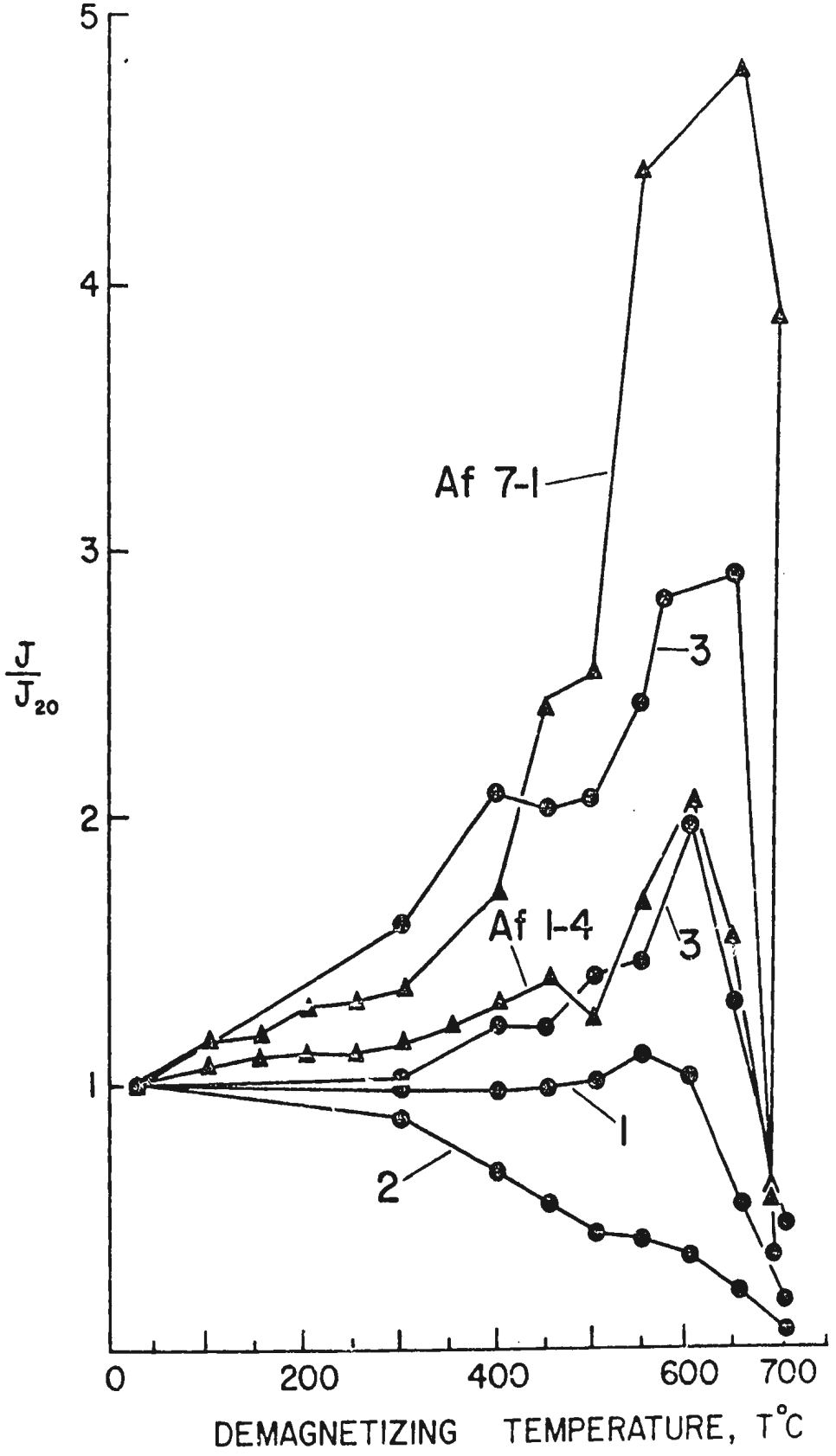

Fig. 3.6 Normalized intensity, J/J_{20}, of single specimens

Numbers refer to type curves; see Section 3.3.2.

suggested in the case of Silurian Bloomsburg redbeds (Irving and Opdyke, 1965) and Maringouin formation (Roy and Robertson, 1968). An alternative or contributing cause of type-3 curves may be the formation of a new ferromagnetic component during heat treatment, as observed in the present study (Chapter 5).

3.3.3. Stepwise thermal demagnetization

Thermal demagnetization may be thought of as the converse of the acquisition of thermoremanent magnetization (TRM), the procedure of which is based upon the addition law of partial TRM (PTRM) (Nagata, 1961). For example, above the curie temperature T_c of a cooling lava, the thermal energy exceeds the magnetic energy and the material is paramagnetic. As the temperature falls through T_c the material acquires an equilibrium magnetization which moves freely into the direction of an applied field. At a certain temperature called the blocking temperature, T_b, the magnetization is blocked and can resist changes in fields applied on a short time scale (Néel, 1955). The magnetization produced in the case of CRM exhibits a behaviour upon demagnetization similar to that of total TRM (Kobayashi, 1959), the only difference being that TRM or PTRM is acquired by grains of constant volume cooling from a high temperature, whereas CRM may be acquired at relatively constant atmospheric temperatures through a process involving a volume increase (Haigh, 1958). In stepwise thermal demagnetization, as the temperature rises above T_b for a given component, the domain orientations of that component will tend to be randomized and, in the absence of an external field, a laboratory PTRM

is not acquired upon cooling; hence components with successively higher blocking temperatures are progressively eliminated.

Thermal demagnetization methods were introduced by Thellier (1938) and have since been developed further (Leng, 1955; Doell, 1956; Irving et al., 1961; Wilson and Everitt, 1963; Chamalaun and Creer, 1964). Their main advantage over the steady and alternating-field treatments is that two or more hard components having different Curie points may be separated.

3.3.4. Thermal demagnetization unit

The unit used in the present investigation for progressive thermal demagnetization of rocks was mostly constructed at Memorial University, where it is located in a favourably situated laboratory within the otherwise magnetically noisy Chemistry-Physics building. The location was chosen for optimum uniformity of the permanent magnetic background field and was relatively remote from a.c and d.c sources and movable ferromagnetic objects (Deutsch and Somayajulu, 1970). The unit is described by Somayajulu (1969), and closely follows the design by Irving et al. (1961), the principal changes being (i) the reduction in the oven size (diameter of the cylindrical heating system is 13.0 cm in the present unit) and (ii) addition of a flux-gate monitoring assembly as an aid in controlling the field nulling.

Prior to this investigation, the helmholtz coils used by Somayajulu (1969) were replaced by square parry coils of twice the linear dimensions of the former (sides 1.7 to 1.9 m), similar to

Irving et al. (1961), thus increasing by nearly an order of magnitude the working space within which the field gradients are smaller than some specified maximum. Moreover, the nichrome wire, which was ferromagnetic below 300°C, was replaced with relatively non-magnetic chromel-A wiring, which eliminated the awkward "empty run" procedure used previously to reduce stray fields. The base plate at the bottom of the oven was wrapped in asbestos sheeting and no significant traces of ferromagnetic impregnations were found in this or in any other material used in the unit.

The three orthogonal parry coils are powered by two d.c power supplies (Power Designs, Inc.) and regulated by a resistor unit for fine control of field-nulling. Three identical, orthogonally oriented fluxgate detectors were installed outside the oven, though still within the region enclosed by the parry coils. This was to monitor residual magnetic fields at the oven center where the detectors could not be placed during heating experiments.

With the aid of a direct-reading Schonstedt Model HSM-1 station magnetometer, capable of measuring fields to 1 gamma ($1\gamma = 10^{-5}$ oersted), each external detector was located in a position at which the field was approximately equal to the corresponding field component at the oven center. The output of each detector is connected to an oscilloscope through an amplifier, while the input for exciting the primary winding at 400 Hz is obtained from a signal generator. In the absence of an external magnetic field, the output contains instrumental noise in the form of harmonics, totalling about 50γ. If

during experiments the field in the working space departs from zero, this field, combined with the above harmonics, results in an unsymmetrical wave form on the oscilloscope screen. Zero field is restored manually for any parry coil component, and is checked with the aid of a symmetry test; i.e. one assumes that the fundamental mode is zero when in the composite harmonics pattern corresponding amplitudes above and below the field axis are equal. The error in judging this symmetry by direct observation was estimated to be 5γ or less for any component, or $< 10\gamma$ for the total field error, on the most sensitive scale; let this error be e_1 (Section 3.3.4.1). The estimated total field error in comparing the centrally mounted and external probes, when the fields independently compared with the Schonstedt probe were equal, was approximately the same as the symmetry error, e_1.

The magnetic field in the oven working space, a cylindrical region of 11.5 cm diameter and 9.5 cm height was surveyed in 1969, prior to the start of the demagnetization program, and checked in 1970; at both times, magnetic disturbances were minimal. The Schonstedt magnetometer probe was oriented successively parallel to each parry coil axis and moved so as to scan the field in a horizontal plane for each orientation. This was done at three levels corresponding to the mean heights of specimens placed at the three shelves of the specimen stand. During the majority of experiments, eight specimens at a time were placed on the stand, four at the central shelf and two each at the top and bottom shelves. On any shelf, the specimen centers were displaced 3.5 cm from the central vertical axis of the oven, with a minimum separation of 1.2 cm between any two specimen surfaces; such a separation

was judged to be quite sufficient to avoid possible magnetic interactions between specimens (see intensity figures, section 3.1). From the results of the survey it was estimated that for zero field at the oven center the total field acting at the center of any specimen was within 10-15γ (the oven gradient error, e_2).

3.3.4.1. Field-nulling errors

Before each demagnetization run the three components of the field at the oven center were adjusted with the aid of the Schonstedt magnetometer (step 3 in section 3.3.5). While the reading error of the instrument was only 1γ, the estimated nulling error, e_3, in the total field (incorporating reading error) was within 4γ, most of this being due to limitations in adjusting the nulling current, and possibly some drift of the current. When repeating the field-nulling measurements after the run (step 11) the total field was within 10-15γ in the great majority of experiments, though in a few cases fields of 20-25γ were found. In all runs this may be within about one hour of the last field-nulling adjustment with the external probes, though the maximum time covered between steps 3 and 11 (for runs where specimens were heated to 600^{o}C or above) is about 3½ hours.

The experiments were conducted only at magnetically quiet times, i.e. in the absence of geomagnetic disturbances (such as magnetic storms, etc.) and mostly at night time, on weekends and on holidays. Therefore the observed departures from field-nulling at the end of heating experiments may be attributed to either diurnal variations, or

drift of the nulling currents, or both. The diurnal variation of the laboratory field was recorded in three components for 24 hours under magnetically quiet conditions using the Schonstedt probe and a strip recorder.

The total field variations obtained in this way were always < 10γ/hr and typically < 7γ/hr. By comparison, the combined adjustment and symmetry error in using the external fluxgate probes, $e_4 = e_1 + e_3$, is typically within 10-15γ. Thus both the diurnal variation and the adjustment-symmetry errors could account for the observed departures from zero field at the oven center during step 11.

From the above considerations it was concluded that the magnitude of the total field-nulling error at the specimen sites during demagnetization runs is the sum of e_4 and the oven gradient error, e_2, due to the off-center position of the specimens; in the great majority of cases, these errors are 10-15γ each, and the combined field-nulling error, $e_5 = e_2 + e_4$, was taken to be 25γ or less. In exceptional cases, e_5 may have been as large as 35γ.

An imperfectly nulled total field as high as 25γ would only represent 0.1% of the uncancelled laboratory field and was unlikely to be sufficient to impose a partial thermoremanent component upon specimens cooling even from high temperatures. However, to minimize in a statistical sense the effect, if any, of such stray fields upon the resultant specimen remanence directions, the standard practice (e.g. Irving et al., 1961) was adopted, in which the previously determined remanence vectors were always oriented in the oven as nearly randomly

as possible prior to any demagnetization run. Thus generally half the specimens (4) were in rolling positions, and the other half upright or upside down, with two remanence vectors each pointing north, east, south and west, and with an approximately uniform distribution of inclinations ranging from steep upward to steep downward.

As a final precaution the specimens when not being treated or measured were always stored in magnetically shielded cans, in which the field is < 10γ (Somayajulu, 1969).

3.3.4.2. Control and measurement of temperature

The oven temperature was measured at a point close to the centre of parry coils, using platinum-platinum/10% Rhodium thermocouples calibrated at the National Research Council, Ottawa; the hot junction is inserted through the base of the specimen stand. A direct-reading Leeds and Northrup potentiometer used with the thermocouple was calibrated to correlate ^{o}F scale readings with true centigrade values corresponding to the NRC standardization.

The heating current is obtained from the 220-volt mains through a variac and is continuously controlled at the desired temperature through manual adjustment. This could be done within ± 5^{o}C at 350^{o}C and within ± 3^{o}C at 600^{o}C and higher temperatures, during the time intervals when the temperature is maintained constant; this was always at least 15 minutes (Step 8; section 3.3.5).

Thermal gradients were measured by Somayajulu (1969) with a movable platinum-platinum/10% Rhodium thermocouple at various fixed mean

temperatures in the central part of the oven normally occupied by the specimen stand. From his results it was estimated that at 350°C the excess temperature, ΔT, at a distance of 3.5 cm from the central oven axis (where all specimens were placed in the present investigation) is within +5°C whereas at 600°C and higher temperatures ΔT is within +2°C. The temperature gradients remain small up to distances greater than 4 cm from the oven axis where they rise appreciably. Similar gradients were found in a further test by the present author, who concluded that for the actually adopted specimen positioning (i.e. 3.5 cm from the oven axis) the excess temperature, while constituting a systematic rather than random error, was less than the magnitude of the combined measurement/control error at all temperature levels. For this reason, all temperature values quoted here refer to the oven center. The maximum departures of the actual specimen temperature from this value were estimated to be of magnitude 5°C and 10°C in the ranges > 550°C and 300° - 550°C, respectively.

As a precaution during these measurements and also during actual demagnetization runs, the specimen stand region is enclosed by an inverted copper pot acting as a secondary radiator of heat (Step 6, section 3.3.5); without this arrangement the thermal gradients in the working space would have been much larger than the actually observed values. In future work with this unit, it is planned to improve the temperature control, particularly in the critical high-temperature ranges, by replacing manual adjustment of the heating current by a thermostat.

3.3.5. Procedure of thermal demagnetization

(1) The remanent magnetization directions and intensities of the specimens are measured with the spinner magnetometer.

(2) About 30 minutes before starting the experiment the d.c power supplies for field compensation and the electronic units for field monitoring are switched on to ensure stabilizing.

(3) The Schonstedt station magnetometer probe is kept inside the oven, and the field of each pair of parry coils in turn is adjusted to zero value with the estimated error ($e < 4\gamma$) discussed in section 3.3.4.1. For each component the procedure is repeated with the probe in the reversed (180^0) position. At the end the probe is moved freely in all directions until the estimated total field near the oven center is $e < 4\gamma$. The external fluxgate units are checked for symmetry, corresponding to zero parry coil fields.

(4) The specimens are arranged on the three shelves in the specimen stand, in random positions, with 1.2 cm minimum separation between their surfaces (Section 3.3.4.1).

(5) The thermocouple cold junction is placed in ice at 0^0C and the temperature potentiometer is balanced.

(6) The specimens are covered with the inverted copper pot to reduce temperature gradients.

(7) The oven is closed and the variac is switched on with the voltage set to the desired temperature.

(8) When the desired temperature has been approximately reached it, is measured, adjusted if necessary, during which time the field is

regularly monitored, and maintained constant for at least 15 minutes.

(9) The heating current is switched off and the oven is quickly raised to the highest position (unless nitrogen is used, in which case it remains closed). The three field components are carefully monitored with the external fluxgate probes throughout the cooling period, and any necessary adjustments in the parry coil currents are made.

(10) When the specimens have cooled to the laboratory temperature, they are quickly transferred into a can containing three concentric layers of magnetic shielding, inside which the magnetic field is $< 10\gamma$, i.e. several orders less than the surrounding laboratory field. This greatly reduces the risk that the specimens may acquire a significant VRM in the laboratory between the time of treatment and measurement.

(11) The magnetic field at the oven center is remeasured with the Schonstedt probe, 30 - 45 minutes after step 10.

3.4. Pilot thermal demagnetization in air

A detailed initial demagnetization of a few representative specimens only is generally the most efficient procedure for determining optimum demagnetization temperatures; this eliminates the need for intermediate steps in subsequent systematic treatments that may involve all samples. Such a "pilot" study was carried out with 28 red sandstone specimens selected from 22 sites of the Wabana (9 sites, 12 specimens), Airfield (12 sites, 14 specimens) and Townsquare (1 site, 2 specimens) formations (Fig. 2.2) using the "vector rotation" criterion (Irving, 1964) to determine optimum temperatures. Results are shown in Figs. 3.7

to 3.10 and Tables 3.6 to 3.8 are discussed below for five representative specimens taken in a stratigraphically descending order.

3.4.1.1. Specimen Wa 4-3

This specimen is from one of the uppermost exposures on Bell Island (Fig. 2.2). Heat treatment to 300°C (five steps) caused little change in the NRM vector, which had NE declination and shallow, downward inclination (D = 46°, I = +17°), typical of "group A" (Section 3.2). Above 300°C, the remanence directions changed progressively, the declination being NW at 350°C, then W (400°C) and SW (600°C); the intensity of magnetization (J) gradually increased, reaching a maximum (J = 6.1 emu/cm^3) near 600°C, with J_{600}/J_{20} = 1.7, where J_{600} and J_{20} correspond to 600°C and atmospheric temperature (NRM), respectively. An intermediate (southerly) direction at 640°C lies approximately on a great circle between the directions at 600°C and 685°C (D = 126°, I = -17°), at the latter temperature, which is close to the Curie point of hematite, the intensity had dropped again (J_{685}/J_{20} = 0.6).

3.4.1.2. Specimen Wa 10-6

The NRM direction, contrary to that of specimen Wa 4-3 (above), is nearly aligned with the axial dipole field (D = 0°, I = +65.5°) and the 1968 field (D = 332°, I = +71°), though of opposite (negative) polarity. This site (No. 10; Table 3.6) was the only one at Bell Island at which steep NRM inclinations were found; this was also confirmed by preliminary measurements with the astatic magnetometer (Murthy, 1966)

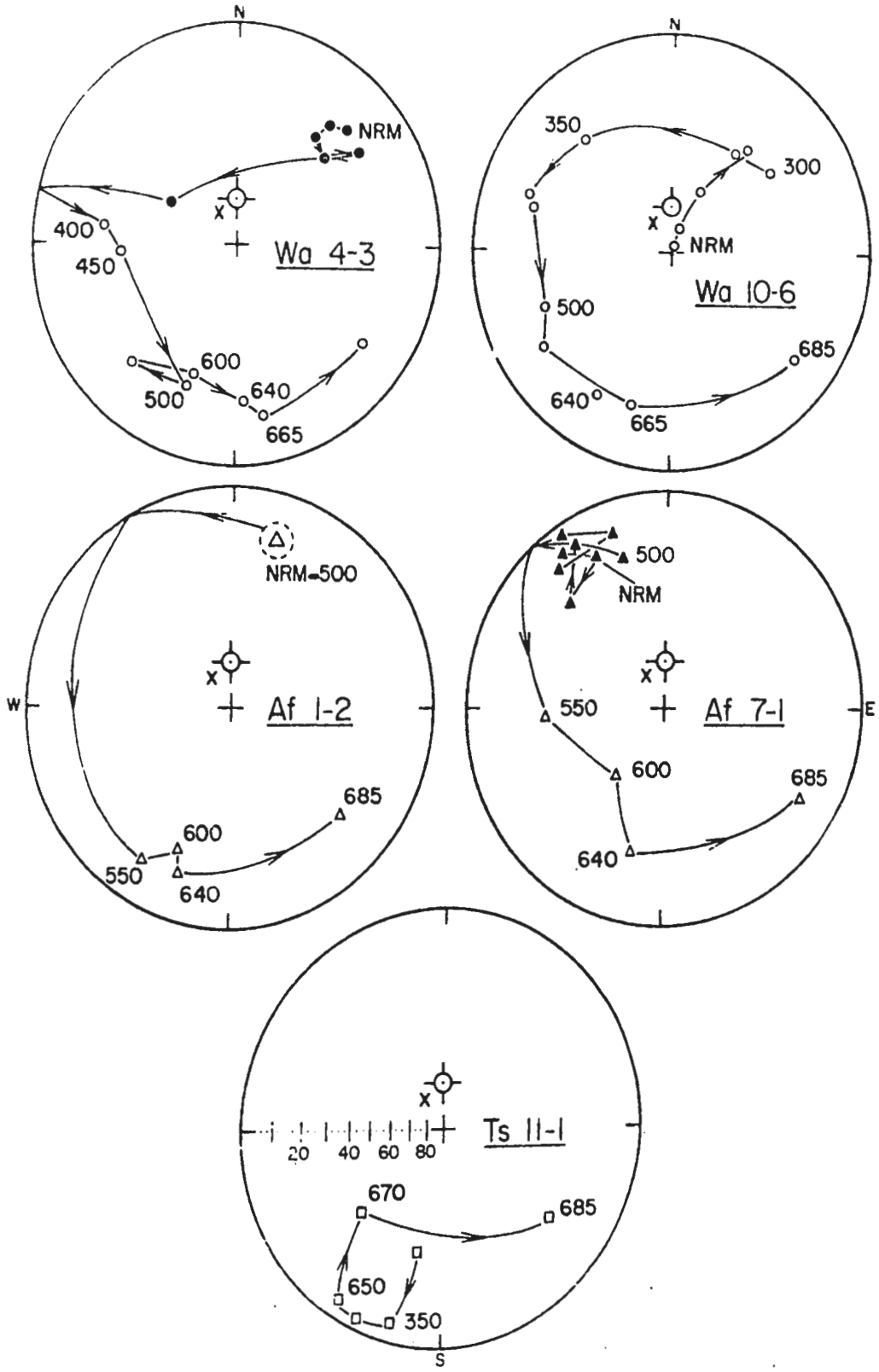

Fig. 3.7 Directional changes after pilot thermal demagnetization of single specimens in air

(See Tables 3.6, 3.7 and 3.8.) Symbols as in Figs. 3.1, 3.3 and 3.4.

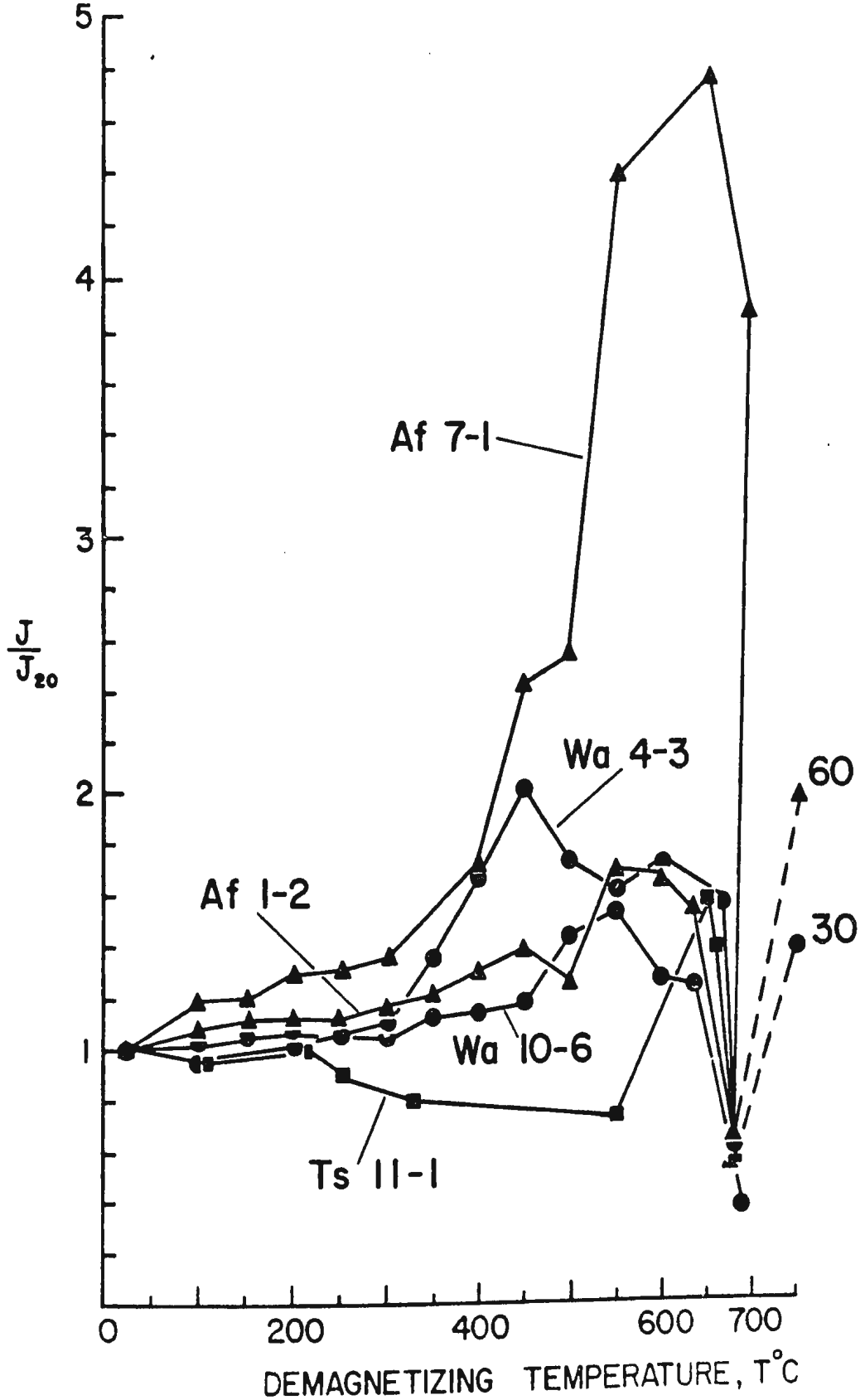

Fig. 3.8 Normalized intensity, J/J_{20}, of single specimens (Corresponding to Fig. 3.7.) The two numbers (30,60) refer to off-scale values of J/J_{20}.

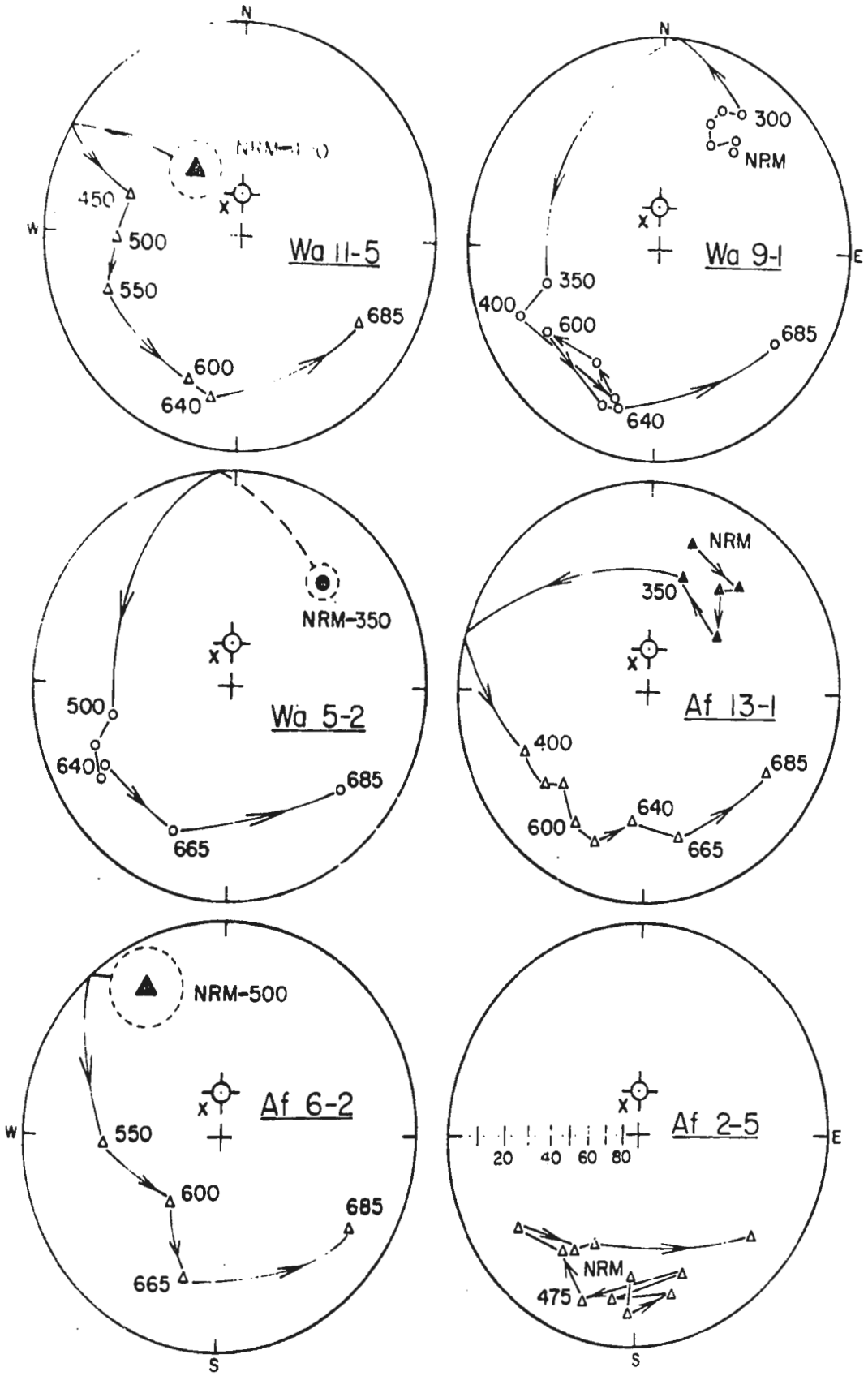

Fig. 3.9 Directional changes after pilot thermal demagnetization of single specimens in air

Symbols as in Fig. 3.7.

Fig: 3.10 Normalized intensity of 6 specimens, after stepwise thermal demagnetization

(See Section 3.4; not tabulated.)

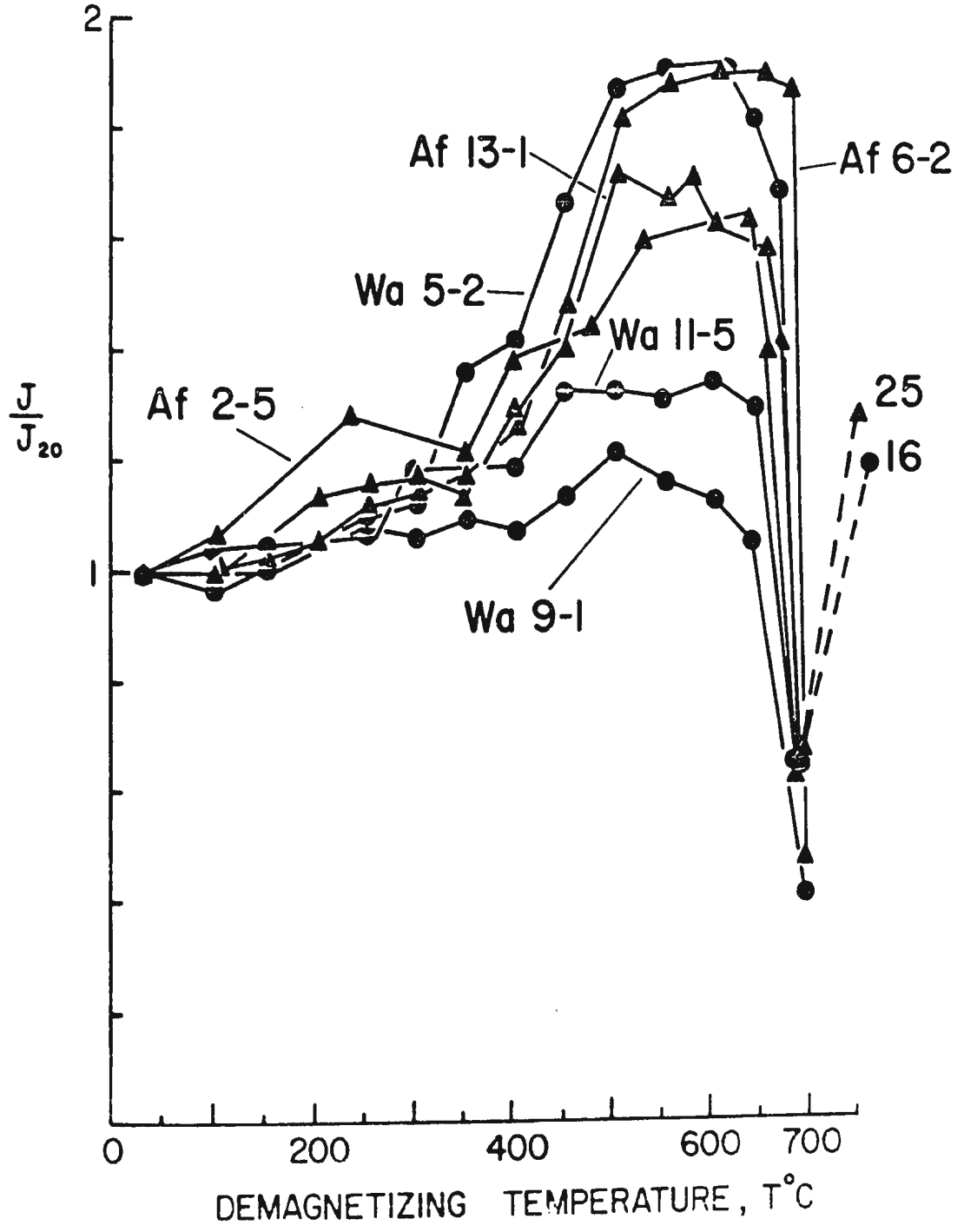

The two numbers (16,25) at 750°C refer to off-scale values of J/J_{20}.

TABLE 3.6

Pilot thermal demagnetization of red sandstone specimens from Wabana formation

T, demagnetization temperature (^{o}C); D, declination (degrees taken clockwise from north through 360^{o}); I, inclination (degrees, + indicates north pole in the lower hemisphere); J, intensity of magnetization (emu/cm^3):

Specimen Wa 4-3				Specimen Wa 10-6		
D	I	J x 10^{-5}	T	D	I	J x 10^{-5}
45.6	+17.2	3.8	20	9.6	-86.4	7.8
40.4	+19.9	3.7	100	10.4	-76.3	8.0
37.8	+26.3	3.9	150	26.3	-54.6	8.2
45.2	+29.1	4.0	200	38.1	-27.8	8.0
55.3	+17.7	4.2	250	34.8	-30.2	8.2
300.2	+48.9	5.2	300	50.3	-26.6	8.2
277.6	-23.8	6.4	350	320.1	-21.7	8.8
268.4	-30.4	7.7	400	290.8	-14.8	8.9
200.1	-23.2	6.6	450	287.3	-17.8	9.2
225.7	-17.9	6.2	500	250.6	-21.7	11.2
200.8	-24.3	6.5	550	237.8	-14.8	12.0
177.5	-19.9	6.1	600	197.4	-18.5	10.0
170.1	-14.7	6.0	640	210.3	-17.8	9.8
125.6	-17.2	2.7	685	128.2	-14.8	3.0

TABLE 3.7

Pilot thermal demagnetization of red sandstone specimens from Airfield formation

T, demagnetization temperature (^{o}C); D, declination (degrees taken clockwise from north through 360^{o}); I, inclination (degrees, + indicates north pole in the lower hemisphere); J, intensity of magnetization (emu/cm^{3}):

Specimen Af 7-1				Specimen Af 1-2			
T	D	I	J x 10^{-5}	T	D	I	J x 10^{-5}
20	326.0	+ 1.2	3.6	20	11.2	-10.4	5.7
100	340.3	+ 9.8	4.3	100	10.4	-10.2	6.2
150	319.8	+10.5	4.3	150	14.3	-14.8	6.3
200	323.6	+ 7.6	4.7	200	12.1	-14.6	6.4
250	330.4	+13.6	4.8	250	14.3	-12.8	6.4
300	344.4	+13.6	4.9	300	12.6	-14.3	6.6
400	313.6	+21.2	6.2	350	15.3	-20.3	6.9
450	329.0	+ 6.7	8.8	400	20.1	-14.2	7.2
500	341.7	+18.0	9.2	450	30.3	-14.4	7.3
550	266.5	-28.0	16.0	500	20.4	-14.8	7.2
600	219.3	-48.2	17.4	550	210.3	-12.1	8.9
640	194.1	-21.6	14.1	600	200.6	-20.6	8.8
685	120.6	-13.9	2.4	640	199.1	-14.1	8.1
				685	131.2	-19.3	3.3

TABLE 3.8

Pilot thermal demagnetization of red sandstone specimen from Zone 1 (Townsquare formation)

T, demagnetization temperature (^{o}C); D, declination (degrees taken clockwise from north through 360^{o}); I, inclination (degrees, + indicates north pole in the lower hemisphere); J, intensity of magnetization (emu/cm^3):

Specimen Ts 11-1			
T	D	I	$J \times 10^{-5}$
20	196.1	-30.2	3.0
350	195.6	- 3.8	2.3
450	193.4	- 7.9	2.2
550	205.6	- 0.5	2.2
650	211.2	- 3.6	4.8
670	228.5	-34.0	4.2
685	126.8	-21.6	2.0

reported from preliminary measurements. However, after the 300°C step, the direction had changed to D = 50°, I = -27°, similar to the NRM direction of specimen Wa 4-3, suggesting that a fairly steep viscous (VRM) component, possibly of quite recent origin, had been removed. On the basis of similar behaviour that was later observed for all samples from Wabana site 10 (Table A1.1, Fig. 3.2), the NRM of these samples was assigned to "group A" (Section 3.2) despite the presence of this steep, low-temperature VRM. Above 300°C, the response of specimen Wa 10-6 was quite similar to that of Wa 4-3, described above, up to the final step at 685°C.

3.4.1.3. Specimens Af 1-2 and Af 7-1

These specimens were from sites (Nos. 1 and 7, Fig. 2.2), respectively, above and below the Commerical Dominion bed of the Airfield formation. Both NRM vectors belong to group A, though the directions are quite far apart (D = 11°, I = -10° and D = 326°, I = +1° for specimens Af 1-2 and 7-1, respectively). This illustrates the large scatter of site mean directions for group A with D ranging from NW to NE, and I, both positive and negative, at sites of the Airfield formation (Table 3.7). After 8 demagnetization steps up to 500°C, the remanence directions of both specimens had changed only by small amounts but after the 550°C step they moved through large angles to the southwest, with small negative inclinations. This is similar to the findings for 600°C in the case of the Wabana pilot specimens (Sections 3.4.1.1, 3.4.1.2) and the 600°C directions will be denoted "group C". The group C site mean directions

(Tables 4.2 and 4.5) show a large scatter, mainly in declination, as suggested also by the pilot results discussed here. At 685°C, the directions of both specimens Af 1-2 and 7-1 move southeast, close to the direction of the Wabana pilot specimens; these will be denoted "group D", which is characterized by a close grouping of 685°C site mean directions for all 25 sites studied at Bell Island (Tables 4.3 and 4.6). Whereas both specimens Af 1-2 and 7-1 become progressively more negative in the range 20° - 600°C (Fig. 3.8), the increase of J in the former case was spectacular reaching a maximum for $J_{650}/J_{20} = 4.8$. At 685°C, the normalized intensity of both specimens had again dropped to about 0.6, similar to the case of the Wabana pilot specimens.

3.4.1.4. Specimen Ts 11-1

This specimen is taken from zone 1 of the Townsquare formation (Fig. 2.2), and is stratigraphically well below 200 m bottom of the Airfield formation. The NRM direction (D = 196°, I = -30°) is roughly opposite to the group A directions, and is representative of group B. Contrary to the four pilot specimens from the higher levels (Sections 3.4.1.1 - 3.4.1.3), the NRM direction is relatively undisturbed until the 670°step (D = 229°, I = -35°) and up to 550°C, J decreased moderately rather than increasing. Moreover, after 650°C, the normalized intensity had increased to $J_{650}/J_{20} = 1.6$ before dropping to $J_{685}/J_{20} = 0.6$ at 685°C. At that temperature, both the intensity and the direction are typical of the group D results (Section 3.4.1.3).

The changes in the directions of magnetization and intensity for 6 additional pilot specimens are given in Figs. 3.9 and 3.10. Results for the remaining 17 pilot specimens were similar but are not listed individually. Fisher statistics applied to all 28 specimens are given in Table 3.9 for NRM and 685°C only.

3.5. Analysis of pilot study

Thermal demagnetization of the 28 pilot specimens was helpful in determining the best estimate for the subsequent systematic thermal treatment. The observed major trends in the pilot study were as follows:

(1) The NRM directions fall into two opposed groups, A and B, with northerly and southerly declinations, respectively (Figs. 3.1 - 3.4).

(2) No significant changes in the NRM directions of magnetization were generally observed until treatment to 350°C or more (Figs. 3.7 and 3.9), the only exception being site Wa 10, which was discussed earlier (Section 3.4.1.2) in terms of a probable low-temperature VRM component.

(3) After the 350°C step both the group A and B vectors change towards the apparently stable, intermediate group C directions, becoming stabilized between 550 - 600°C, mainly with southwest declinations and intermediate to shallow inclinations (Section 3.4.1.3). The intensity of magnetization generally has its maximum in the 550 - 650°C range.

(4) After the 640°C treatment the remanence vectors tend to move along great-circle routes towards the southeast (Figs. 3.7 and 3.9, Table 4.11).

TABLE 3.9

Fisher analysis for the pilot study

	NRM		After 685°C
	group A specimens	group B specimens	all specimens
N[1]	20	8	28
D[2]	20.6	181.7	124.8
I[3]	+9.3	-21.9	-18.0
R	15.094	7.904	27.9
k	3.9	73	230
α_{95}	19.2	6.6	1.8

[1]Number of specimens (combined Wabana, Airfield and Townsquare formations).

[2]D = declination, degrees.

[3]I = inclination, degrees.

(5) Between 670°C and 685°C the vectors become closely grouped, with group D directions (Section 3.4.1.2, Tables 3.9 and 4.11) and a sharp decrease in intensity, usually to one-half the NRM intensity or less. This grouping generally remains stable up to 690°C - 695°C; at and above 700°C the directions become much more dispersed, and intensities increase by 1-2 orders of magnitude (Figs. 3.8 and 3.10).

Hence for the systematic treatment of all samples the demagnetization steps were chosen to be at 350, 600 and 685°C. Two specimens per sample were demagnetized in every case. This procedure will be termed a 3-step demagnetization (Chapter 4) to distinguish it from additional 1-step and 10-step tests using different specimens from some of the samples, mainly to assess possible physical-chemical effects due to the heat treatment itself (Chapter 4).

CHAPTER 4

SYSTEMATIC THERMAL DEMAGNETIZATION STUDY

Systematic thermal demagnetization was made on all the samples collected from 24 sites of the Wabana and Airfield formation as outlined in section 3.5. In the following discussion (Section 4.1), Figure 3.5 shows the site-mean directions of magnetization, which are also listed in Tables 4.1 - 4.6, along with Fisher statistics and the intensities for both formations at the demagnetization steps corresponding to 350, 600 and 685^{o}C.

4.1. Statistical analysis of site-mean directions and intensities

4.1.1. Wabana formation

The site 8 mean NRM direction (Table 3.2) is southerly, corresponding to group B, while the other ten site-mean directions correspond to group A, having north to east declinations, except site 11 where the declinations are northwest (D = 339.6^{o}). The A and B groupings were discussed in section 3.2. The mean inclinations are downward (positive), except at sites 8 (group B), 9 and 10, and are shallow to intermediate except at site 10 where their value, I = -78.6^{o}, is similar to the steep, upward inclinations found in the pilot study (Section 3.4).

After treatment to 350^{o}C, most of the site-mean directions show little change from their NRM values (compare Tables 3.2 and 4.1), but with some large changes in the within-site precision (see k values).

TABLE 4.1

Site mean directions for Wabana formation after stepwise demagnetization to 350°C

Group	Site No.	N	D	I	J x 10^{-5}	R	k	α_{95}
A	1	4	44.7	+15.9	6.2	3.992	390	4.7
	2	6	40.9	+22.7	4.6	5.917	60	8.7
	3	5	39.2	+23.1	5.1	4.942	69	9.3
	4	5	40.1	+29.6	5.2	4.614	10	25.0
	5	3	55.0	+26.7	6.1	2.986	150	10.2
	6	2	45.2	+30.0	6.3	—	—	—
	7	2	77.1	+26.5	6.4	—	—	—
	9	8	45.7	-40.4	8.7	7.200	8.7	20.0
	10	6	9.8	-33.6	7.4	5.691	16	17.2
	11	5	249.1	+30.6	5.7	4.123	4.6	40.3
B	8	10	196.4	-19.0	8.2	9.838	56	6.5

Symbols and conventions for rounding k are as in Table 3.2.

In the course of these systematic demagnetizations, specimens sometimes broke during a particular step, so that their remanence could not be measured; in that case, they were replaced for subsequent steps by fresh specimens from the same core; thus, values of N for certain sites quoted in Tables 3.2, 3.3 and 4.1 - 4.6 may vary between different steps. For N < 3, Fisher statistics are inapplicable; hence no data for R, k and α_{95} are shown in that case.

TABLE 4.2

Site mean directions for Wabana formation after stepwise demagnetization to 600°C

Group	Site No.	N	D	I	J x 10^{-5}	R	k	α_{95}
A	1	4	230.1	-23.4	8.4	3.904	31	16.7
	2	6	216.9	-27.0	7.0	5.087	5.5	31.5
	3	5	231.1	-21.9	6.9	4.690	13	22.1
	4	5	247.8	-30.5	7.7	4.838	25	15.7
	5	3	259.3	-23.7	6.9	2.970	68	15.1
	6	2	302.2	-19.9	6.6	–	–	–
	7	2	278.1	-20.7	6.8	–	–	–
	9	8	299.8	-17.1	8.8	7.882	59	7.3
	10	6	306.9	-27.2	9.9	5.897	49	9.7
	11	4	269.7	-36.6	7.8	3.292	4.2	50.9
B	8	8	264.3	-23.4	11.0	7.729	26	11.1

Symbols and conventions for rounding k are as in Table 3.2.

TABLE 4.3

Site mean directions for Wabana formation after stepwise demagnetization to 685°C

Group	Site No.	N	D	I	J x 10^{-5}	R	k	α_{95}
A	1	5	128.1	-18.2	2.9	4.962	100	7.5
	2	6	125.6	-21.0	2.9	5.972	180	5.1
	3	5	123.3	-19.1	3.2	4.950	81	8.6
	4	5	127.4	-19.3	2.9	4.980	200	5.4
	5	5	127.6	-18.8	2.9	4.988	320	4.3
	6	3	117.4	-20.3	3.0	2.974	76	14.3
	7	3	120.5	-15.9	3.1	2.978	89	13.1
	9	8	126.7	-19.2	3.1	7.983	410	2.7
	10	6	128.5	-19.0	3.1	5.954	110	6.5
	11	7	141.4	-19.9	3.1	6.986	430	2.9
B	8	9	121.7	-17.1	3.8	8.810	42	8.0

Symbols and conventions for rounding k are as in Table 3.2.

TABLE 4.4

Site mean directions for Airfield formation after stepwise demagnetization to 350°C

Group	Site No.	N	D	I	J x 10^{-5}	R	k	α_{95}
A	1	5	19.2	-19.1	7.4	4.970	140	6.6
	5	2	5.2	+17.4	6.2	—	—	—
	6	2	328.0	+30.3	7.1	—	—	—
	7	5	347.0	+23.5	6.0	4.710	14	21.4
	8	5	20.4	+20.9	7.3	4.945	73	9.0
	9	4	35.5	+19.3	7.2	3.920	37	15.3
	10	2	17.0	+23.5	4.9	—	—	—
	11	4	17.4	+29.0	6.1	3.965	86	9.9
	12	4	18.2	+22.7	5.1	3.957	70	11.0
	13	2	17.9	+21.0	5.1	—	—	—
B	2	6	183.0	-18.0	6.8	5.968	160	5.4
	3	3	186.2	-22.0	6.9	2.968	62	15.9
	4	3	184.9	-15.3	7.2	2.960	50	17.7

Symbols and conventions for rounding k are as in Table 3.2.

TABLE 4.5

Site mean directions for Airfield formation after stepwise demagnetization to 600°C

Group	Site No.	N	D	I	J x 10^{-5}	R	k	α_{95}
A	1	5	207.7	-18.1	8.6	4.931	58	10.1
	5	2	183.2	-16.6	7.1	–	–	–
	6	2	198.2	-26.3	7.0	–	–	–
	7	5	229.1	-25.4	10.6	4.795	20	17.8
	8	5	204.0	-25.2	10.0	4.893	37	12.7
	9	4	210.5	-28.9	10.1	3.850	20	21.0
	10	2	239.2	-17.8	8.0	–	–	–
	11	4	275.2	-23.2	9.2	3.873	24	19.3
	12	4	247.4	-29.4	6.2	3.934	45	13.8
	13	2	288.8	-27.6	6.1	–	–	–
B	2	6	221.7	-19.6	7.7	5.725	18	16.2
	3	3	214.3	-23.6	7.8	2.987	150	10.1
	4	3	216.8	-26.7	8.9	2.815	11	39.5

Symbols and conventions for rounding k are as in Table 3.2.

TABLE 4.6

Site mean directions for Airfield formation after stepwise demagnetization to 685°C

Group	Site No.	N	D	I	J x 10^{-5}	R	k	α_{95}
A	1	5	120.4	-16.0	3.4	4.959	98	7.8
	5	3	124.8	-18.5	2.6	2.995	440	5.9
	6	4	128.2	-21.6	3.0	3.975	120	8.4
	7	5	125.4	-18.7	3.2	4.992	480	3.5
	8	5	129.0	-18.9	3.1	4.991	440	3.6
	9	4	123.6	-17.9	3.1	3.987	230	6.0
	10	2	114.4	-11.8	2.9	—	—	—
	11	4	122.3	-15.9	2.9	3.975	120	8.5
	12	6	121.6	-17.1	3.0	5.965	140	5.6
	13	3	112.8	-17.3	3.3	2.982	110	11.9
B	2	6	119.3	-17.1	3.0	5.994	840	2.3
	3	3	119.5	-15.0	3.2	2.991	220	8.4
	4	3	121.9	-13.8	3.6	2.995	430	6.0

Symbols and conventions for rounding k are as in Table 3.2.

The largest directional changes occurred at site 10, as discussed in section 3.4 in connection with the pilot study. At 350°C, k had increased at three sites (1, 3, 5) and decreased at six (2, 4, 8 - 11), so that on the whole, the within-site scatter is somewhat greater than in the case of NRM.

Comparison of results before and after 600°C treatment shows large changes in the site-mean directions of magnetization, all of which have shallow to intermediate upward inclinations, but with a large spread of declinations ranging from D = 217° (site 2) to D = 307° (site 10). Similar results were obtained previously in the pilot study (Section 3.5) and denoted as group C directions.

The 685°C treatment is found to have improved the within-site grouping over that at 600°C at all eight sites, though at three sites (1, 8, 10), the NRM groupings are tighter than for 685°C. The 685°C site-mean directions of magnetization are closely grouped and similar to those obtained in the pilot study (Table 3.9), having southeast declinations and negative shallow inclinations (group D).

4.1.2. Comparison between Airfield and Wabana formations

Results of the systematic treatment for the Airfield formation mostly were comparable to those obtained from the Wabana samples (Section 4.1.1) and will not be separately discussed. In turn, the site-mean data for both formations (Tables 3.2, 3.3, 4.1 - 4.6) are comparable with those obtained from the respective pilot studies. The site-mean directions of the single site of the Townsquare formation are also

included in Fig. 3.5, and at all demagnetization steps are similar to the directions for the group B sites (where "group B" refers to the NRM grouping) of the Wabana and Airfield formations. The main differences in the site-mean statistics between the two latter formations are:

(1) The group A declinations of the site-mean NRM are more easterly in the case of the Wabana formation, remaining more easterly after the 350°C step. The corresponding site-mean directions after the 600°C step for Wabana again tend to be larger (i.e. more westerly) than for the Airfield formation.

(2) Up to the 350°C treatment, inclinations irrespective of sign tend to be larger for the Wabana formation, which includes also one site (Wa-10) with steep NRM inclination ($I = -78.6^{o}$), probably associated with a VRM (Section 3.5).

(3) The NRM site-mean precisions of the two formations are comparable, but show a greater range in the case of the Airfield formation. For the 350°C to 685°C steps, the values of k tend to be larger (i.e. site-mean groupings are better) for Airfield than for Wabana.

The most remarkable feature of these results is that such a tight condensation of directions, as found in group D, occurred at all 24 sites of the 150-meter section (plus the Townsquare site 180 m below), with virtually no aberrant results for individual specimens, and that this was observed only after treatment to a temperature as high as 685°C, close to the Curie point of hematite. Moreover, the D grouping is the end result of a large directional change, roughly along great-circle routes, from the C (600°C) grouping (Figs. 3.7, 3.10; Table 4.11).

The author has not found in the paleomagnetic literature any results from similar studies in which a directional change of comparable magnitude and consistency occurred at such high temperature over a thick section of sedimentary rocks. However, several case histories in which thermal treatment resulted in significant regrouping of vectors have been published. Prominent examples are (i) the condensation of a smeared vector distribution by thermal cleaning at the 300°C step in Carboniferous glacial sediments of New South Wales (Irving et al, 1961) and (ii) the isolation of a possibly primary Devonian component after thermal demagnetization above 600°C of the Old Red Sandstone of the Anglo-Welsh Cuvette, believed to have been remagnetized in the late Paleozoic (Chamalaun and Creer, 1964).

4.1.3. NRM decay curves

Another interesting feature of the present investigation is the increase of remanent intensity observed during demagnetization up to the 600 - 650°C steps, along with a sharp intensity drop with a narrow range between 650 and 685°C, shown with strikingly similar trend in all decay curves (Figs. 3.8, 3.10). Between NRM and about 600°C, the samples from both the Wabana and Airfield formations exhibit a gradual intensity increase by a total factor of 2-3, and in some cases spectacularly by about 5 times. The intensity values obtained in the systematic demagnetization and in the 1-step and 10-step procedures (Section 4.1.5) confirm the earlier results of the pilot study (Section 3.4).

Thus the shape of the intensity curves obtained during stepwise thermal demagnetization illustrates a useful concept, namely that of thermally-discrete and thermally-distributed components (Irving and Opdyke, 1965, and Roy et al., 1967). A thermally-discrete component is defined as a component having a narrow spectrum of blocking temperatures, being concentrated in a small range below T_C; for the purpose of the present discussion, this range is taken as $< 25^{o}C$. Thermally-distributed components are generally characterized in the decay curves by gradual intensity changes with temperature, suggesting the existence of a wide spectrum of blocking temperatures.

From the foregoing discussion, it was concluded that the group D ($685^{o}C$) directions of magnetization reside in a thermally-discrete component, whereas the components responsible for the other groupings (A, B and C) are perhaps mainly thermally distributed. The demagnetization curves (Figs. 3.8, 3.10) indicate that the Curie point of the group D component is slightly above $685^{o}C$, ruling out magnetite and suggesting hematite as the significant carrier of that magnetization. This is plausible also from the fact that untreated rock contained 50 - 70% of hematite and no significant magnetite (Section 2.3).

The NRM decay curves obtained in the present investigation belong to Schwarz' (1969) type-3 NRM decay curves (Section 3.3.2), in

which the intensity increases up to a certain temperature and falls beyond that; the downward section of the curve includes the (generally narrow) range of blocking temperatures.

One possible explanation for the intensity increase up to about 600°C in the NRM decay curves obtained in the present investigation is that two opposed, thermally-distributed components in the rock are removed in unequal proportions at progressively higher temperatures. Thus it is conceivable that in each of the roughly antiparallel "A" and "B" NRM groupings, the opposed component is also present, though with smaller magnetic moment; i.e. the "A" group magnetization contains a weaker "B" component that is preferentially removed by the treatment, and vice versa. The geometry of this mechanism is further complicated by the additional presence in the NRM of the "C" and "D" components in unknown proportions.

In a study of the Silurian Bloomsburg red beds, Irving and Opdyke (1965) identified three behaviour patterns, "A", "B" and "C", in the NRM decay curves during stepwise thermal demagnetization, as discussed also by Schwarz (1969) (Section 3.3.2). In the case of type B curves, a sometimes spectacular increase in intensity, similar to certain examples in the present study (pilot specimens, Figs. 3.7 - 3.10), was found to be associated with large directional changes up to 100°. Irving and Opdyke explained these findings by assuming that the NRM is composite, being made up of thermally-discrete (Roquet, 1954) and thermally-distributed components roughly antiparallel to each other, which are not coupled magnetically but are believed to have arisen from physically

separated phases. At progressively higher temperatures during stepwise thermal demagnetization, the selective removal of the distributed component, characterized by a large spectrum of blocking temperatures in the range 300 - 550°C, should then explain the increase of intensity (Fig. 3.6). Irving and Opdyke attributed the distributed component in the Bloomsburg rocks to a late Paleozoic origin, possibly a "moderate temperature VRM" acquired during deep burial of the rocks at about the time of the Appalachian orogeny. The oppositely-directed discrete component becomes isolated from the distributed component after thermal demagnetization above 550°C and disappears between 650 - 700°C; this is also similar to the results obtained in the present study (Figs. 3.6 to 3.10).

Briden (1965) studied the ancient secondary magnetizations in rocks and considers them to have been acquired under the action of the Earth's field during geologically long times, after which remanence was stabilized due to an increase in relaxation time of the magnetic grains. Alternative causes for this could be a fall in temperatures (during geological uplift or end of igneous activity) or growth of grains. Similar conclusions were reached by Chamalaun (1964) from his study of the Old Red Sandstone of the Anglo-Welsh Cuvette.

Thus the type B curves in the Bloomsburg red beds as well as in the present investigation (equivalent to the type-3 NRM decay curves of Schwarz; section 3.3.2) were probably associated with the occurrence of two or more NRM components of different direction and thermal stability in the same sample. The NRM decay curves obtained in the present investigation will be discussed further in sections 4.4 and 4.5 and Chapter 5.

4.1.4. Group and formation mean statistics

Tables 4.7 - 4.9 list the group and formation mean statistics for steps 350, 600 and 685°C. Fisher statistics were not quoted for the group A means in Tables 4.7 and 4.8, as the mean direction obtained was based on a smeared distribution with a wide spread in longitudes. Thus, the mean NRM directions of the Wabana and Airfield formations differ by 30° in declination (D = 42° and 12°, respectively), but very little in inclination (I = +19° and +16°), while the mean NRM vectors at the four group B sites are closely grouped (Table 3.5).

The changes in group and formation mean directions after subsequent demagnetization steps follow largely the pattern of the sample and site mean directions, already described. Thus only small directional changes are observed after the 350°C step (Table 4.7), while after 600°C, both the group A and B directions in both formations change over to group C directions (Table 4.8).

Fisher statistics were not calculated in the case of the group C directions, again because of a smeared distribution (Fig. 3.5). An interesting result of the thermal treatment between 600 and 685°C is that, irrespective of the formation or the NRM (A or B) groupings, all the vectors pass from group C to group D (685°C) directions (Table 4.9); that this directional change occurs progressively along great-circle paths is suggested by the detailed observations above 650°C (Table 4.11).

TABLE 4.7

Group and formation mean directions after stepwise demagnetization to 350°C

Group	Formation	N	D	I	J x 10^{-5}	R	k	α_{95}
A	Airfield	10	11.3	+20.0	6.2	9.321	14	13.8
	Wabana	10	41.4	+18.2	6.2	7.198	3.2	32.2
	[1]Airfield and Wabana	20	24.5	+19.9	6.2			
B	Airfield	3	184.8	-18.4	7.0	2.996	500	5.5
	Wabana	1	196.5	-19.0	8.2	—	—	—
	Airfield and Wabana	4	187.7	-18.6	7.3	3.982	170	7.1

Symbols and conventions for rounding k are as in Table 3.5.

[1]The group A mean direction is based on a smeared distribution of site mean vectors, and Fisher statistics are not quoted.

TABLE 4.8

Group and formation mean directions after stepwise demagnetization to 600°C

Group	Formation	N	D	I	J x 10^{-5}	^{2}R	^{2}k	$^{2}\alpha_{95}$
^{1}A	Airfield	10	226.9	-27.6	8.3	–	–	–
	Wabana	10	259.0	-29.5	7.7	–	–	–
	Airfield and Wabana	20	245.8	-29.2	8.0	–	–	–
^{1}B	Airfield	3	217.6	-23.3	8.1	2.993	270	7.6
	Wabana	1	264.3	-23.4	1.1	–	–	–
	Airfield and Wabana	4	228.8	-24.7	8.9	3.789	14	25.2
^{1}Group A and Group B		24	242.6	-28.6	8.5	–	–	–

Symbols and conventions for rounding k are as in Table 3.5.

^{1}Groups "A" and "B" refer to NRM groupings, whereas the directions assumed by both the NRM groupings after 600°C treatment (i.e. all directions quoted in this table) will be referred to as group "C".

^{2}Except for the sites having Group B NRM directions, Fisher statistics are not quoted, as the formation mean directions after 600°C treatment are based on a smeared distribution of site mean vectors.

TABLE 4.9

Group and formation mean directions after stepwise demagnetization to 685°C

Group	Formation	N	D	I	J x 10^{-5}	R	k	α_{95}
[1]A	Airfield	10	122.2	-17.4	3.1	9.956	210	3.4
	Wabana	10	126.6	-19.2	3.0	9.945	180	3.7
	Airfield and Wabana	20	124.4	-18.3	3.1	19.889	170	2.5
[1]B	Airfield	3	120.2	-15.3	3.3	2.9986	1400	3.3
	Wabana	1	121.7	-17.1	3.8	—	—	—
	Airfield and Wabana	4	120.6	-15.8	3.4	3.9980	1500	2.4
[1]Group A and Group B		24	123.8	-17.9	3.2	23.877	190	2.2

Symbols and conventions for rounding k are as in Table 3.5.

[1]Groups "A" and "B" refer to NRM groupings, whereas the directions assumed by both the NRM groupings after 685°C treatment (i.e. all directions quoted in this table) will be referred to as group "D".

4.1.5. Comparative demagnetization study by 1-step and 10-step procedures

As previously mentioned (Section 3.5), systematic thermal demagnetization experiments were made using 1-step and 10-step procedures besides the major 3-step procedure in order to study the possible effects of the heat treatment on the specimens (Table 4.10.1). One specimen from each of the 112 samples was subjected to the 1-step procedure, which involved demagnetization directly to 685°C. Similarly, a smaller batch of 64 specimens, representing 9 of the 11 Wabana sites and all 13 Airfield sites, was treated up to 685°C, but in a 10-step procedure.

The mean directions of magnetization obtained in the three (1-, 3- and 10-step) procedures were found to be identical at the 95% probability level. This is shown in Table 4.10.2, based on equal numbers of specimens (N = 22), where each specimen represents one sample and one site (excepting sites Wa 6 and 7). Besides the directions, the intensity values at 685°C are also quite similar for the three procedures.

However, the values of the precision parameter k (in Tables 4.10.1, 4.10.2) show some increase (i.e. improved grouping) when the 1-step and 10-step procedures are compared. Still, in the case of all three procedures, the k values are relatively large (i.e. the grouping may be considered "good"), so that the increase in k noted above is possibly fortuitous. Therefore it was concluded that the procedure adopted in the stepwise demagnetization had no significant effect on the direction and intensity of the 685°C component, and at most only a marginal effect on the precision.

TABLE 4.10.1

Results of thermal demagnetization to 685°C for two different procedures[1]

	Wabana		Airfield	
	1-step	10-step	1-step	10-step
$^{2}\bar{D}$	126.4	128.7	122.0	126.0
$^{2}\bar{I}$	-18.7	-18.9	-18.1	-17.1
$^{2}N_S^s$	60_{60}^{11}	41_{9}^{9}	52_{52}^{13}	23_{23}^{13}
R	58.877	40.687	51.683	22.873
k	53	130	160	170
α_{95}	2.6	2.0	1.6	2.3
$^{3}J \times 10^{-5}$	3.03	3.14	3.12	3.13

[1]For details see section 4.1.5.

[2]Mean declination and inclination for N specimens, selected irrespective of site for either formation, and s, S = number of sites (s) and samples (S) represented.

[3]Arithmetic mean of the intensity of magnetization (emu/cm^3) for the N specimens.

TABLE 4.10.2

Results of thermal demagnetization to 685°C for three different procedures[1]

	Procedure		
	1-step	3-step	10-step
$^2\bar{D}$	124.0	124.8	129.1
$^2\bar{I}$	-18.3	-17.6	-17.4
^2N	22	22	22
R	21.741	21.805	21.880
k	81	110	180
α_{95}	3.5	3.0	2.3
$^3\bar{J} \times 10^{-5}$	3.11 ± 0.42	3.02 ± 0.36	3.09 ± 0.30

[1]For details, see Table A2.1.

[2]Mean declination and inclination for one specimen each from N samples representing 22 sites of the Wabana and Airfield formations (one sample per site, excluding sites Wa 6 and Wa 7). Different specimens from the same samples were compared in each procedure.

[3]Arithmetic mean (N = 22) of the intensity of magnetization (emu/cm^3), with the standard deviation.

4.1.6. High-temperature demagnetization in the range 650 - 750°C

To confirm whether, in the systematic thermal demagnetization, the 685°C treatment constituted effective thermal cleaning, the same treatment was applied in 10°C steps from 650 - 700°C with a further step at 750°C to five specimens taken from the Wabana and Airfield formations (Table 4.11). A further objective was to confirm whether the group C (600°C) directions move progressively towards the group D (685°C) directions along great circle paths, as one would expect them to do if the group C component were being preferentially demagnetized.

The results in Table 4.11 do confirm a progressive change, roughly along great circles, between the group C and D directions, the latter obtained after 690°C treatment as 685°C was not used. This is consistent with the results of the pilot study (Figs. 3.8, 3.10) which was less detailed at the higher temperatures.

Upon heating to 700°C, the five specimen directions became considerably scattered (k = 7.1) (Table 4.11) while all five intensities increased (Fig. 4.2). After further treatment to 750°C the five vectors approached a random grouping (k = 2.2) and now included both positive and negative inclinations. At the same time, the intensity of magnetization increased by factors 15 to 60 compared with the NRM intensity (see section 4.4.1).

To confirm the above results for 750°C, 9 specimens (7 samples) from the Wabana and Airfield formations were subjected to a single-step demagnetization to 750°C. The NRM and 750°C mean directions are shown

TABLE 4.11

Directional changes and precision for five specimens after detailed thermal demagnetization in the 650 - 750°C range

Treatment	Wa 1-4		Wa 4-3		Wa 5-2		Af 2-5		Af 7-1		k
°C	D	I	D	I	D	I	D	I	D	I	(N=5)
650	214	-21	256	-28	220	-24	192	-32	196	-22	2.5
660	211	-27	170	-12	194	-18	158	-18	177	-20	17
670	190	-16	163	-28	167	-20	137	-20	150	-22	18
680	179	-13	157	-20	141	- 7	130	-10	142	-14	18
690	121	-17	127	-19	126	-15	121	-14	122	-18	580
700	132	-22	148	-22	100	+22	110	-28	100	-41	7.1
750	148	-31	93	-41	112	+68	166	+18	80	-22	2.2

For normalized precision and mean intensity of magnetization, see Fig. 4.2.

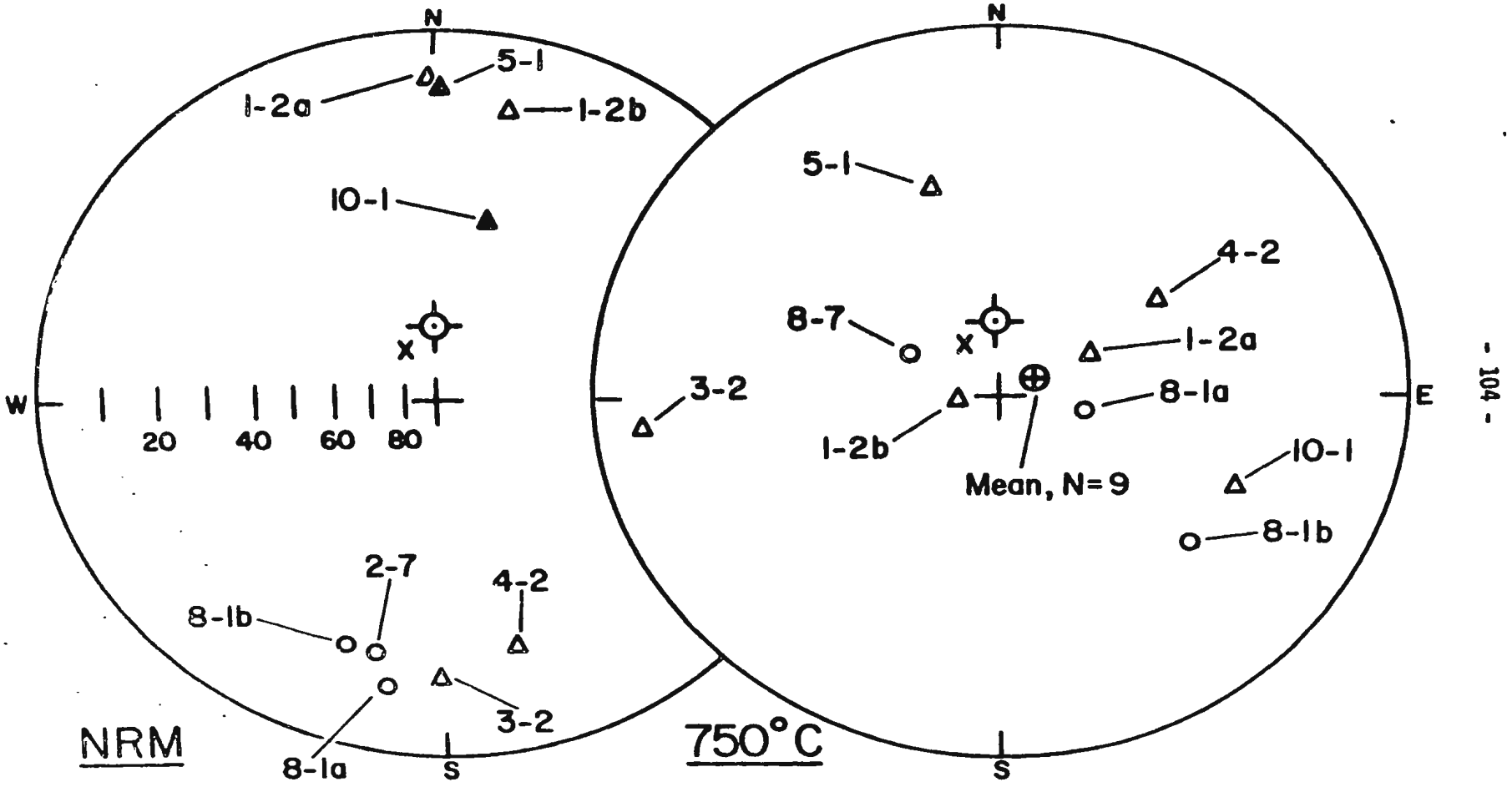

Fig. 4.1 Directions before and after one-step thermal demagnetization to 750°C of single specimens in air

Numbers refer to site, sample and specimen (e.g. 1-2a, site 1, sample 2, specimen a) from the Wabana or Airfield formations. Other symbols as in Figs. 3.1, 3.3 and 3.4.

Fig. 4.2 Normalized precision, k/k_0, and arithmetic mean intensity of magnetization, J, after stepwise thermal demagnetization in the temperature interval 600 - 750°C (Wabana and Airfield formations)

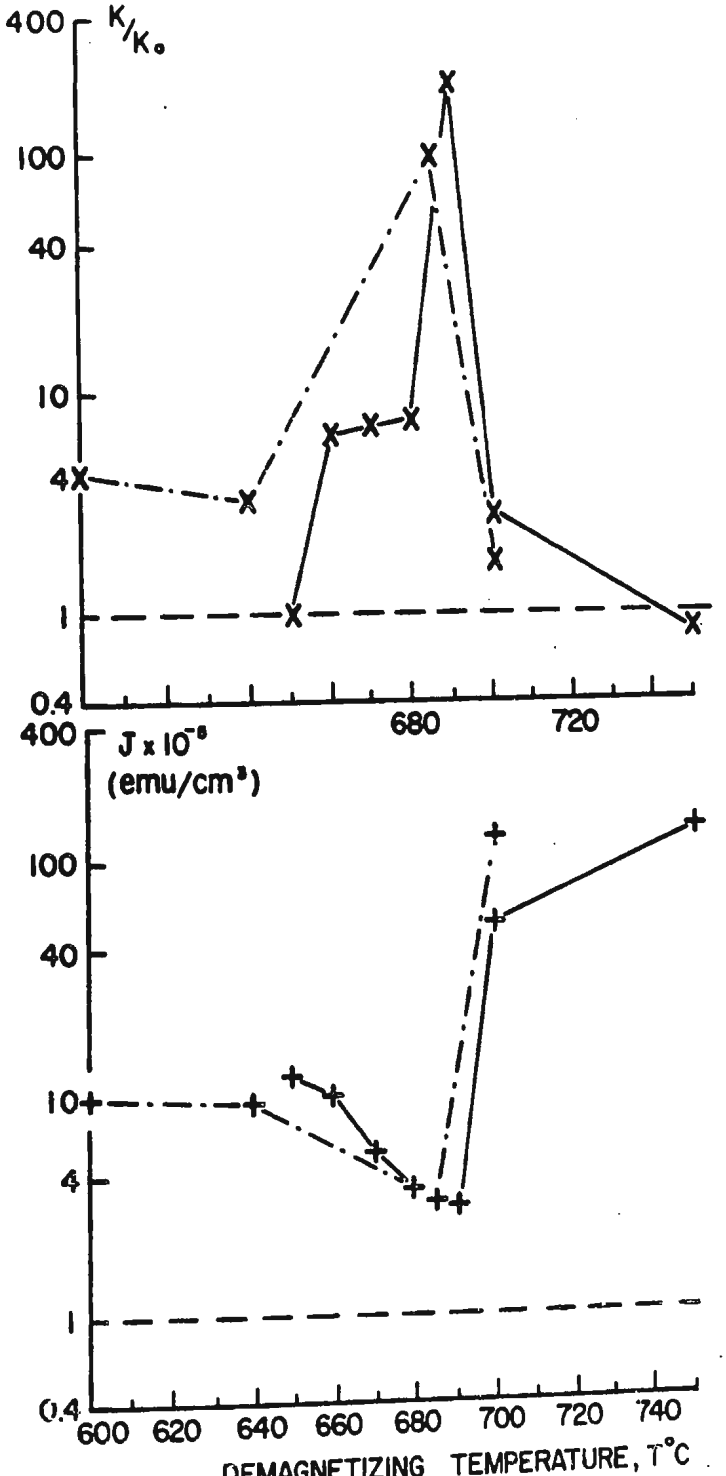

X——X + ——+ mean of 1 specimen each from 5 samples, 650 - 750°C (see Table 4.11)

X-·-·-X +-·-·-+ mean of 1 specimen each from 4 samples, 600 - 700°C (see Pilot study, Section 3.4)

in Fig. 4.1. The grouping of the 9 specimen vectors for 750°C is again quite poor (k = 2.7).

4.1.7. Change of precision parameter with temperature

Results of the pilot and systematic thermal demagnetizations (Sections 3.4 and 4.1) and their extension to temperatures above 685°C (Section 4.1.6) show that at all levels of comparison (i.e. between samples, sites or zones), the 685°C step tends to be associated with (i) maxima in the precision of mean directions; (ii) minima in the intensity of magnetization.

To depict this graphically, the normalized precision, k/k_0, and the intensity J were plotted against demagnetization temperature for the five specimens (Table 4.11) and the pilot specimens discussed in section 4.1.6. The resulting curves are shown in Fig. 4.2. Similarly, k/k_0 values are plotted for a 13-step thermal demagnetization of six fresh specimens (sites Wa 8 and Af 7, Table 4.12) and for the site and zone means (Fig. 4.3). The normalized precision parameter (e.g. Robertson, 1969) is given by

$$k/k_0 = (N - R_0)/(N - R) \qquad (4.1)$$

where $k = (N - 1)/(N - R)$ is the actual precision parameter for N unit vectors of resultant length R (Fisher, 1953),

$k_0 = (N - 1)/(N - R_0)$ is the corresponding precision parameter for a random vector distribution, and

TABLE 4.12

Selected site mean remanence direction and normalized precision, k/k_o, after detailed stepwise thermal demagnetization, based on single specimens

	Site Wa 8, $^1N = 6$				Site Af 7, $^1N = 6$			
Step (^oC)	^1D	^1I	^1R	$^2k/k_o$	^1D	^1I	^1R	$^2k/k_o$
NRM	182	-19	5.912	24	26	+18	5.964	60
100	185	-17	5.972	77	21	+23	5.918	26
150	187	-18	5.948	41	26	+17	5.951	44
200	189	-19	5.951	44	25	+22	5.890	20
250	194	-22	5.884	19	30	+21	5.934	33
300	191	-18	5.822	12	25	+18	5.927	29
350	198	-19	5.899	21	11	+15	2.125	0.55
400	191	-25	5.897	21	250	-28	4.719	1.7
450	210	-23	5.747	8.5	238	-23	5.305	3.1
500	237	-21	5.686	6.8	231	-22	5.462	4.0
550	276	-20	5.794	10	231	-18	5.423	3.7
600	248	-25	4.878	1.9	218	-25	4.931	2.0
640	207	-24	5.296	3.1	193	-21	5.771	9.4
685	123	-19	5.982	119	122	-18	5.983	126

[1] Mean values of D, I and R (see definition, Table 3.4) at each site are based on unit weight being given to N specimens selected from N different samples.

[2] Normalized precision, $k/k_o = (N - R_o)/(N - R)$, where R_o is Stephens' (1964) resultant of N random vectors at probability P = 0.05.

Fig. 4.3 Normalized precision of site, group and zone mean directions, for the Wabana and Airfield formations, after stepwise thermal demagnetization

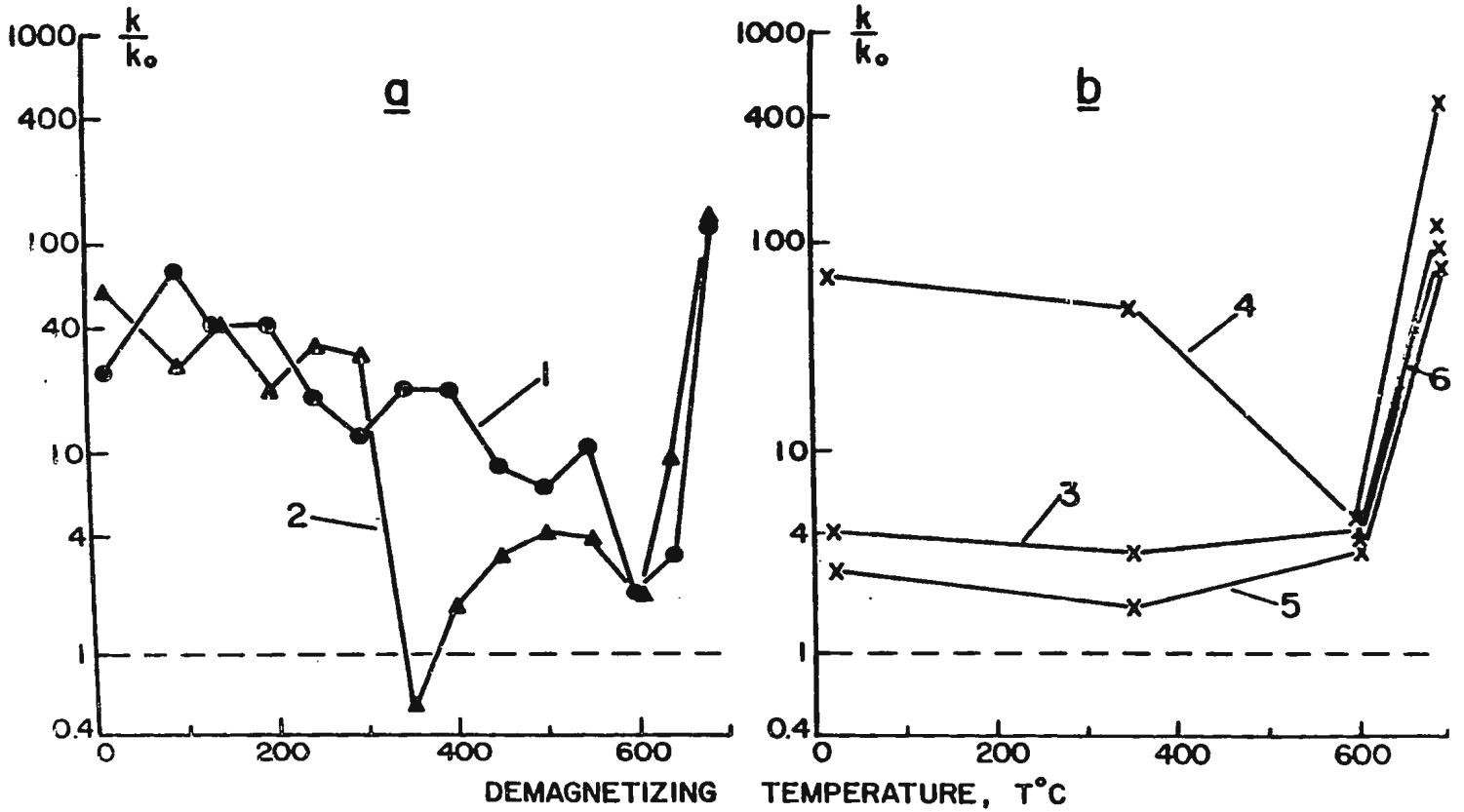

(a) 13 steps, for N = 6 single specimens (= 6 samples) each, from two sites: curve 1, site Wa 8; curve 2, site Af 12

(b) 3 steps, equal weight given to: curve 3, N = 20 group A sites; curve 4, N = 4 group B sites; curve 5, N = 9 group A zones; curve 6, N = 11 groups A+B zones (see also Tables 3.5, 4.6 - 4.9, 4.20 - 4.23)

R_0 is Stephens' (1964) resultant of N random vectors, which is a function of N and the specified probability level, P. Usually P is taken as 0.02 or 0.05.

The advantage of using k/k_0 rather than k is that it enables one to assess at a glance the approach to randomness of a given vector distribution. This is because for probability P, $k/k_0 = 1$ corresponds to a random distribution, whereas $k/k_0 > 1$ denotes significant grouping.

For the various groupings represented in Figs. 4.2; 4.3, the curves (based on P = 0.05) show that, over the entire range NRM-750°C, the distributions are nearly always non-random. However, k/k_0 varies over three orders of magnitude, reaching a maximum usually near 685°C where J tends to be smallest. The results confirm the successful isolation by thermal cleaning of a magnetically hard component having a narrow range of blocking temperatures above 650°C; this will be discussed further.

4.2. Statistical comparison of mean directions of magnetization

4.2.1. Sources of dispersion

The main aim of statistical tests in paleomagnetism (Fisher, 1953; Watson, 1956; Watson and Irving, 1957; Stephens, 1964; McElhinny, 1967; Larochelle, 1967), is to estimate the accuracy of calculated mean directions of magnetization, which depends upon the inherent, very hierarchial nature of the sampling scheme (Irving, 1964) and also upon a number of other factors [see (1) - (7), below]. Sedimentary rock

formations sampled for paleomagnetic study usually represent a continuous time sequence that is significantly long on the geological time scale. However, because of differences in the conditions of deposition, the time intervals represented by the same rock thicknesses at different sites are not necessarily the same, nor are the different sites necessarily contemporaneous. Therefore, in analyzing the sources of dispersion in a set of paleomagnetic directions obtained from independently oriented samples taken at different sites, it is useful to compare both the within-site and between-site dispersions, thus comparing two sampling levels. The magnitude of these dispersions will be determined by some or all of the following contributing factors (considering sedimentary rocks only):

(1) Sampling and measurement errors;

(2) (i) Inhomogeneity of magnetization;

(ii) Inclination and bedding errors;

(iii) Shape and magnetocrystalline anisotropy;

the latter being especially relevant to hematite-bearing red sandstones. Any of the effects under (2) may result in failure of the rocks to record faithfully the ambient field direction.

(3) Structural deformation between sites, or between samples at the same site, subsequent to their acquisition of the original magnetization. Examples are tilting, folding and slumping.

(4) Secondary magnetizations acquired during or since the diagenesis of the rock through chemical changes or time- and temperature-dependent processes affecting the primary magnetization, or through such phenomena as lightning.

(5) Significant differences in ferromagnetic properties between or within sites, as caused by differences in rock composition or in environmental conditions during deposition and lithification. An example is the presence or absence at different sites of a suitable oxidizing environment for the precipitation of hematite.

(6) Changes in the direction of the main field caused by polar wandering and/or continental drift.

(7) Paleosecular variation or possible field asymmetries of longer time period (Hide, 1967), resulting in significant differences in the ancient field direction at different sites.

Of the above factors, sampling and measurement errors (1) can be estimated and are usually small compared to the observed dispersions (Irving, 1964). Inhomogeniety of magnetization (2, i) can usually be detected by the measurement procedure (Tarling, 1967). An inclination error (2, ii) is not expected to occur in sediments whose magnetization is of CRM origin (Collinson, 1965). The effect of anisotropy (2, iii) on the magnetization directions can be estimated from measurements (Howell, 1962; Fuller and Uyeda, 1962; Graham, 1967). The geometrical effect of structural deformation (3) can often be determined and corrected for; this may be difficult, however, in the case of large, regional deformations.

Secondary magnetizations (4) can generally be detected and often minimized by demagnetization techniques, though this is not always possible (Section 3.3). Variations in the lithology within a formation (5) may result in differences in parameters such as the intensity of magnetization, the effect of which can be estimated from within-sample,

within-site and between-site dispersions. Rates of change in the mean direction of the dipole field caused by displacements of the pole relative to the site (6) can generally be expected to be small (e.g. a few centimeters per year in the case of continental drift) and will have little effect on the between-site scatter if the sites span a few million years.

4.2.2. F-ratio tests

The significant contribution of some or all of these effects [(1) - (7)] to the within- and between-site variations may be judged with the aid of a variance-ratio (or "F"-ratio) test (Watson, 1956; Larochelle, 1967), in which the ratio $\bar{\delta}_b^2/\bar{\delta}_w^2$ is compared with the statistic $F_{2(B-1),\,(N-B),\,\alpha}$ obtainable from standard tables. Here $\bar{\delta}_b^2$ and $\bar{\delta}_w^2$ are the angular variances (measured in radians) between sites and within sites, respectively. N is the total number of samples distributed over a total of B sites, and α is the probability level. The angular variances are given by

$$\bar{\delta}_b^2 = 2(\Sigma R_i - R)/(B - 1) \qquad \bar{\delta}_w^2 = 2(N - \Sigma R_i)/(N - B) \qquad (4.2,\ 4.3)$$

where R_i and R are the magnitudes of the unit vector resultants for the i^{th} site and the N samples, respectively. Then, if

$$\bar{\delta}_b^2/\bar{\delta}_w^2 > F_{2(B-1),\,(N-B),\,\alpha} \qquad (4.4)$$

the B site-mean directions may be said to differ significantly with a probability exceeding $1-\alpha$. The same test can be applied to other

hierarchial levels, e.g. in comparing between-formation and within-formation (i.e. between-site) angular variances, in which case N and B become the total number of sites and formations, respectively.

Among the possible causes of dispersion (Section 4.2.1), effects (1) - (3) can be considered small or may be allowed for as a result of experiments or field observation. Among the remaining effects, (4) - (7), (4) and (5) could result in the condition given by inequality (4.4), i.e. between-site dispersions are significantly greater than within-site dispersions; this will be the case if effects (4) and (5) occurred over thicknesses or lateral distances comparable with the separation between sites.

However, both these effects are closely related to the ferromagnetic history of the rocks, and it will often be difficult to estimate the stratigraphic thicknesses over which they result in significantly different dispersions. For example, a viscous PTRM acquired by Upper Silurian red sediments in Oslo region, Norway (Storetvedt, 1968), due to the heating effect of adjacent large plutonic masses during some millions of years, resulted in the within-flow dispersion being equal to, or even greater than, the between-flow dispersion; in such cases any magnetization/time relationship would be practically impossible to establish. Relative polar wandering (effect 6), if it were significant, would be expected to contribute mainly to the apparent value of $\bar{\delta}_b^2$ rather than $\bar{\delta}_w^2$, resulting in an increase of $\bar{\delta}_b^2/\bar{\delta}_w^2$ [inequality (4.4)].

While some of the sources of dispersion (e.g. experimental errors) would represent random errors, the others may be systematic to a varying extent; the effect of random errors can be reduced, e.g. by a large collection and measurement of samples, whereas systematic errors must be recognized and separated from the others, as they do not contribute to a true "fisherian" dispersion. Systematic polar wandering (see above) would be a case in point.

In general, if the various sources of dispersion can be separated, the scatter of site-mean directions of magnetization will be due only to effect (7), namely, the secular variation and other asymmetries of the paleogeomagnetic field, which would satisfy condition (4.4) if they were of sufficient magnitude. Results of F-ratio tests were applied as discussed below.

4.2.3. Discussion of F-ratio test results

Application of the F-ratio test in comparing the between-site/within-site ratio with F (inequality 4.4) is permissible only if the within-site dispersions, $\bar{\delta}^2_w$, are not significantly different (Watson and Irving, 1957). For this reason it is first necessary to satisfy the condition

$$\bar{\delta}^2_I / \bar{\delta}^2_{II} \leq F_{2(N_I - 1),\, 2(N_{II} - 1),\, \alpha} \qquad (4.5)$$

where α is the probability level, previously defined;

N_I and N_{II} are the numbers of samples at two sites, I and II, having respectively the largest and smallest values of dispersion, $\bar{\delta}^2$,

among the total number (B) of sites being compared; and

$\bar{\delta}^2_I$ and $\bar{\delta}^2_{II}$ are the dispersions at sites I and II, the remaining (B-2) sites having intermediate values of $\bar{\delta}^2$.

The same F-ratio test (condition 4.5) can be applied at other hierarchial levels, e.g. between formations (B) and sites (N). It should be noted that

$$\bar{\delta}^2 = 2/k = 2(N - R)/(N - 1) \qquad (4.6)$$

where k is Fisher's precision parameter.

In practice, condition (4.5) could not be met in the case of the group D (685°C) directions for either the 11 Wabana sites or the 13 Airfield sites mainly because $\bar{\delta}^2$ assumed extreme values at a few sites, compared with the majority of sites. This can probably be explained by local variations in the geology, as will be discussed in Chapter 5.

Hence it became necessary to apply the F-test in a more restricted way, by dividing each formation into two groups of sites, those with high (H) and low (L) sample dispersions, respectively. By specifying sites I and II, as defined in equation (4.5), separately for the H and L groups in each formation, it was possible to satisfy the equation for both 99% and 95% probability levels (Table 4.13.1).

The same initial F-ratio test was also applied to the assumption (necessary in comparing the between- and within-formation dispersions) that the within-formation (i.e. between-site) dispersions for Wabana and Airfield are not significantly different. Condition (4.5) can now be written

$$\bar{\delta}^2_1/\bar{\delta}^2_2 \leq F_{2(N_1 - 1),\ 2(N_2 - 1),\ \alpha} \qquad (4.7)$$

TABLE 4.13.1

F-ratio test of variance of sample mean directions at different Bell Island sites after 685°C treatment

(1)	(2)	(3)	(4)	(5)	(1)	(2)	(3)	(4)	(5)
Formation	Wa(H)[1]	Wa(L)[1]	Af(H)[1]	Af(L)[1]	Formation	Wa(H)[1]	Wa(L)[1]	Af(H)[1]	Af(L)[1]
[2]Site I	Wa 8	Wa 2	Af 6	Af 5	$\bar{\delta}_I^2/\bar{\delta}_{II}^2$	2.59	2.44	2.87	2.08
^3N_I	9	6	4	3	$^5F_{2(N_I-1),2(N_{II}-1),\alpha}$	$F_{16,10,\alpha}$	$F_{10,12,\alpha}$	$F_{6,6,\alpha}$	$F_{4,10,\alpha}$
$^4\bar{\delta}_I^2$	0.0476	0.0112	0.0250	0.0050	$^5F(\alpha = 0.01)$	4.52	4.33	8.47	5.99
[2]Site II	Wa 10	Wa 11	Af 9	Af 2	$^5F(\alpha = 0.05)$	2.82	2.77	4.28	3.48
$^3N_{II}$	6	7	4	6	Sites included in groups[6]	8,6,3	2,4,5	6,1,13	5,4,8
$^4\bar{\delta}_{II}^2$	0.0184	0.0046	0.0087	0.0024		7,1,10	9,11	11,12,3,9	7,2

TABLE 4.13.1, continued

[1] H, L = groups of sites with relatively high (H) and low (L) sample variances.

[2] I, II = sites being compared, having respectively the largest and smallest variance in the group.

[3] N_I, N_{II} = numbers of samples at sites I and II.

[4] $\bar{\delta}^2_I$, $\bar{\delta}^2_{II}$ = variances corresponding to sites I and II.

[5] $F_2(N_I-1),2(N_{II}-1),\alpha$ = F-ratio, for the N_I and N_{II} samples respectively at 99% and 95% probability levels.

[6] Included are all sites of the Wabana and Airfield formations except site Af 10 (N = 2 samples only). For each group the sites are listed in descending order of $\bar{\delta}^2$, from $\bar{\delta}^2_I$ to $\bar{\delta}^2_{II}$ (intermediate values of $\bar{\delta}^2$ are not shown).

where $\bar{\delta}_1^2$ and $\bar{\delta}_2^2$ are the dispersions within the Wabana and Airfield formations (the former being larger). Table 4.13.2 shows that this condition is indeed met in the case of the 685°C directions for Wabana and Airfield, at both the 99% and 95% levels.

The F-ratio test was now applied to 685°C directions for the two groups (H and L) of Wabana and Airfield sites. Table 4.14 shows that in one of the groups of sites having high within-site dispersions [i.e. Wa(H) and Af(H)], condition (4.4) is fulfilled at neither probability level. On the other hand, for the groups having low values of $\bar{\delta}_w^2$ [Wa(L) and Af(L)], inequality (4.4) is satisfied at both levels, i.e. the probability that these site-mean directions differ significantly is greater than 99%. The results of the test in this case are therefore somewhat inconclusive. This is partly because of the need to group the sites into H and L groups, for the reasons given. Taking all site-mean directions together it may be argued that, with the possible exception of the Wa(L) group of sites, where $\bar{\delta}_b^2$ is esceptionally large (0.0805), there is a fairly close approach to isotropic conditions in the case of both formations.

The reason for arguing this is that both the numerators and denominators in the $\bar{\delta}_b^2/\bar{\delta}_w^2$ ratio are relatively small at most of the sites; i.e. the between-site and within-site precisions (Tables 4.3, 4.6 and 4.9) are large, where $\bar{\delta}^2 \propto 1/k$ (equation 4.6). At the same time relatively minor geological differences may cause fairly large variations in $\bar{\delta}_w^2$, including cases where the grouping of the few samples at a given site may be exceptionally good, resulting in very small $\bar{\delta}_w^2$. However, since $\bar{\delta}_w^2$ appears in the denominator of the ratio $\bar{\delta}_b^2/\bar{\delta}_w^2$, it does not, in that case,

TABLE 4.13.2

F-ratio test of variance of site mean directions for Wabana and Airfield formations, after 685°C treatment

Formation	Wabana	Airfield
^1N	$^1N_1 = 11$	$^1N_2 = 13$
$^2\bar{\delta}^2$	$\bar{\delta}_1^2 = 0.0110$	$\bar{\delta}_2^2 = 0.0080$
$^2\bar{\delta}_1^2/\bar{\delta}_2^2$	1.38	
$^3F_{2(N_1-1),\ 2(N_2-1),\ \alpha}$	$F_{20,24,\alpha}$	
$F(\alpha = 0.01)$	2.74	
$F(\alpha = 0.05)$	2.03	

^1N = number of sites occupied in Wabana (N_1) and Airfield (N_2) formations.

$^2\bar{\delta}^2$ = Variances corresponding to Wabana ($\bar{\delta}_1^2$) and Airfield ($\bar{\delta}_2^2$) formations, respectively.

$^3F_{2(N_1-1),\ 2(N_2-1),\ \alpha}$ = F-ratio for the N_1 and N_2 sites, respectively, at 99% and 95% probability levels.

TABLE 4.14

Estimates of between-site (between-formation) and within-site (within-formation) dispersions after 685°C treatment

Groups of sites and formations	$3\bar{\delta}_b^2$	$4\bar{\delta}_w^2$	$\bar{\delta}_b^2/\bar{\delta}_w^2$	$F_{2(B-1),2(N-B),\alpha}$		
					$\alpha = 0.01$	$\alpha = 0.05$
[1]Wa(H)	0.0264	0.0298	0.89	$^1F_{10,50,\alpha}$	2.72	2.04
[1]Wa(L)	0.0805	0.0070	11.50	$^1F_{8,52,\alpha}$	2.88	2.13
[1]Af(H)	0.0257	0.0151	1.70	$^1F_{12,44,\alpha}$	2.66	2.00
[1]Af(L)	0.0240	0.0039	6.15	$^1F_{8,34,\alpha}$	3.08	2.22
[2]Wabana and Airfield	0.0400	0.0094	4.26	$^2F_{2,44,\alpha}$	7.24	4.05

[1]Groups of sites with relatively high (H) and low (L) sample variances, and the corresponding F-ratio of N samples in B sites of 99% and 95% probability levels, respectively.

[2]Wabana and Airfield formations with N_1(=11) and N_2(=13) sites (see Table 4.13.2) and the corresponding F-ratio of N sites (=24) and B(=2) formations at 99% and 95% probability levels.

3,4 $\bar{\delta}_b^2$, $\bar{\delta}_w^2$ = between-site (between-formation) and within-site (within-formation) dispersions.

require a major increase in the between-site dispersion to satisfy $\bar{\delta}_b^2/\bar{\delta}_w^2 > F$ for a given group of sites. This is illustrated by the case of the Af(L) group of sites where $\bar{\delta}_b^2 = 0.0240$ is actually smaller than the corresponding values in the other three cases, though the F-ratio test indicates a significant difference between site-mean directions.

A similar difficulty in interpretation exists in the case of the comparison between the Wabana and Airfield formations (Table 4.14), where the condition was met for $\alpha = 0.05$ but not $\alpha = 0.01$; hence, it may be said that the probability of the two formation-mean directions being identical is just under 5%. Again, a ratio between relatively large precision values (for the between- and within-formations) is involved, and it may be argued that the difference in mean directions between the Wabana and Airfield formations, though significant, is not much more than marginal.

The results obtained in the F-ratio test will be further discussed in Chapter 5.

4.3. Statistics based on stratigraphic zones

A given stratigraphic thickness will tend to represent a relatively long time interval in the case of sedimentary rocks compared with lavas. However, the extent to which the magnetic record might be contemporaneous with the sedimentary record is generally uncertain, so that an adequate statistical analysis of directional grouping must be made. A Fisher analysis based on equal weighting of site-mean directions, as in

section 4.1, may bias the results in favour of those stratigraphic levels at which the sampling was relatively extensive, e.g. where several sites have significant overlap.

In order to reduce this bias, the sampling sites of the Wabana and Airfield formations were combined into stratigraphic "Zones" (Fig. 2.2; Table 4.15) containing one to four sites each in such a way that no vertical overlap occurs between any two sites from different zones. Mean directions and intensities of magnetization and Fisher statistics based on the N = 11 zones are calculated without tilt correction for NRM and for 350, 600 and 685^{o}C treatments.

4.3.1. Tilt correction

Obtaining the direction of a magnetic component with the use of Fisher statistics, as in section 4.3, and showing it to be stable, one is generally safe to assume that this represents the direction of the Earth's magnetic field at the time the rock acquired this component. There are some exceptions, e.g. strong anisotropy. However, the field direction is measured relative to the present horizontal plane, and if the rock formation has been tectonically deformed since the time of magnetization, the remanence direction relative to the bedding plane (assumed to be the ancient horizontal) is mainly of interest. This may be computed by means of a "tilt correction". In cases (including Bell Island) where only a gentle, uniform tilt is involved, this correction simply consists of "tilting back" the strata into a horizontal position about the strike axis.

TABLE 4.15

Non-overlapping stratigraphic zones

Formation	Site number	Stratigraphic zone number	Stratigraphic location (Fig. 2.2)
Wabana	1 - 4	Z1	above Hayes' zone 5
	5	2	Upper bed (U.b)
	6, 7	3	bottom of U.b
	8	4	Scotia bed (S.b)
	9, 10	5	just below S.b
	11	6	bottom of Wabana formation
Airfield	1	Z7	just above Dominion bed
	2 - 4	8	D.b
	5 - 7	9	just below D.b
	8, 9	10	below D.b
	10 - 13	11	bottom of Hayes' zone 2

A tilt correction applied to the remanence vectors at opposite limbs of a fold may be used in the "fold test" (Section 3.3.1); a positive result of this test, i.e. one in which the remanence vectors across the fold are significantly better grouped after "unfolding" than before, constitutes strong evidence for a pre-folding origin of the remanence.

Despite the excellent stability evidence, the Bell Island formations suffer from the limitation that a fold test is not applicable; moreover, the age of tilting, though possibly Devonian (Chapter 5), is not known. Without a fold test it is generally difficult to assess the age of the magnetization, though some criteria for estimating roughly the age of the NRM and 685°C magnetizations at Bell Island will be discussed in Chapter 5. On that basis it is considered plausible, though not proven, that the 685°C component is a primary (Ordovician) magnetization residing in the precipitated hematite layers of the oolites. If this can be assumed, the acquisition of the 685°C component almost certainly predated the tilting of the Bell Island beds, so that the "correct" values of direction of magnetization are those obtained <u>after</u> tilt correction (i.e. relative to bedding). This has been done in Tables 4.16 - 4.20. In the case of group and formation mean directions for NRM, 350°C and 600°C, which probably represent the secondary and subsequent magnetic episodes but may or may not predate the tilting, the mean directions of magnetization are quoted both before and after tilt correction (Tables 4.20 - 4.22).

The tilt is quite uniform throughout the Bell Island sequence and, for the purpose of applying the tilt correction to the present results, it was always taken as

Strike: 75°; Dip: 10°NNW .

TABLE 4.16

Zone-mean directions (NRM) after tilt correction

Zone[1]	Fisher Statistics[4]							J[5]
	N[2]	Group[3]	D	I	R	k	α_{95}	
Z1	4	A	37.0	+16.2	3.997	1100	2.8	4.6
2	1	A	38.0	+17.7	–	–	–	4.4
3	2	A	72.2	+29.6	–	–	–	4.3
4	1	B	190.7	-10.5	–	–	–	8.0
5	2	A	45.9	-57.0	–	–	–	7.3
6	1	A	340.2	+30.1	–	–	–	5.7
7	1	A	11.8	-21.4	–	–	–	6.4
8	3	B	181.2	- 5.6	2.999	2800	2.3	6.4
9	3	A	351.6	+11.0	2.987	150	10.1	4.6
10	2	A	24.0	+12.1	–	–	–	5.1
11	4	A	19.6	+14.3	3.988	240	5.9	4.8

[1]See Table 4.15.

[2]Number of sites given unit weight.

[3]See Table 4.8.

[4]Symbols are as in Table 3.2.

[5]$\times 10^{-5}$ emu/cm^3, intensity of magnetization.

TABLE 4.17

Zone-mean directions (350°C) after tilt correction[1]

			Fisher Statistics					
Zone	N	Group	D	I	R	k	α_{95}	J
Z1	4	A	38.3	+17.1	3.983	180	6.9	5.3
2	1	A	36.1	+23.6	—	—	—	5.2
3	2	A	56.3	+26.4	—	—	—	6.4
4	1	B	195.1	-10.4	—	—	—	8.2
5	2	A	33.3	-45.5	—	—	—	8.1
6	1	A	255.1	+13.1	—	—	—	5.7
7	1	A	21.7	-27.3	—	—	—	7.4
8	3	B	184.0	- 9.0	2.996	500	5.5	7.0
9	3	A	347.2	+14.5	2.901	20	28.2	6.4
10	2	A	26.0	+12.9	—	—	—	7.3
11	4	A	15.7	+15.4	3.994	530	4.0	5.3

[1]Symbols are as in Table 4.16.

TABLE 4.18

Zone-mean directions (600°C) after tilt correction[1]

Zone	Fisher Statistics							
	N	Group	D	I	R	k	α_{95}	J
Z1	4	A	227.3	-21.8	3.936	47	13.6	7.5
2	1	A	242.2	-28.8	–	–	–	7.7
3	2	A	286.5	-26.2	–	–	–	6.7
4	1	B	259.9	-24.6	–	–	–	11.0
5	2	A	300.0	-29.5	–	–	–	9.4
6	1	A	262.1	-38.5	–	–	–	7.8
7	1	A	206.0	-10.6	–	–	–	8.6
8	3	B	214.8	-17.1	2.993	270	7.6	8.1
9	3	A	200.8	-15.9	2.852	14	34.9	8.2
10	2	A	204.4	-19.5	–	–	–	10.1
11	4	A	257.4	-26.7	3.787	14	25.4	7.4

[1]Symbols are as in Table 4.16.

TABLE 4.19

Zone-mean directions (685°C) after tilt correction[1]

			Fisher Statistics					
Zone	N	Group	D	I	R	k	α_{95}	J
Z1	4	A	127.8	-11.5	3.998	1200	2.7	3.0
2	1	A	129.2	-10.8	–	–	–	–
3	2	A	120.8	-11.1	–	–	–	3.1
4	1	B	123.3	- 9.7	–	–	–	3.8
5	2	A	129.3	-11.1	–	–	–	3.1
6	1	A	142.5	-10.7	–	–	–	3.1
7	1	A	121.9	- 8.8	–	–	–	3.4
8	3	B	121.7	- 8.1	2.999	1380	3.3	3.3
9	3	A	127.9	-11.7	2.998	1100	3.7	2.9
10	2	A	127.9	-10.5	–	–	–	3.1
11	4	A	119.3	- 8.7	3.987	230	6.1	3.0

[1]Symbols are as in Table 4.16.

TABLE 4.20

Group and formation mean directions (NRM) before and after tilt correction

Group and formation	N[1]	J[2]	Tilt correction: before D	before I	after D	after I
Group A						
Wabana	5	5.2	36.8	+17.6	35.1	+11.5
Airfield	4	5.2	12.5	+13.2	11.8	+ 4.3
Wabana and Airfield	9	5.2	24.4	+15.7	23.2	+ 8.0
Group B						
Wabana	1	8.0	191.9	-19.5	190.7	-10.5
Airfield	1	6.4	181.6	-15.2	181.2	- 5.6
Wabana and Airfield	2	7.2	186.7	-17.4	185.9	- 7.2

[1] N = number of stratigraphically non-overlapping zones (Table 4.15) given unit weight. All other symbols are as in Table 4.12.

[2] $\times 10^{-5}$ emu/cm^3, intensity of magnetization.

TABLE 4.21

Group and formation mean directions (350°C) before and after tilt correction[1]

NRM Group and formation	N	J	Tilt correction: before D	before I	after D	after I
Group A						
Wabana	5	6.1	34.8	+23.2	31.4	+18.9
Airfield	4	6.6	13.4	+13.3	12.7	+ 4.4
Wabana and Airfield	9	6.4	22.6	+18.0	20.7	+10.9
Group B						
Wabana	1	8.2	196.4	-19.0	195.1	-10.4
Airfield	1	7.0	190.8	-18.4	184.0	- 9.0
Wabana and Airfield	2	7.6	193.6	-18.7	189.5	- 9.7

[1]Symbols are as in Tables 4.16 and 4.20.

TABLE 4.22

Group and formation mean directions (600°C) before and after tilt correction[1]

NRM Group and formation	N	J	Tilt correction: before D	before I	after D	after I
Group A						
Wabana	5	7.8	271.5	-28.2	263.2	-21.9
Airfield	4	8.6	218.9	-25.8	215.6	-19.6
Wabana and Airfield	9	8.2	248.0	-29.7	240.8	-28.4
Group B						
Wabana	1	8.1	264.3	-23.4	259.9	-14.6
Airfield	1	8.1	217.6	-23.3	214.8	-17.1
Wabana and Airfield	2	9.6	240.9	-25.2	236.8	-22.4
Group A and Group B	11	8.9	246.6	-28.8	239.9	-27.3

[1]Symbols are as in Tables 4.16 and 4.20.

From measurements made by the author at 9 sites of the Wabana and Airfield formations, these values are estimated to apply within ± 5^{o} (strike) and ± 3^{o} (dip) in the great majority of cases. Since a 10^{o} dip is used in the tilt correction, the maximum change in direction of the remanence vector is $\leq 10^{o}$.

4.3.2. Statistical analysis of the results

Within-zone Fisher statistics are not given in the case of zones Z2 - Z6 (Wabana formation) and Z10 (Airfield formation) because the number of sites is only 1 or 2. Statistics for group and formation mean directions were also omitted in the case of groups A (NRM) and C (600^{o}C) because they are based on smeared distributions, each having a wide spread in longitudes.

The group D (685^{o}C) mean directions for the 11 non-overlapping zones are well-grouped (k = 160) and give an overall mean direction after tilt correction of D = 126.5^{o}, I = -10.3^{o} (Table 4.23) for the 150-meter Wabana-Airfield sequence. This is not significantly different from the corresponding directions based on 24 sites (D = 125.4^{o}, I = -10.3^{o}; k = 190). Since, in the latter case, the weighting is biassed towards certain stratigraphic levels at which two or more sites occur, the similarity between these two directions suggests that throughout the Wabana-Airfield sequence, vertical as well as horizontal changes in the 685^{o}C direction are insignificant. This is consistent with the relatively large between-site and betwee-zone precisions, k. Geological and paleomagnetic implications of this finding will be discussed in Chapter 5.

TABLE 4.23

Group and formation mean directions (685°C) after tilt correction[1]

NRM Group and formation	Fisher Statistics						
	N	D	I	R	k	α_{95}	J
Group A							
Wabana	5	129.9	-11.1	4.964	110	7.3	3.0
Airfield	4	124.2	-10.0	3.991	320	5.1	3.1
Wabana and Airfield	9	127.4	-10.6	8.944	140	4.3	3.1
Group B							
Wabana	1	123.3	- 9.7	—	—	—	3.3
Airfield	1	121.7	- 8.1	—	—	—	3.3
Wabana and Airfield	2	122.5	- 8.9	—	—	—	3.5
Group A and Group B	11	126.5	-10.3	10.937	160	3.6	3.3

[1]Symbols are as in Tables 4.16 and 4.20.

4.4. Thermomagnetic analysis

4.4.1. Effect of heat treatment

In section 4.1.6, it was seen that the scattering of remanence directions above the effective cleaning range (685 - 690°C) is accompanied by an intensity increase of 1 - 2 orders of magnitude. This may be due to some unknown physical or chemical changes produced by heat treatment. Although stepwise thermal demagnetization is used extensively to study stability in red sandstones, the effect of heat treatment on their magnetic properties has not been widely examined, though results of work on magneto-chemical effects of heating have been reported by Kobayashi and Schwarz (1966) and Stephenson (1967).

According to Stephenson, the reduction of the external field to zero during demagnetization does not necessarily mean that any magnetic material produced during heating will fail to acquire a magnetization. It is possible that superexchange processes may be effective across the boundaries between old and new material, or else, the newly forming mineral may be acted upon by the magnetostatic field due to a nearby magnetic grain.

Therefore, the cause for the increase in intensity beyond 690°C was further investigated by a thermomagnetic analysis.

4.4.2. Thermomagnetic measurements

Broadly defined, a thermomagnetic analysis is any study of the change of a magnetic parameter with temperature; the stepwise demagnetization

described in section 4.1 fall in this category. However, the stepwise technique has the serious drawback that an irreversible chemical or physical effect on the magnetization brought about by heating may remain undetected, since the remanence is remeasured only at room temperature. More information, including better clues about the minerals responsible for the remanence, might be obtained from experiments in which the magnetization is measured continuously during a heating-cooling cycle, e.g. by high-temperature astatic magnetometer (Collinson et al., 1967).

In the present investigation, the immediate aim of a continuous analysis was to test the explanation proposed in section 4.1.3 for the observed increase in the intensity of magnetization after stepwise treatment: namely, that preferential demagnetization of opposed components present in the NRM is responsible. For this purpose, the high-field intensity of some powdered Bell Island specimens was measured in air at normal pressure during heating to 700°C and cooling. In the following text, use of the term "thermomagnetic analysis" will be restricted to these measurements.

The instrument used was a magnetic balance designed and built by Mr. L. G. Kristjansson of the Physics Department, who also kindly carried out the experiments described below; this instrument which is described in Deutsch et al. (1970) is capable of measuring Curie points in most basaltic and red sedimentary rocks to ± 15°C.

The powders are heated in a small, stationary furnace surrounding the sample cup, the heating current being adjusted by a variac. Temperatures are measured to about ± 5°C with a Pt-Pt/10% Rh thermocouple. Heating to 685°C and cooling to room temperature takes

40 - 50 minutes each. For the present experiments an 0.5-gram sample of rock was powdered to sand texture in a mortar. The field at the gap centre (usually 1,100 oersteds) was maintained constant during an experiment. The compensating currents required to null the deflection were plotted for different temperatures and Curie points obtained from the slopes of the heating curves in the usual way. These curves are roughly analogous to curves of high-field magnetic susceptibility vs. temperature.

4.4.3. Results of thermomagnetic measurements

Ten previously untreated powdered samples from the Wabana and Airfield formations were studied. In all cases during the initial heating stage, the magnetizations increased significantly over the temperature inverval 20 - 650°C, and decreased sharply during further heating to 675 - 685°C, at which temperatures the normalized magnetic moment, M/M_{20}, had usually fallen to 0.2. Fig. 4.4a shows a typical M-T curve for a Wabana specimen, with a Curie point of about 680°C. This is close to the Curie point of hematite, suggesting strongly that the component of discrete magnetization described as the 685°C (group D) component in section 4.1 is, in fact, hematite. Moreover, the absence of any sharp drop of magnetic moment with increasing temperature up to 600°C suggests that magnetite is absent or insignificant. Similar behaviour was shown earlier by stepwise treatment (Figs. 3.8, 3.10), though it must be remembered that the observations made with the magnetic balance

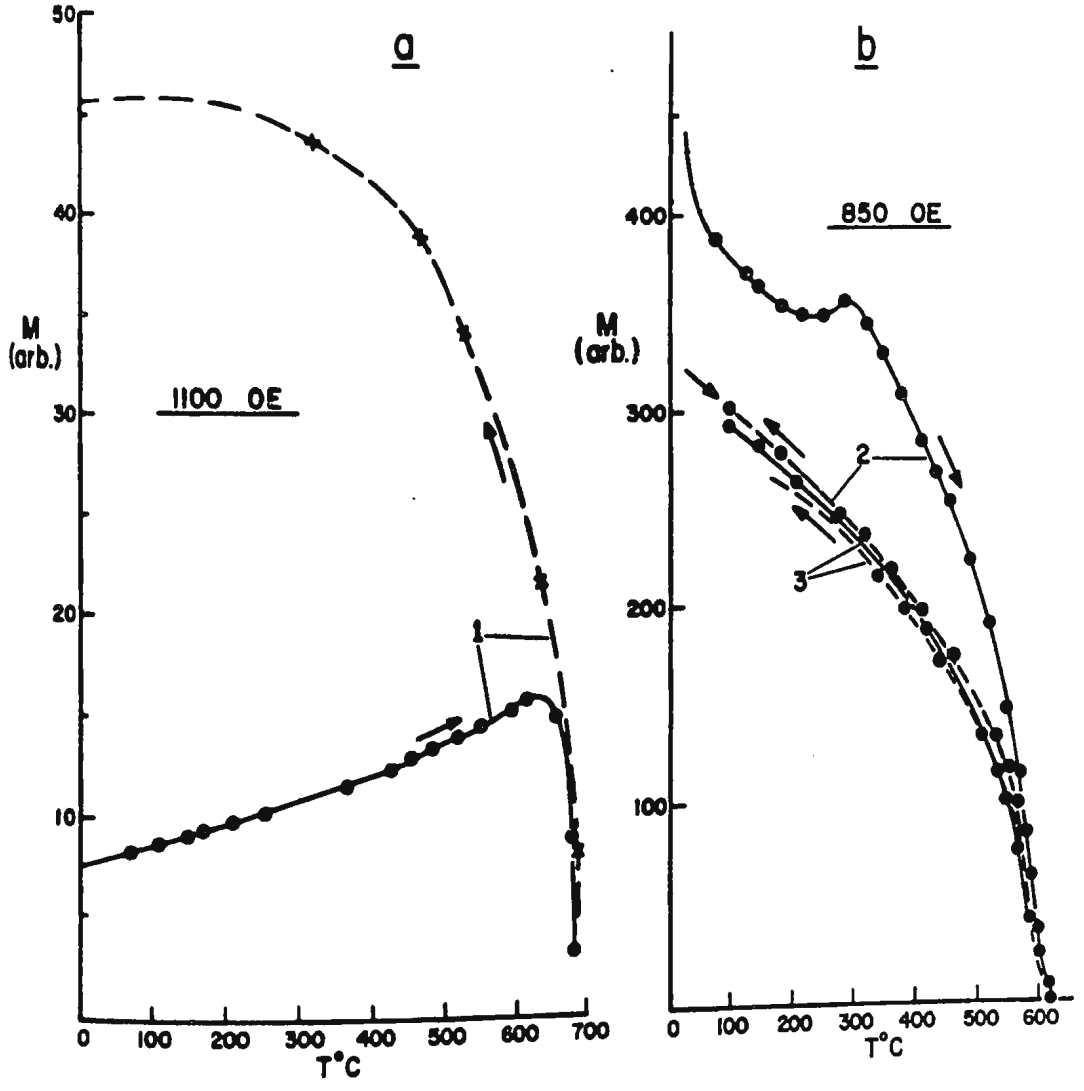

Fig. 4.4 Thermomagnetic (M-T) curves for single powdered specimen from Wabana formation

(a) Heating (solid line) and cooling (broken line) of fresh powder (1) in 1100 oersted
(b) Further heating-cooling cycles (2,3) of the same powder in 850 oersted

M: magnetic moment (arbitrary units)

differ fundamentally from those in the stepwise treatment, which represent remanence measurements on whose specimens that have cooled to atmospheric temperature in zero field.

The most interesting feature of all ten curves (see example in Fig. 4.4a) is the significant increase in M up to 600°C, which cannot be caused by a directed remanence, as the specimens in the present experiments were powdered. Therefore, the thermomagnetic analysis shows conclusively - at least in the case of the samples subjected to both types of analysis - that the J/J_{20} increase up to 600°C in the stepwise analysis cannot be due simply to the preferential demagnetization of two opposed components in the NRM, though the directed remanence may play a part. In view of the close similarity in behaviour of all Bell Island samples in the stepwise study, this conclusion most probably applies to all samples studied.

Examination of the cooling curves in the first heat treatment always produced a sharp increase in the magnetic moment, e.g. by a factor of 6.2 in the example shown in Fig. 4.4a. This type of thermal irreversibility can have several causes (Nagata, 1961) such as the transformation of an unstable ferromagnetic substance to a more stable phase, or remixing of exsolved phases or possible chemical changes during heating. Chevallier (1951) reports many examples of irreversible thermomagnetic curves for hematite obtained in moderately strong magnetic fields ($\sim 10^2$ oersteds). Nagata (1961; p. 142, 211) mentions that for hematite and titanohematites the thermomagnetic curves are always irreversible in a fairly strong field, pointing out, however, that the reason is not well understood.

The thermal irreversibility noticed in the present thermomagnetic experiments would be consistent with the formation of a strongly magnetic component through chemical change during heat treatment. This possibility was further investigated by subjecting the powders to a second heating-cooling cycle, in 850 oersteds (Fig. 4.4b, curves 2). In the heating stage, the magnetization, unlike previously, decreased gradually and fell almost to zero at 600 - 620°C; the curve obtained during the subsequent cooling lies above the heating curve, as before, though the irreversibility is now less pronounced. The experiment was repeated again, giving off curves (Fig. 4.4b, curves 3) that closely reproduced the second heating-cooling cycle.

The experiment was repeated again, yielding now almost identical heating and cooling curves, which again disappear at or just below 620°C (Fig. 4.4b, curves 3).

4.4.4. Summary of thermomagnetic results

Thermomagnetic experiments using powdered Bell Island material in air have shown that:

(1) In the first heating, the magnetization always increased until 600°C, after which it decreased sharply up to 675 - 685°C (Fig. 4.4a), suggesting a Curie point near 685°C, which is close to that of hematite.

(2) The heating curves obtained in (1) resemble the stepwise demagnetization curves (e.g. Figs. 3.8, 3.10), which also had intensity maxima at 600°C and minima at 685°C. This is despite the fact that the

stepwise procedure, in contrast to the thermomagnetic one, measures remanence components acquired in an ancient field and only after the rock has cooled to room temperature.

(3) The thermomagnetic cooling curves following the first heating show a very large intensity increase (by factors of 6.2 to 7.3) compared with the heating curves. This irreversibility in the first heating-cooling cycle (Fig. 4.4a, curves 1) resembles results from hematite-bearing samples reported in the literature (Chevallier, 1951).

(4) The above large intensity increase may be compared with that observed in stepwise demagnetization to 750°C (Fig. 4.2).

(5) After the second heating-cooling cycle, the extent of irreversibility was reduced, and a new Curie point was indicated at, or just below, 620°C (Fig. 4.4b, curves 2). A similar apparent Curie point resulted from the third heating and cooling, which gave nearly reversible curves (no. 3).

Interpretation of the above data must remain limited, pending a more complete investigation of certain experimental factors, such as the grain size of the samples as well as their preparation, and the atmosphere surrounding the sample as well as the heating rate and maximum temperature in the experiment.

With this limitation in mind, the most plausible explanation of these results is that a strongly magnetic component with a Curie point in the range 610 - 620°C is formed during heat treatment, both in the stepwise and thermomagnetic procedures and that, in the latter procedure, the process of formation continues until completion of the third heating-cooling cycle to 700°C. The excellent directional grouping associated with the D-component suggests that the mineral responsible (most probably

hematite) co-exists up to about 685°C with the new material produced by the heating, which is non-ferromagnetic above 620°C. The new material appears to have no effect on the remanence direction of the D-component, which is an important conclusion enabling one to interpret this component paleomagnetically.

Assuming the above explanation is correct, it remains to identify the new, heat-produced component. The only two likely iron oxides capable of producing the large observed magnetizations seem to be magnetite (Fe_3O_4) and maghemite (γ-Fe_2O_3). However, magnetite is almost certainly ruled out because of its low Curie point (578°C, which is further reduced in titanomagnetite), and probably also by the results of the AF demagnetization of the D-component (Section 4.6), which suggests that the bulk coercivity of the mineral responsible (probably hematite) is much higher than would be expected if magnetite were significantly present. The possibility that maghemite may be responsible for the heat-produced component will be discussed in sections 4.4.5 and 4.4.6.

4.4.5. Preliminary X-ray diffraction data

In a further attempt to identify the heat-produced component, some X-ray diffraction spectra were obtained with the Philips unit, available in the Geology department at Memorial University, through the kind assistance of Mr. H. Keats of that department. Two powders were prepared from one sample each of the Wabana and Airfield formations; for each sample, the first powder was fresh and the second was derived from a specimen that had been heated to 700°C in air.

Typical diffraction spectra obtained from one heated and one unheated powder of the Wabana sample (Wa 2-1) are shown in Fig. 4.5, where relative intensity (I/I_1) is plotted against Bragg angles (2θ). In the unheated sample, two prominent peaks (I/I_1 = 95 and 80) corresponding to $2\theta = 42^0$ and 45^0, respectively, reveal the presence of hematite.

In the heated sample, one observes (i) a pronounced peak (I/I_1 = 34) at $2\theta = 38^0$; (ii) a larger peak (I/I_1 = 90) at $2\theta = 42^0$ which is slightly reduced in intensity compared with the unheated sample; and (iii) an M-shaped peak, which is superposition of two peaks, at $2\theta = 45^0.2$ and $45^0.4$, with I/I_1 = 80 and 95, respectively, and which replaces the 45^0 (I/I_1 = 80) peak for the untreated sample. Peak (i) which was absent in the heated sample can be due to magnetite or maghemite (but not hematite) for which the I/I_1 values quoted in standard tables are 60 and 34, respectively; the latter value is identical to the observed value, though this in itself is insufficient evidence to rule out magnetite. The larger observed intensity in the M-shaped peak (iii) cannot be due to hematite, but again could be either magnetite or maghemite (quoted I/I_1 = 100 in both cases). The similarity in the spectra for the latter minerals is due to their close minerological similarity, both being inverse spinels (cubic), with approximately equal cell dimensions. Maghemite may be considered to be approximately equivalent to magnetite that is deficient in one out of nine Fe sites in the unit cell (Nagata, 1961).

Thus, the preliminary X-ray diffraction data suggest that a new mineral, which could be either magnetite or maghemite is formed after heat treatment to 700^0C in samples that contained hematite, but no

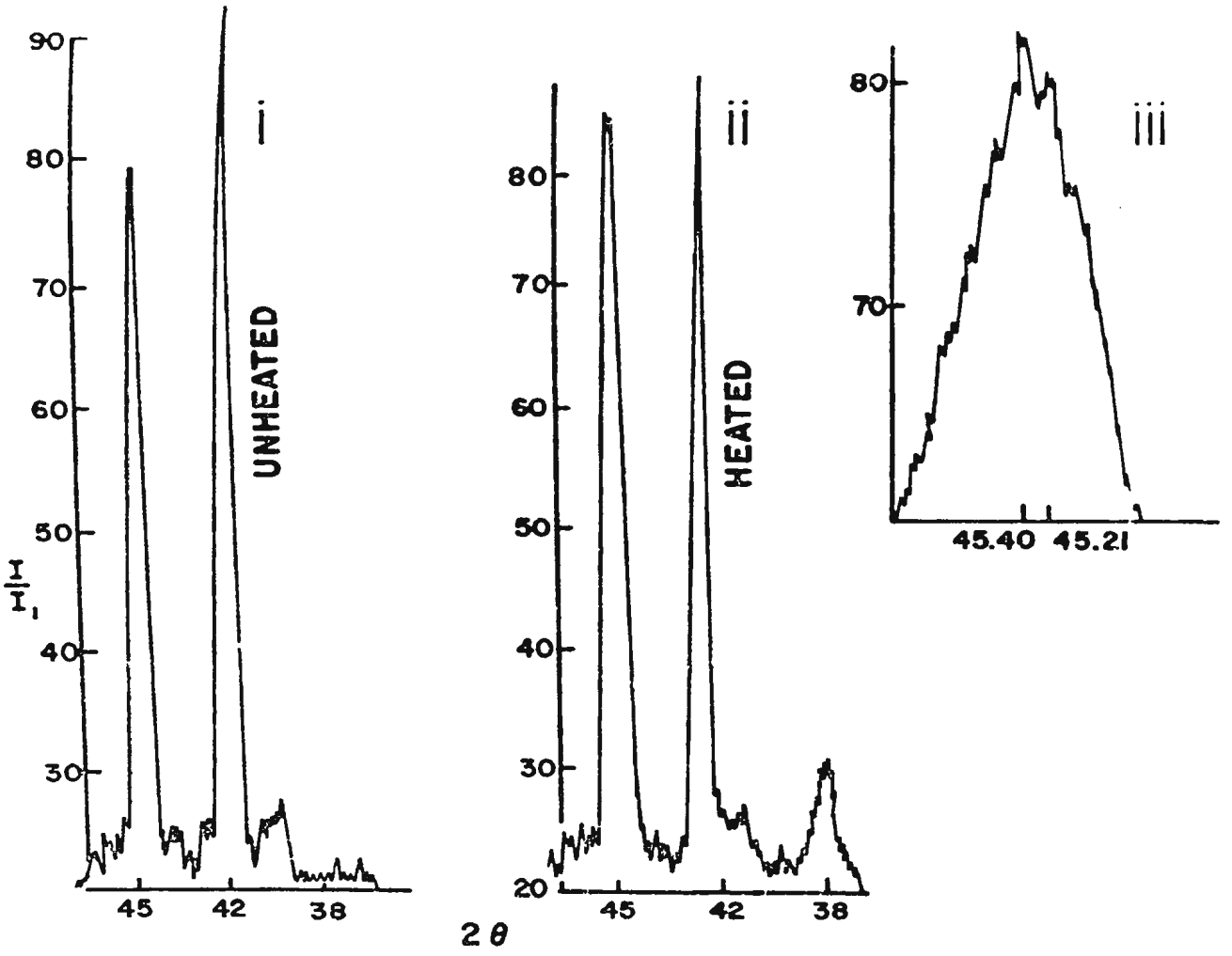

Fig. 4.5 X-ray diffraction spectra for a Wabana sample

(See p. 142 of text)

significant amounts of either magnetite or maghemite before the treatment. That a new ferromagnetic material has been formed by the heat treatment, is fully consistent with the results of the stepwise and thermomagnetic experiments.

Reasons for discounting magnetite as a plausible product of the heat treatments have been given (Section 4.4.2). It was therefore concluded that maghemite is the most likely mineral responsible for the heat-produced mineral responsible for the heat-produced phenomena described. It should be emphasized, however, that this conclusion is tentative pending confirmation by further X-ray diffraction and other analyses.

4.4.6. Occurrence of maghemite

Van der Marel (1951) and Van Houten (1968) report maghemite (γ-Fe_2O_3) as a common mineral in sediments rich in iron and organic matter, where it can also be produced by moderate heating (100 - 300^{o}C) through dehydration of oxyhydroxides such as lepidocrocite (γ-FeOOH). Kelly (1956) reports that poorly crystallized goethite (α-FeOOH) can break down to maghemite and then to hematite at atmospheric temperatures. Van Houten mentions the presence of maghemite both in the specularite and pigment of red sandstones.

While the existence of maghemite at atmospheric temperature or its production through moderate heating is well established, the rock magnetic literature seems to include no clear evidence for the generation of maghemite at higher temperatures, nor are the high-temperature

properties of that mineral, including Curie point, as yet adequately understood. At first sight this is not surprising, in view of the well-documented metastability of maghemite and its common inversion to hematite at low temperatures, often < 300°C (e.g. Bagin, 1961; Nagata, 1961).

Under the right conditions, however, the persistence of stable maghemite to temperatures well in excess of 300°C may not be exceptional. E. Thellier (discussion in Creer, 1962) believes that the tendency of destruction of maghemite by moderate heating has been overemphasized in the literature and cites Michel (1963) who found that under certain chemical conditions maghemite very stable to heating can be produced. As Collinson (1968) points out, a major increase in susceptibility is often observed in thermal demagnetization experiments to 500 - 700°C[1]; this could be due to magnetite (Stephenson, 1967) or "possibly" maghemite production, though Collinson considers magnetite to be an unsatisfactory alternative, when the specimens are heated in an oxidizing atmosphere.

A mechanism that may be pertinent to the present investigation was proposed by Rowland and Jonas (1949) who found that heating siderite ($FeCO_3$) in air to 700°C produced hematite and a spinel, which they suggest might be maghemite, though magnetite cannot be ruled out. Since

---

[1]This is borne out also by susceptibility measurements, carried out in the earth's field on three Bell Island specimens (Af 3-3, 4-1 and Wa 2-1) using a Scintrex (Model SM-4) bridge. The specimens were measured before heating and after cooling successively from 300, 500, 600, 700 and 850°C. The specimens gave comparable results, showing increases in susceptibility by factors of about ten and twenty, after the 600°C and 850°C steps, respectively.

siderite (which, along with chamosite, does not normally occur in red-beds) is a major constituent of the oölitic matrix at Bell Island, it thus might serve as the source for the production of maghemite by heating. Rowland and Jonas, repeating their experiments with nitrogen as an atmosphere, found that at 700°C an even larger amount of spinel was generated than in air, while in their differential thermal analysis, an exothermic peak attributed to oxidation of FeO was suppressed. These findings appear to be compatible with the results using nitrogen, described in section 4.5.

In section 4.1 it was shown that the 685°C remanence direction belived to reside in hematite seems to be unaffected by the new material (maghemite?) produced during heating. In attempting to explain this rather surprising result, one might obtain a clue from some experiments performed by Porath (1968), in which artificial specimens containing only maghemite were heated to 580°C in a small applied field. In this process, most of the maghemite inverted to hematite (compared with the production of maghemite in hematite-bearing rock inferred at Bell Island), but the CRM of the hematite was not controlled by the host mineral, maghemite. Porath explained the results by invoking spin exchange interactions which would align the magnetization direction of the residual maghemite along the direction of the hematite.

Results pointing to high-temperature stability of maghemite have also been reported by Van der Marel (1951), who found that maghemite originally present in soils (but not when produced by oxidation from magnetite) persisted without inversion to hematite during 2 hours of heating at 600°C. Similarly, Wasilewski (1969) found maghemite to be more stable than magnetite above 300°C.

The considerable uncertainty regarding the Curie point of maghemite arises from its metastability and the difficulty of identifying the mineral at high temperatures. In view of this, indirect methods are used: e.g. O'Reilly (1968), applying an extrapolation technique, calculated the AB lattice interactions of various spinels, obtaining T_c = 770°C for maghemite. Other estimates of T_c for maghemite are lower, Michel and Chaudron (1935) obtaining 675°C, and Wasilewski (1969), 550 - 600°C and in one case 620°C. Bannerjee (1965) quotes a still lower value (545°C) that may be simultaneously the Curie point and the inversion temperature of the mineral. From Irish laterites, Wilson (1961) reports Curie points slightly over 600°C, attributed to maghemite. Possibly relevant to this are results quoted by Wilson and Smith (1968), who found that heating had increased T_c in various volcanic and baked rocks, probably due to oxidation. Values of T_c = 600 - 620°C were common in their samples such as Icelandic laterite, though maghemite was not necessarily the carrier.

The foregoing discussion shows that (i) under certain conditions, maghemite in rocks may remain stable without inverting to hematite, even when maintained for some hours above 600°C; and (ii) a Curie point of about 610 - 620°C for maghemite, though far from definite, is compatible with some of the reported data. Hence the proposal in the present investigation that maghemite is produced during heating (possibly due to the presence of siderite) does not conflict with the published evidence.

4.5. Pilot thermal demagnetization in nitrogen

Stepwise thermal demagnetizations in nitrogen were performed on eight fresh specimens representing two and six samples from the Wabana and Airfield formations, respectively. Five of these were successively heated to 300, 500, 575 and 685°C, the other three only to 500°C step. These experiments were performed to compare the results with those of in air.

The NRM directions of magnetization (not shown) changed only moderately up to the 500°C step, similar to the earlier results using air. However, in the five specimens taken to 685°C, the grouping became poor, particularly with respect to declination, and the D-component was not observed. The intensity changes are plotted in Fig. 4.6, showing that, contrary to all results of the stepwise treatment in air, J decreased rather than increased up to 500°C. However, after the 685°C step, J has increased spectacularly by up to two orders of magnitude.

These results are consistent with the production of magnetite above 500°C (presumably through reduction of the hematite), though verification of this would require further tests, e.g. to measure T_c. Blackett (1956) reports that thermal demagnetization of redbed samples in nitrogen caused them to darken, though without the production of magnetite; on the other hand, Leng (1955), Chamalaun and Creer (1964), Irving and Opdyke (1965) all report anomalous results after heating in nitrogen, which they ascribe to generation of magnetite. To avoid this, the thermal demagnetization of redbed samples for paleomagnetic purposes should be carried out in air or oxygen-rich atmospheres (Schwarz, 1969).

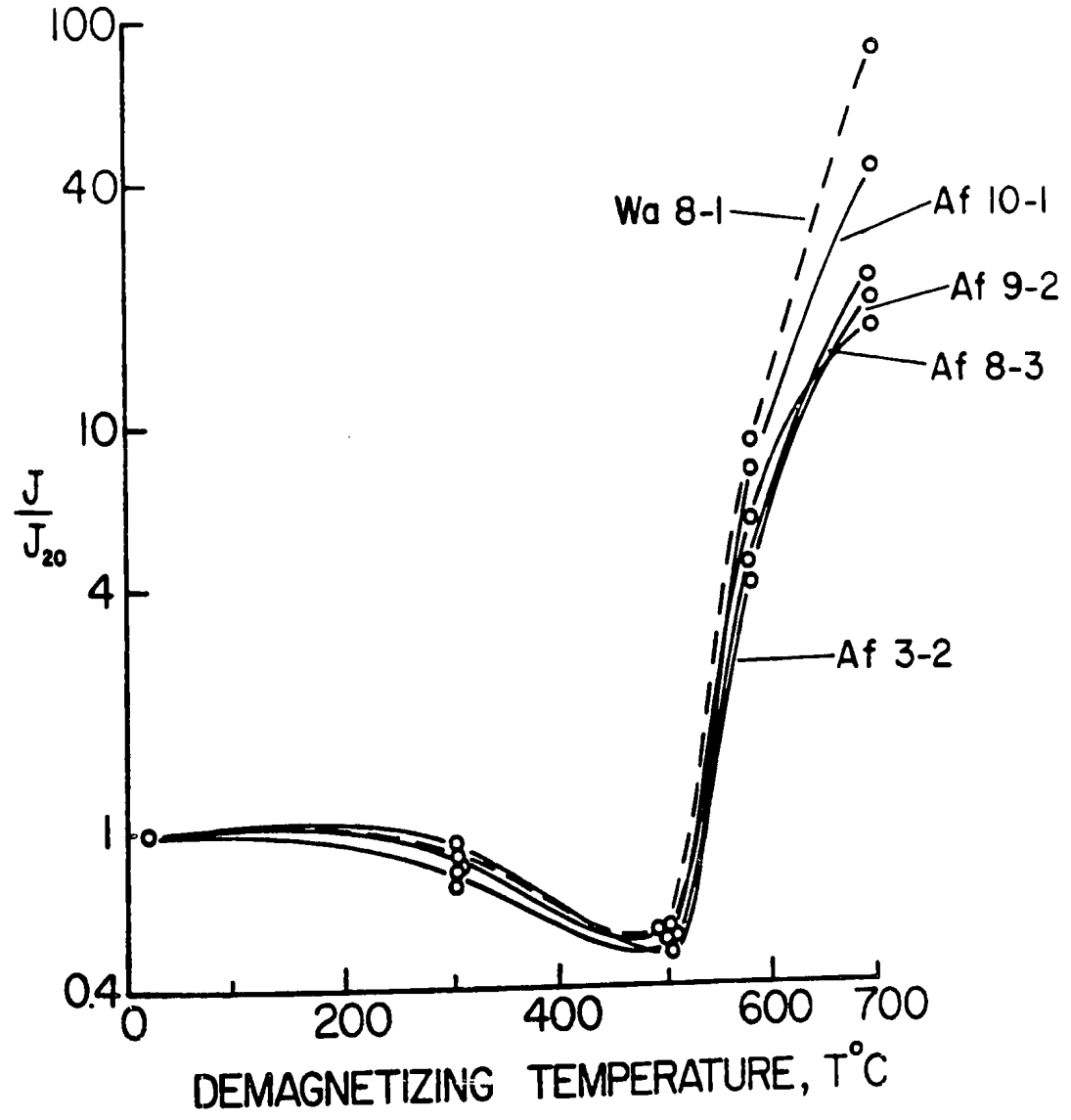

Fig. 4.6 Normalized intensity, J/J_{20}, of single specimens after stepwise thermal demagnetization in nitrogen

If, in the present test, the material formed in nitrogen was indeed magnetite, then production of magnetite in the treatments using air was probably suppressed. From the previous discussions, this would be compatible with the proposed production of maghemite by heating.

4.6. Pilot alternating-field (AF) demagnetization

AF demagnetization is useful for removing components of relatively low coercivity from the NRM, leaving intact the remanence directions of the magnetically harder, perhaps original, components. The method has proved successful in the case of igneous rocks where unstable VRM's of relatively recent origin can often be separated from the component of interest.

AF techniques are now standard, and details can be found in Collinson et al. (1967). The unit with 3-axis tumbler used in the Physics Department is described by Pearce (1967). AF treatment has the substantial advantage over thermal methods that chemical changes are avoided. However, its sole use in the case of redbed specimens is not generally recommended (Irving, 1964), since redbeds often contain hard secondary components that are difficult to distinguish in the coercivity spectrum from the primary component.

The present AF test was made (i) to obtain a check on the thermal results in terms of stability, and (ii) to compare the AF-stability of the group D component with that of the NRM.

One fresh specimen each from the Wabana and Airfield formations was subjected to successively higher fields up to 800 peak oersteds. The

changes in intensity and direction of magnetization are shown in Fig. 4.7 (curves 1 and 2). Clearly, the entire remanence is highly stable against alternating fields of the order of 800 oersteds. This is probably due to the presence of hematite, which is characterized by high coercivity commonly exceeding 1000 oersteds in rocks (Irving, 1964).

A third specimen (Wa 2-1; curve 3, Fig. 4.7), which had been thermally demagnetized to 685°C and hence retained only the group D remanence, was similarly treated. The results show the same remarkable stability against alternating fields as was displayed by the fresh specimens. Assuming that these results are representative, they strongly suggest that magnetite is insignificant in both the NRM and the 685°C component, since otherwise Fig. 4.7 would have shown some directional scatter or a major reduction in intensity after AF treatment. The results are also comparable with the idea (Section 4.1.3) that the group D component resides in hematite, possibly in association with the heat-produced material, and that this material is maghemite.

Finally, the results provide an excellent example of the limitations of the AF technique in the case of redbeds, for in the absence of thermal treatment, the C- and D-components, and hence the presumed primary magnetization, would not have been discovered, possibly not even if higher fields had been used. Thus, paleomagnetic results in the literature based on redbed studies in which stability tests comprised only AF treatment to a few hundred oersteds or less must be regarded as inconclusive.

Fig. 4.7 Normalized intensity, J/J_{20}, and direction, after stepwise alternating-field demagnetization of single specimens from the Airfield (▲) and Wabana (O) formations

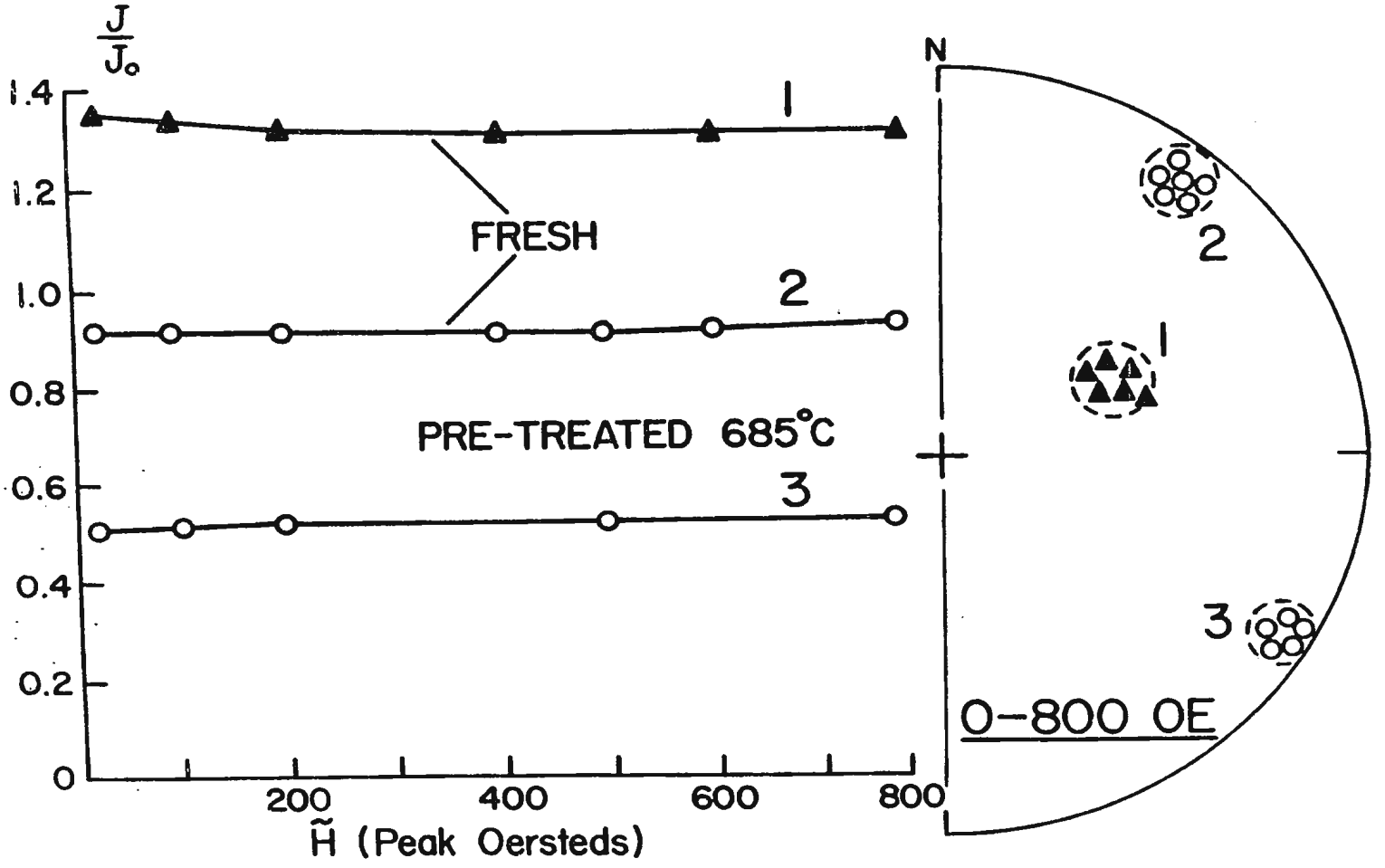

1,2: fresh specimens. 3: specimen previously demagnetized in air to 685°C.
Solid symbols: N. Pole down, open symbols: up.
Dotted circles denote limits of directional change during treatment.

CHAPTER 5

THE ORDOVICIAN GEOMAGNETIC FIELD RELATIVE TO EASTERN NEWFOUNDLAND

5.1. Calculation of pole position

Paleomagnetic pole positions were calculated from the mean direction of magnetization for the NRM and the D-component (Table 5.1) in accordance with the axial dipole assumption (Chapter 1). The tilt correction was applied only to the D-component, which is plausibly of primary origin, as will be further discussed in section 5.2. Hence in Fig. 5.1, the pole corresponding to the D-component is shown with its associated 95% error oval, based on the 11 non-overlapping zones. Table 5.1 also shows the alternative statistics based on 24 sites; the pole positions for the two weightings are identical within experimental error, but the more conservative weighting based on zones ($dp = 1.8^{o}$, $dm = 3.6^{o}$) was preferred for the reasons discussed in section 4.3. For comparison, poles for the NRM groups A and B were also calculated and plotted in Fig. 5.1. Here, the error ovals are omitted because the mean directions are vector resultants incorporating the C- and D-components, and because of the large spread of declinations in the case of Group A.

5.2. Origin of magnetization of the Bell Island redbeds

According to Hayes (1915), the origin of the Bell Island iron ore deposits is due to oxidation of the precipitated hydrates of iron derived from earlier rocks. The decomposition of iron hydroxides

TABLE 5.1

Paleomagnetic pole positions for the Bell Island oölitic red beds from the mean directions of magnetization, before and after laboratory treatment (685°C)

Group and treatment	N	Mean directions of magnetization[1] D	I	k	α_{95}	Pole position	Antipole position	dp	dm
A (NRM)[2]	20 sites	25.8	+18.1	--	—	46°N 89°E	46°S 91°W	—	—
B (NRM)[2]	4 sites	184.1	-16.3	220	6.3	51°S 59°W	51°N 121°E	3.4	6.5
D (685°C)[3]	24 sites	125.4	-10.3	190	2.2	27°S 13°E	27°N 167°W	1.1	2.2
D (685°C)[3]	11 zones	126.5	-10.3	160	3.6	28°S 12°E	28°N 168°W	1.8	3.6

[1] See Tables 3.5, 4.9 and 4.19.

[2] Relative to present horizontal.

[3] After tilt correction (10°NNW).

dp, dm - semiaxes of the 95% oval of confidence.

Underlined pole and antipole positions and oval dimensions are as in Fig. 5.1.

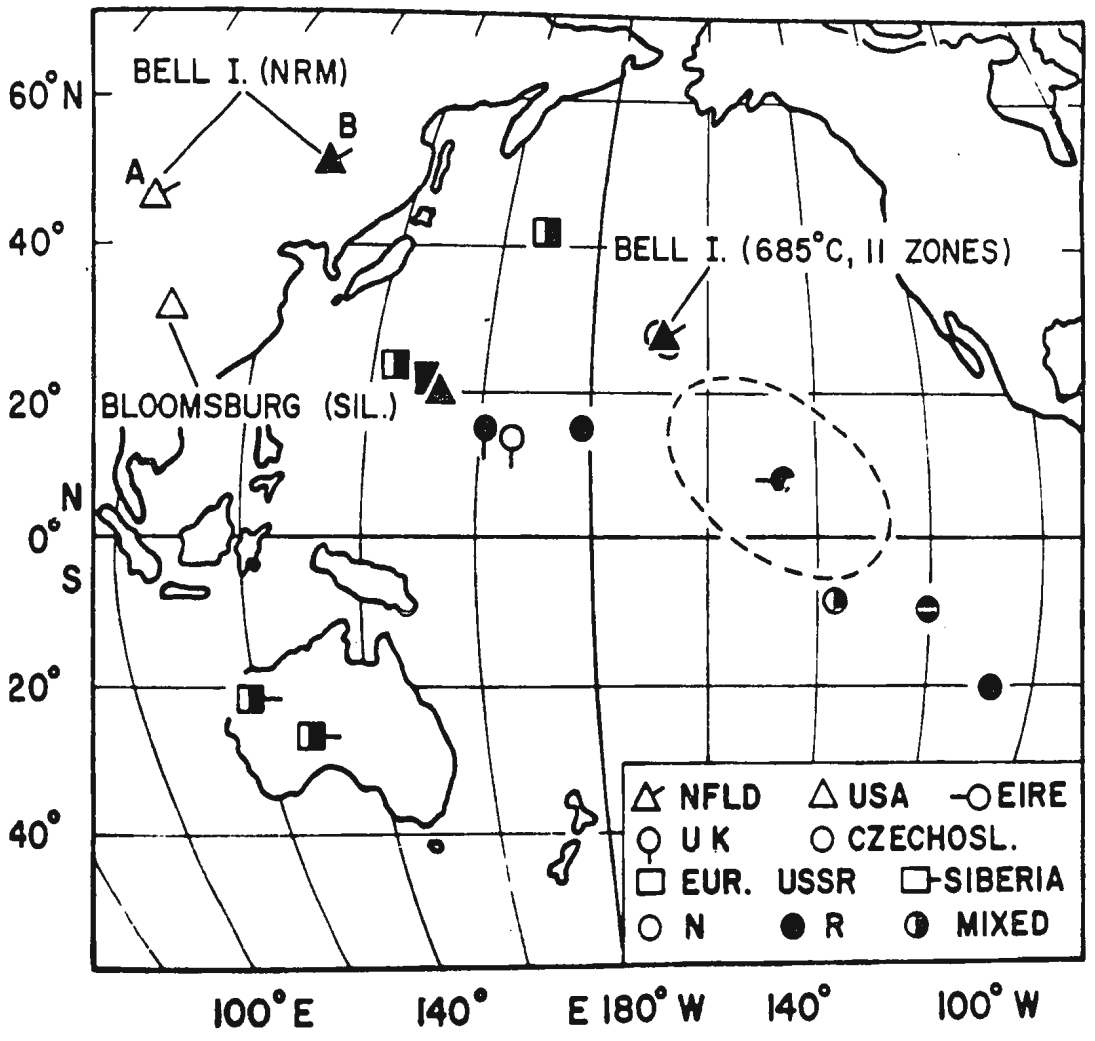

Fig. 5.1 Pole positions corresponding to the zone mean directions at Bell Island, compared with Paleomagnetic poles inferred from other Ordovician rocks in North America and northern Eurasia

Symbols refer to location of study and presumed polarity (see also Fig. 4 in Deutsch and Somayajulu, 1970). The 95% confidence ovals are shown along with the Bell Island (685°C pole and for comparison with the pole relative to Eire (4 Killary Harbour ignimbrite bands). The Bell Island NRM poles are based on site mean directions. The pole for the Silurian Bloomsburg formation (Roy et al., 1967) is shown for comparison. See also Table 5.1.

responsible for the formation of red sandstones is an example of a process favourable to magnetization, which may be acquired through the growth of iron oxide (e.g. hematite) particles by "nucleation" (Nagata, 1961) and in the present case would first occur near the nucleus of an oölite, which is almost always the site of grain growth during diagenesis. This would be accompanied by an increase in relaxation time when a critical size for domain formation has been attained, which would in turn favour the acquisition of a stable magnetization contemporaneous with the primary iron deposit.

5.2.1. Oölites as primary chemical sediments

Hayes' (1915) mechanism, corresponding to a primary, shallow-water, marine origin for the Bell Island ore zones, is still unchallenged in the literature, though Rose (1952, p. 51) quotes a view by T. L. Tanton, who considers these as replacement iron deposits by primary precipitates from mineralized solutions introduced into the already consolidated, fossil-bearing rocks of Arenig (Lower Ordovician) age; in this case, the time of the magnetization associated with ore formation is unknown and could be significantly later than the Ordovician. However, Tanton's view was not elaborated and hardly seems to be supported by the evidence.

Thus it would be difficult to explain the oölitic structure other than by original precipitation and accretion of alternating layers of hematite and chamosite about nuclear, clastic grains. The observed penetration of oölite grains by tubules of boring algae (Hayes, 1915) indicated their contemporaneity with ore deposition. Castaño and

Garrels (1950) made some experiments on the deposition of iron with special reference to the Clinton iron ore deposits, and inferred that formation of the iron ore by chemical precipitation in a marine environment is reasonable.

5.2.2. Diagenesis in oölitic ores

Processes that convert newly deposited grain into an indurated rock are defined as "diagenetic" (Pettijohn, 1957). Mainly diagenesis includes the processes of formation of new minerals; redistribution and recrystallization of substances in sediments; and lithification (Fig. 5.2). According to Fairbridge (1967), diagenesis begins at the moment a sedimentary particle comes to rest on the sea floor, and continues in three phases, namely (i) the sedimentation phase - "syndiagenesis", (ii) the compaction-maturation phase - "anadiagenesis", and (iii) the emergent-pre-erosion phase - "epidiagenesis".

The initial stage of phase (i), in which the composition of primary particles is controlled by the chemistry of the superjacent water is followed by the early burial stage, in which the particle gets entrapped and chemically modified by the bacteria and other subsurface organisms. Fersmann (1922) for the first time intended the term "syndiagenesis" to define oölite as a primary chemical sediment. Donahue (1969) suggests a "splash-cup" mechanism in which drops of solution fall from a ceiling into a depositional depression that gradually develops into the oölite due to repeated precipitation. Formation of oölites in situ in an oxidizing environment as a result of diagenesis pre-dating consolidation is mentioned in Amstutz and Bubenick (1967).

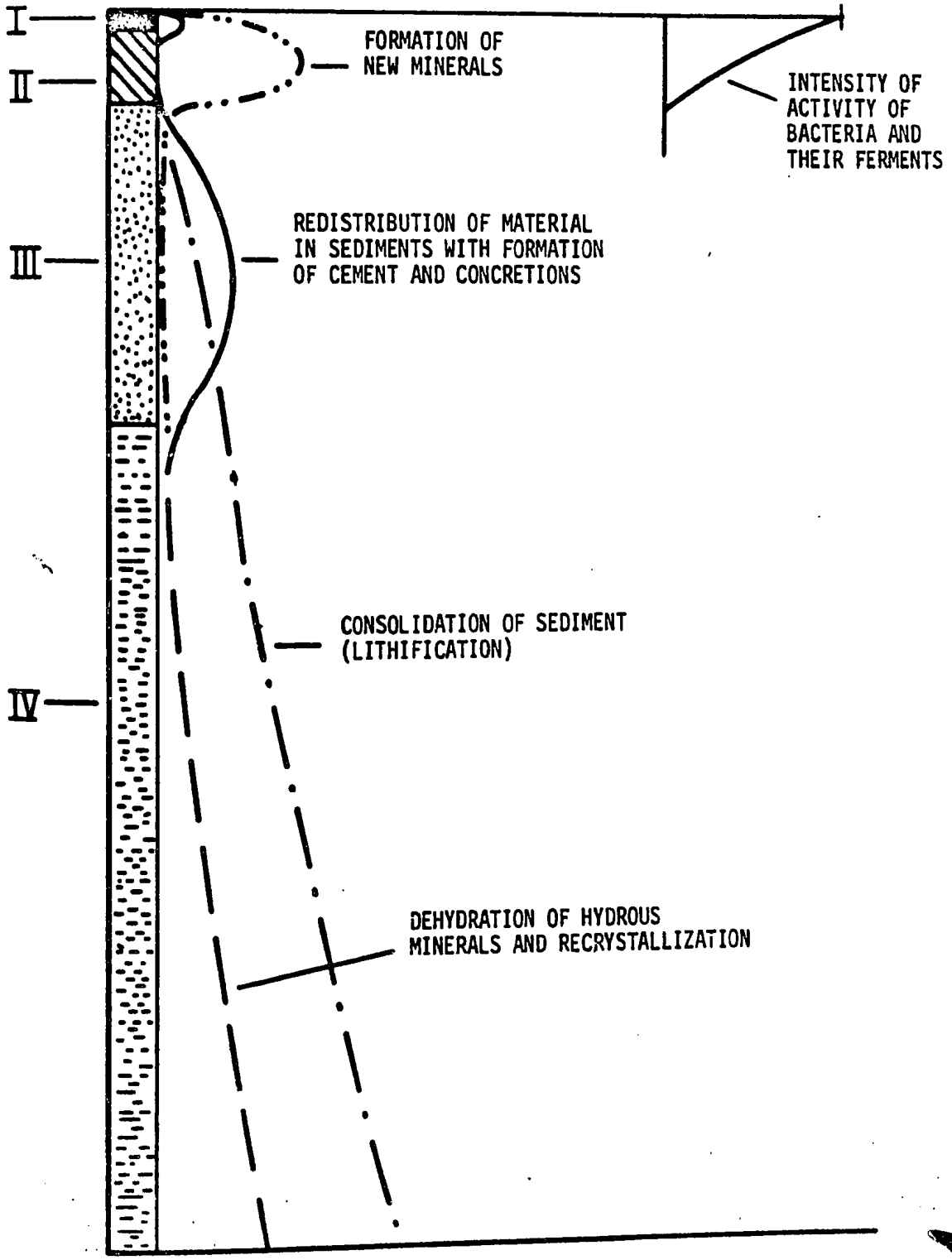

Fig. 5.2 Diagenetic stages in sediments
(Slightly modified after Strakhov et al., 1954)

The early burial stage is characterized by redistribution of material within the sediments, with formation of cement and concretions. This is the stage where breakdown of organic matter occurs, giving rise to formation of secondary minerals such as siderite (Fairbridge, 1967). These early processes appear to apply to the Bell Island ore where the oölites are penetrated by algae borings, whereas the siderite resulted from diagenetic replacement (Hayes, 1915). The duration of the initial stage of phase (i) varies from several days to 10^3 years (Larsen and Chillingar, 1967), whereas the whole syndiagenetic phase lasts for 10^3 - 10^5 years (Fairbridge, 1967).

The compaction and maturation phase (ii) is called lithification, which is characterized by cementation of the sediments during compaction, dehydration of minerals occurs, e.g. change of goethite into hematite. Perhaps the secondary hematite, which at Bell Island nearly always occurs at the outer rims of the oölites, is the result of phase (ii). Fairbridge quotes wide limits for the estimated duration of cementation from 10^3 - 10^5 years to 10^7 - 10^8 years.

The epidiagenetic phase (iii) is characterized by long-term compactional processes, the nature and distribution of which depends upon the changing environments and upon the extent to which phase (ii) was completed.

5.2.3. Origin of the high-temperature component

Petranek (1966) discusses certain common features of the shallow-water origin of early Paleozoic, particularly Ordovician oölitic iron ores

(Section 2.3). The paleogeographical setting of such ores reveals that most of them were deposited close to the shore on shallow flats in well-aerated environments.

From the foregoing discussion, one can infer that precipitated hematite layer in the growing oölite will have increased from very small dimensions to beyond critical size for the formation of a stable CRM through nucleation in the presence of the ambient field. This appears to be the most plausible mechanism responsible for the primary magnetization of the three redbed formations at Bell Island, all of which contain hematite oölites of similar structure.

Whether the D-component is, in fact, equivalent to this primary magnetization cannot be established beyond doubt in the absence of a fold test. It is not self-evident even that the D-component predates the A, B or C group magnetizations, which also give evidence of being stable and are possibly all CRM's. However, it was shown in Chapter 4 that the D-component is the only one associated with a discrete range of blocking temperatures and a Curie point close to that of hematite, above which the remanence tends to become random. It therefore seems almost certain that this component predates those in the A, B and C groups.

Assuming this, it does not necessarily follow that the D-component is the primary one, since no evidence of the primary field might have been preserved in the rock. However, if one accepts the view of oölite formation and diagenesis outlined above, it is difficult to escape the conclusion that at least the innermost hematite layers must have been magnetized as the beds were first laid down; conversely, if the D-component were due to some post-Ordovician event, one would then have to ask why the magnetization of the inner hematite layers should have disappeared.

It was therefore concluded that the D-component is most likely to represent a primary (Ordovician) direction of the geomagnetic field.

5.3. Paleomagnetism of the Bell Island rocks

The hypothesis that the Earth's magnetic field, when averaged over an adequate time span, closely approximates a geocentric axial dipole, and has done so in the past, was the basic assumption in calculating the geographical pole positions (Table 5.1). This is plausible on the basis of dynamo theory (e.g. Stacey, 1969) and is supported by some evidence from paleomagnetism (Opdyke and Henry, 1969) and paleoclimatology (Blackett, 1961), though it is difficult to confirm paleomagnetically with Lower Paleozoic and older rocks. Thus the Ordovician data for North America and Western Europe are still quite inadequate for a test of dipolar behaviour, as illustrated by the scatter of poles in Fig. 5.1. However, Rodionov (1966), measuring sedimentary rocks from a large area in Siberia, found his results consistent with a dipolar field during the Ordovician and late Cambrian. In summary, the assumption that the Bell Island redbeds were magnetized in a (presumably geocentric) axial dipole field is likely to be justified, though not proved.

5.3.1. The Paleosecular variation[1]

Assuming that the pole computed from the D-component (Fig. 5.1)

[1] "(Paleo) secular variation" is here used in a broader sense, to include both the actual secular variation (10^3 - 10^4 y.) and possible longer-term asymmetries (10^5 - 10^6 y.; Hide, 1967).

indeed corresponds to a primary field, one might at first expect the dispersion about its mean direction to provide knowledge about the paleosecular variation during Ordovician time; this requires also that the latter be distinguishable in the data from the various other sources of scatter (Section 4.2). A direct measure of this dispersion is the size of the error oval in Fig. 5.1 ($dp = 1.8^{o}$. $dm = 3.6^{o}$). On any basis of comparison (e.g. tabulations in Irving, 1964), this reflects remarkably close grouping of the mean directions, even more so, if one considers that the most conservative statistics (i.e. unit weight given to 11 zones) were applied. The absence of a significant between-site scatter is also indicated by the F-test (though not clearly, for the reasons given in section 4.2.3).

Khramov (1967) quotes present rates of accumulation for littoral-type deposits (which includes the Bell Island redbeds) as 0.3 - 3 meters per millenium, pointing out that considerably smaller rates must have prevailed in the geological past. This would correspond roughly to 10^4 - 10^5 years or perhaps much longer, for the deposition of the 450-meter section including the Townsquare, Airfield and Wabana formations. If rate of deposition and total thickness were the only relevant factors, one might conclude that this is adequate for preserving a record of the paleosecular variation.

However, if the D-component is a CRM acquired through nucleation (Section 5.2.3), then the time required for stabilizing this magnetization was probably at least as long as the duration of the syndiagenetic phase, i.e. 10^3 - 10^5 years. This is not less than the secular variation, which therefore could have been smoothed out. This would support the conclusion

by Creer (1962) who maintains that redbeds whose magnetization is of chemical origin are unsuitable for paleosecular variation studies.

From this context it is interesting to estimate the expected magnitude of secular variation. Cox (1962) and Creer (1962, 1965) have plotted the results of analyses of the latitude-dependence of the dispersion ($\delta = \cos^{-1} R/N$). The paleolatitude corresponding to the D-component at Bell Island is 5^{o}, consistent with the low-latitude origin ascribed to redbeds. For this latitude, the dispersion obtained from Creer's (1962) curve is about 20^{o}, whereas the actual value, based on $N = 11$ zones, is only 6^{o}. This would agree with the proposal that the secular variation has been smoothed out.

However, if the smoothing-out process did not occur, then the D-component was perhaps acquired during a short time compared with the secular variation. However, an alternative explanation for the low value of δ may be that, during the relevant part of the Ordovician period, the magnitude of the secular variation was substantially less than today. It is difficult to test this explanation in view of the scarcity of adequate paleomagnetic data from well-dated Ordovician rocks, most of which are sedimentary. From his extensive study of Siberian rocks, Rodionov (1966) finds that, during the Ordovician, the amplitude of the secular variation may not have been substantially greater than today. However, his data are also from redbeds, and the dispersion he observed may be due to causes other than secular variation.

It is concluded that, while the smoothing-out mechanism appears to explain best the observed low dispersion about the mean direction of the D-component, the two alternative explanations, i.e. that the secular variation

was either small or inadequately sampled, cannot be ruled out. Similar explanations would apply also to mechanisms involving a change in field direction during the time the Bell Island sequence was laid down, i.e. mainly polar wandering or continental drift. Thus these processes were either insignificant, or the evidence has been suppressed in the magnetic record.

5.3.2. Origin of the NRM

The natural remanence (groups A and B) of the Bell Island rocks was shown to be composite and residing mainly in a thermally distributed component (possibly CRM) with a wide spectrum of blocking temperatures. The difference in the directions of the distributed and discrete (685^{o}C) components suggests that they originated at different times, the main component in the NRM being almost certainly younger. If this component was acquired by some process such as viscous PTRM (Briden, 1967) (Section 4.1.3), then a possible time of origin for this secondary magnetization is the late Paleozoic, at which time the rocks may have been heated during burial and uplifted as part of the Appalachian orogeny. However, since the Bell Island beds were relatively unaffected by orogenic episodes, this explanation is not too convincing. Irving and Opdyke (1965) in discussing the NRM of the Bloomsburg redbeds, considered the above possibility along with an alternative explanation which is that the distributed components are of low-temperature chemical origin, perhaps resulting from nucleation aided by moderate heating during burial. This may well apply in the present case.

Whatever the mechanism, a Permian age was considered likely in the case of the secondary component in the Bloomsburg study (Roy et al.,

1967) because its direction corresponded to typical Permian directions in the literature (Irving, 1964). Similarly, the Bell Island "B" group pole in Fig. 5.1[1] is close to typical Permian directions, and would be compatible with a Permian geomagnetic field also because of its polarity, since the prevailing polarity during the Kiaman magnetic interval was also "reversed" (Irving and Parry, 1963). The opposite polarities of the "A" and "B" group poles then might be explained by supposing that these groups were not contemporaneous (though possibly both of late Paleozoic origin), and that the geomagnetic field responsible for the major component in the more recently magnetized group (either "A" or "B") had reversed since the other group became magnetized. Further conclusions cannot be drawn from the NRM data in view of its composite nature.

The smeared group C site-mean vectors (which incorporate an unknown proportion of the discrete group D component) could perhaps be due to differential recrystallization at different sites, giving rise to the formation of secondary hematite at the outer rims of the oölites. That group C is of chemical origin and is stable has not been proved, but seems plausible as these directions prevail to beyond 600°C and the within-site directions are generally well grouped (Tables 4.2, 4.5).

5.4. Comparison with other Paleomagnetic results

For the D-component in Table 5.1, the antipoles rather than the poles seem to correspond to an Ordovician geographical north pole when one

[1] A pole position corresponding to the presumed Permian direction at Bloomsburg is not shown, as none was computed in the original paper (Roy et al., 1967).

compares the data with the published polar wandering curves (Irving, 1964). This assumes that the D-component is stable and primary, and implies that the ambient geomagnetic field was "reversed" compared with its present sense. The antipole position shown in Fig. 5.1 is in the present area of the Pacific Ocean, along with the other published Ordovician poles inferred from sites in North America, Europe and Siberia.

Lower Paleozoic paleomagnetic data from North America are sparse, and the only published result from Ordovician rocks having a plausibly Ordovician remanence and satisfying minimum stability criteria is from the Upper Ordovician Juniata redbed formation (Collinson and Runcorn, 1960). However, the pole computed from the Juniata study (Fig. 5.1) is based on uncleaned NRM directions, unit weight being given to 56 specimens from 12 samples spanning a 425-meter section. NRM stability was partly indicated by the wide divergence of the mean NRM direction from that of the present field.

Thus the pole position (28^{o}N, 168^{o}W) computed in the present study constitutes the first paleomagnetic result from laboratory-treated Ordovician rocks in North America. Fig. 5.1 shows that this presumed Ordovician pole lies far to the east not only of the pole for the Juniata formation (20^{o}N, 153^{o}E), but also of the presumed Silurian pole for the Bloomsburg formation (Roy et al., 1967), which is also based on rocks from the Appalachian system and has been plotted for comparison with the Ordovician results, as it appears to be the only previously published pole position from Lower Paleozoic rocks in North America that have been thermally treated.

5.5. North Atlantic paleogeography

Fig. 5.1 shows also that the spread of the poles calculated from European Ordovician data exceeds 90^{0}. A useful comparison in terms of paleogeography would be between Newfoundland and Ireland; relative to the latter, the single published (mid-) Ordovician pole (9^{0}N, 146^{0}W, Deutsch and Somayajulu, 1970), based on 4 bands of ignimbrite from Killary Harbour, Eire, is shown with its associated error oval, which is large ($dp = 12^{0}$, $dm = 22^{0}$) partly because of the limited sampling. Despite this, the Irish result is backed by fairly good stability evidence, including a positive fold test. The pole positions for Bell Island and Killary Harbour are relatively close (compare error ovals), but it is easily seen that many more stability-tested results from opposite sides of the Atlantic are needed to interpret such results in terms of paleogeography.

Since the published paleomagnetic results from Cambrian and Silurian rocks in North America and Europe (not shown in Fig. 5.1) tend to be as widely scattered as the Ordovician ones, it is premature to test "pre-Wegenerian" models of the North Atlantic, e.g. Wilson's (1966) hypothesis of the proto-Atlantic, or the proposed rotation of Newfoundland (Wegener, 1966 transl.), both of which require reliable comparisons of Lower Paleozoic rocks.

SUMMARY AND CONCLUSIONS

(1) The objective of this work was to study the natural remanent magnetization (NRM) and some magnetic properties, including stability, of the Lower Ordovician redbeds of Bell Island, Newfoundland, and to interpret these paleomagnetically.

(2) A gently dipping ($\sim 10^{0}$) 450-meter section was sampled, including non-ferruginous sandstone and shale showing no significant remanence. Measurements were confined to 480 specimens from 120 samples of oölitic hematite sandstone, spanning a 150-m section (24 sites up to 6 km apart) of the Wabana and Airfield formations, and one site of the Townsquare formation 180 m, further below.

(3) Remanence was measured with a PAR model SM-1 spinner magnetometer and estimated maximum errors (including sampling and orienting) for a single specimen were 2^{0} in direction and ± 2% in intensity (J).

(4) Stepwise thermal demagnetizations to $\leq 750^{0}$ were carried out with a non-magnetic furnace. Field-nulling with a set of 2-meter Parry coils was repeatedly monitored during runs and was < 25γ (exceptionally, 25 - 35γ), i.e. 0.1% of the uncancelled field. Temperature control was to ± 5^{0}C at 350^{0}C and to ± 3^{0}C at 600^{0}C and higher temperature.

(5) A pilot study of 28 representative specimens showed two opposed sets of NRM directions, with northerly (Group A) and southerly (B) declinations and shallow inclinations, except for site Wa-10, where the NRM's were steep. Group B directions occurred in three zones separated vertically by group A sites.

(6) Thermal demagnetizations in air (more than 10 steps) showed only minor directional changes to 350°C, except that the site Wa-10 directions moved into group A positions, probably due to removal of a low-coercivity component.

(7) Treatment to 550 - 600°C deflected both group A and group B vectors mainly SW, with moderate upward inclinations (Group C). Treatment in the range 600 - 695°C redirected the vectors along great circles into shallow, upward positions towards the SE (Group D), with excellent grouping.

(8) The normalized intensity J/J_{20} increased significantly (sometimes more than twofold) to the 600°C step, then dropped sharply after 685°C, and increased by factors of more than 10, after 750°C.

(9) Treating all samples (2 specimens each) to 350, 600 and 685°C in air confirmed the pilot study results. Misalignment with the present field and generally low within-site scatter indicated that the 3 or more superimposed components are relatively stable.

(10) One specimen each from groups A and B, and one pre-treated to 685°C, were virtually unaffected by alternating-field demagnetization to 800 peak oersteds, indicating high stability for the NRM and the D-component. This would be consistent with hematite as the chief remanence carrier.

(11) The directional scatter between sites was large for groups A and C and small for group B. It was least for the D-component (precision parameter $k = 160$ for $N = 11$ zones), where statistical tests indicated that differences of site-mean directions are mostly insignificant

over the vertical section; moreover, $J_{685^{o}C}$ varied by only a few percent from its mean value (3.3×10^{-5} emu/cm^3).

(12) The D-component origin considered most likely is shallow marine precipitation of hematite on the growing oölites under oxidizing conditions favouring formation of primary iron ores, among which Hayes (1915) and others include the Bell Island ore. This would favour acquisition of a stable chemical remanence (CRM), with narrow blocking-temperature range just below the Curie point of hematite, as observed here. Thus the D-component may be primary (Ordovician). Proving this is difficult, as the fold test was inapplicable.

(13) Uniformity of the D-component over the section may be due to: (i) an unusually small secular variation; or (ii) the component was acquired much more quickly than the expected time of laying down a > 150-m sedimentary column; or (iii) during diagenesis of the rock, field asymmetries, being a function of vertical position (i.e. time), were smoothed out, e.g. through nucleation of the hematite. No decision between these alternatives was reached, though (iii) is favoured.

(14) A comparison of 1-, 3- and 10-step treatments to 685^{o}C yielded no significant differences in direction and dispersion. It was concluded that heat treatment had not significantly affected the D-component.

(15) The thermal demagnetization curves suggest that the components other than D are thermally distributed. They are thus more likely to be of secondary (perhaps also CRM) origin.

(16) The NRM may be largely due to remagnetization through modest reheating (e.g. Briden, 1967) connected with the late Paleozoic

Appalachian orogeny. The B-group has the same ('reversed') polarity and similar directions as the secondary component in the Silurian Bloomsburg, Pennsylvania redbeds (Roy et al., 1967), regarded as Permian by the authors.

(17) The intensity rise to 600°C in the stepwise treatment was first attributed to preferential demagnetization of opposed components in the NRM of both A and B groups. In that case, J should not rise when powdered specimens are used. This was tested by heating fresh powders in air to 700°C and cooling in a thermomagnetic balance employing 10^3 oe. fields. Again the magnetic moment rose significantly to 600°C, fell sharply near 685°C, and rose spectacularly upon cooling from 700 - 750°C.

(18) It was concluded that a new, intensely magnetic component was formed during heating, without apparently affecting the direction of the D-component in whole-rock specimens. After two additional heating-cooling cycles to 620°C in the thermomagnetic balance, the curves became reversible, with room temperature magnetic moments 1 - 2 orders of magnitude greater than NRM, and Curie point at 620°C.

(19) The susceptibility k of three specimens was measured at room temperature with an a.c. bridge, before treatment ($k \sim 5 \times 10^{-6}$ c.g.s. units) and after stepwise heating to T = 850°C. Above the 600°C step, k increased 10- to 20-fold, this trend being comparable to the high-temperature trends observed in the J/J_{20}-T and M-T curves.

(20) Two fresh specimens and one pre-treated to 685°C were virtually unaffected by alternating-field (AF) demagnetization to 800 peak oersteds, implying that most of the coercivity spectral range is above that field. Assuming further AF tests confirm these results, this

is as expected for hematite (i.e. in the fresh specimens), but would be an unlikely finding if magnetite were prominent.

(21) Preliminary x-ray diffraction results indicate that this newly formed mineral (item 18) is a spinel, either maghemite (γ-Fe_2O_3) or magnetite (Fe_3O_4). However, the observed Curie point ($T_C \sim 620^oC$) was significantly higher than that of magnetite ($T_C = 578^oC$), whereas $T_C = 620^oC$ could be consistent with maghemite, since a definite Curie point has not yet been established for that mineral. From (20) and (21), it was concluded that maghemite is more likely than magnetite to have been produced by the heat treatment.

(22) However, this would be an unusual finding, in view of the frequently-noted high-temperature instability of maghemite and conversion to the α-form (hematite) at elevated temperatures. Still, in the present case, the relatively uncommon association of much siderite ($FeCO_3$) with the hematite in the rock matrix possibly offers a mechanism for producing maghemite in line with some observations by Rowland and Jonas (1949).

(23) For eight fresh specimens stepwise demagnetized to 700^oC in nitrogen the intensity J decreased up to 500^oC, contrary to the results for air. However, after 685^oC, the D- component grouping became poor and J increased by up to two orders of magnitude. This appears to be due to formation of a very intense component, perhaps magnetite through reduction of the hematite, during heating.

(24) Hematite-bearing sediments often exhibit crystalline susceptibility anisotropy, which may result in a departure of the remanence direction from that of the ambient field. While the present

observations (e.g. directional changes during thermal treatment) suggest that this was not a significant factor, it cannot be ruled out.

(25) Assuming D-component is Ordovician and tilting perhaps mid-Paleozoic or later, mean direction for 11 equally weighted Wabana and Airfield zones without stratigraphic overlap was computed relative to bedding planes: declination, $D = 126.5^{o}$; inclination, $I = -10.3^{o}$; $\alpha_{95} = 3.6^{o}$.

(26) Based on axial dipole assumption this gives a (presumably reversed) pole in the central Pacific Ocean: $28^{o}N$, $168^{o}W$. Despite conservative weighting, the error oval ($dp = 1.8^{o}$, $dm = 3.6^{o}$) is unusually small, reflecting small dispersion.

(27) This is the first Ordovician paleomagnetic result for North America based on reliable tests. The D-component pole lies 90^{o} east of the pole for the Silurian Bloomsburg redbeds (Roy et al., 1967), which had also been studied with thermal techniques.

(28) The few published Ordovician poles for Europe mostly fall in the west-central Pacific, but are too scattered to permit paleogeographic comparisons with eastern Newfoundland. The Lower Paleozoic evidence is still insufficient for testing continental drift models across the North Atlantic.

(29) This suggests further work, some of which is being started here; e.g. comparative paleomagnetic studies between (i) Newfoundland and stable mainland North America; (ii) Newfoundland and western Europe; and (iii) western and eastern Newfoundland.

(30) It is also planned to investigate more thoroughly certain inconclusive aspects of the present work, chiefly (a) the assumption that the D-component is primary (e.g. using chemical demagnetization techniques); (b) the postulated production of maghemite during heating (further thermomagnetic and diffraction studies, Mössbauer effect, etc.); (c) the possible significance of susceptibility anisotropy (see item 24).

(31) Finally, it is proposed to make a magnetic study of oölitic hematites from other land masses for comparison with those from Bell Island.

TABLE A1.1

Remanent magnetization before and after thermal demagnetization

In the following table the values of mean direction and intensity of natural remanent magnetization for all samples and corresponding data after three steps of thermal demagnetization will be listed. Except where noted otherwise, all sample directions quoted are resultants of two specimen directions giving each unit weight and all intensity values represent corresponding arithmetic means.

Wabana formation

Sample No.	NRM			350°C		
	D	I	J x 10^{-5}	D	I	J x 10^{-5}
1-1	45.5	+20.3	4.7	44.4	+15.1	5.3
1-2	27.9	+21.6	3.5	49.0	+15.6	4.3
1-3	30.3	+23.4	3.9	44.7	+19.3	5.5
1-4	45.2	+19.5	6.6	40.6	+13.5	9.6*
1-5	36.2	+21.7	6.2	No measurement		

*Only from one specimen.

TABLE A1.1, continued

Sample No.	NRM D	NRM I	NRM J x 10^{-5}	350°C D	350°C I	350°C J x 10^{-5}
2-1	36.6	+24.2	5.0	44.2	+18.6	6.4
2-2	41.5	+19.0	3.8	29.6	+26.6	5.1*
2-3	59.6	+19.6	4.7	59.1	+22.1	5.0
2-4	39.9	+21.8	4.3	32.4	+19.9	5.1
2-5	40.7	+22.2	4.5	39.1	+19.2	5.8*
2-6	37.2	+22.6	3.9	41.2	+28.3	5.4*
3-1	33.6	+22.4	4.5	39.6	+22.5	5.3
3-2	55.9	+20.6	4.5	39.6	+21.7	5.5
3-3	42.2	+22.0	5.0	43.2	+24.6	4.8
3-4	14.2	+18.0	4.9	51.2	+25.0	5.5
3-5	46.6	+22.5	4.3	22.7	+20.5	4.6
4-1	43.2	+26.6	4.8	35.4	+19.8	4.5
4-2	42.0	+25.7	5.0	47.9	+21.9	5.2
4-3	51.8	+19.3	3.5	23.4	+19.4	4.9
4-4	22.9	+16.3	4.2	62.3	+71.2	5.4*
4-5	46.2	+27.9	4.5	46.2	+16.9	6.2*
5-1	29.6	+17.9	4.0	No measurement		
5-2	45.1	+18.3	3.5	52.6	+21.9	5.8*
5-3	39.2	+29.8	3.5	51.4	+26.8	6.6*
5-4	43.4	+21.6	4.3	61.3	+31.3	5.8*
5-5*	42.1	+26.2	4.0	No measurement		

*Only from one specimen

TABLE A1.1, continued

Sample No.	NRM D	NRM I	NRM J x 10^{-5}	350°C D	350°C I	350°C J x 10^{-5}
6-1	64.2	+34.2	4.0	59.5	+32.1	6.6*
6-2	72.6	+23.2	4.1*	No measurement		
6-3	77.4	+42.3	5.1	31.7	+26.4	6.0
7-1	86.5	+41.8	4.5	80.9	+26.5	6.4
7-2	89.9	+18.2	4.2	73.3	+26.3	6.3
7-3	76.6	+16.1	4.0*	No measurement		
8-1	186.6	-10.8	8.1	185.4	-20.1	10.7
8-2	196.2	-18.1	8.2	200.4	-21.8	8.0
8-3	193.6	-18.2	9.9	183.7	-13.4	9.1*
8-4	183.6	-20.2	9.3	200.6	-19.9	7.2*
8-5	186.0	-23.5	6.8	198.6	-23.1	7.9*
8-6	203.5	-16.1	7.5	208.4	-16.6	8.3*
8-7	194.0	-18.3	6.9	200.8	-26.2	8.4*
8-8	193.4	-22.2	7.7	212.6	-14.3	8.0*
8-9	191.6	-23.4	8.1	181.1	-18.0	7.0
8-10	186.1	-23.6	7.2	192.3	-13.8	7.8*
9-1	48.5	-15.8	10.0	41.3	-71.6	10.0
9-2	47.4	-26.5	8.5	70.6	-33.0	9.7
9-3	51.5	-22.6	9.1	70.4	-19.2	8.7
9-4	28.8	-13.5	5.1	39.0	-34.9	8.3
9-5	26.2	-19.8	5.2	68.8	-66.0	9.6
9-6	28.0	-19.6	5.1	41.5	-20.5	8.1
9-7	49.3	-25.0	5.9	355.9	-29.5	7.7
9-8	50.4	-29.8	6.0	42.2	-30.5	7.4

*Only from one specimen.

TABLE A1.1, continued

Sample No.	NRM D	NRM I	NRM J x 10^{-5}	350°C D	350°C I	350°C J x 10^{-5}
10-1	1.0	-86.9	8.9	21.0	-20.0	8.6
10-2	1.3	-81.4	7.7	1.4	-67.8	6.9*
10-3	0.2	-76.9	7.6	0.9	-32.7	7.5
10-4	1.7	-64.8	7.7*	24.6	-38.2	7.7
10-5	5.2	-80.8	7.0	4.0	-22.2	6.9
10-6	2.2	-80.6	6.8	3.5	-20.1	6.9
11-1	354.7	+36.1	4.6	251.0	+21.8	5.7
11-2	353.7	+22.6	5.1	224.6	+22.5	5.9
11-3	343.2	+48.2	6.1	203.7	+19.5	5.9
11-4	356.3	+41.4	5.8	261.8	+27.2	6.2
11-5	335.9	+53.1	4.8	231.2	+16.6	4.9
11-6	310.4	+41.2	4.9	No measurement		
11-7	320.6	+29.6	5.0	No measurement		

*Only from one specimen.

TABLE A1.1, continued

Sample No.	600°C D	600°C I	600°C J x 10^{-5}	685°C D	685°C I	685°C J x 10^{-5}
1-1	207.8	-21.9	7.0	121.9	-21.4	3.0
1-2	241.2	-22.4	6.9	122.2	-18.5	3.0
1-3	229.9	-26.0	7.5	125.2	-19.6	3.0
1-4	240.8	-21.0	1.23*	130.7	-17.6	2.4*
1-5	No measurement			140.2	-13.2	3.3
2-1	232.4	-24.0	7.0	123.7	-21.4	2.8
2-2	197.8	-26.6	6.6*	121.3	-19.3	2.6
2-3	231.3	-19.3	6.8*	133.5	-21.7	3.6
2-4	153.7	-20.0	6.6	131.8	-21.4	2.8
2-5	211.3	-32.4	7.2*	125.7	-17.3	2.5
2-6	266.4	-14.3	6.9*	117.8	-24.2	3.1
3-1	211.4	-22.2	7.5	113.6	-17.9	2.8
3-2	265.2	-23.3	7.0	118.1	-19.0	3.1
3-3	220.6	-19.3	7.0	120.3	-19.1	3.7
3-4	211.9	-15.5	6.6*	138.2	-20.5	3.1
3-5	249.0	-22.1	6.3	126.5	-18.2	3.2
4-1	241.9	-48.0	8.7	133.3	-19.0	3.2
4-2	236.6	-24.9	7.3	122.2	-21.8	2.9
4-3	236.7	-20.0	7.1	120.3	-20.1	2.8
4-4	260.8	-35.2	6.8	130.2	-17.1	2.8
4-5	263.1	-21.8	8.8	130.6	-18.0	2.9

*Only from one specimen.

TABLE A1.1, continued

Sample No.	600°C D	600°C I	600°C J x 10^{-5}	685°C D	685°C I	685°C J x 10^{-5}
5-1	No measurement			121.9	-18.4	2.9*
5-2	266.4	-19.8	6.8	129.2	-20.4	2.8
5-3	261.5	-20.5	7.0	128.8	-20.3	2.9
5-4	249.3	-30.2	6.9	133.0	-19.5	3.2
5-5	No measurement			125.3	-15.3	2.8*
6-1	303.9	-12.9	6.9	124.0	-19.7	2.7
6-2	No measurement			119.3	-26.4	3.0*
6-3	300.3	-26.8	6.2*	109.1	-14.6	3.2*
7-1	301.7	-15.4	6.7	117.1	-23.8	3.1
7-2	253.3	-22.7	6.8	123.6	-16.0	3.2
7-3	No measurement			120.7	- 7.8	3.0*
8-1	295.1	-16.2	26.1	111.1	-16.5	4.6
8-2	241.2	-20.6	9.3	135.1	-23.6	3.8
8-3	No measurement			113.3	-10.8	6.4*
8-4	257.5	-20.8	7.0	141.8	-11.7	5.0
8-5	267.7	-19.5	8.5	121.7	-25.4	3.1
8-6	257.3	-18.6	10.2*	119.1	-15.2	3.7
8-7	256.7	-21.4	9.3*	118.5	- 8.6	3.2
8-8	272.3	-37.1	9.9*	128.5	-23.1	2.5
8-9	267.8	-27.2	9.9*	106.8	-16.8	2.2
8-10	No measurement			No measurement		

*Only from one specimen.

TABLE A1.1, continued

Sample No.	600°C D	600°C I	600°C J x 10^{-5}	685°C D	685°C I	685°C J x 10^{-5}
9-1	301.4	-13.8	9.7	126.2	-15.2	3.2
9-2	288.2	-21.8	9.7	129.5	-20.0	3.5
9-3	287.5	- 1.7	10.0	123.9	-24.4	3.5
9-4	296.0	-18.3	9.9	123.5	-20.1	3.0
9-5	310.8	-17.7	9.7	130.8	-16.5	2.4
9-6	305.2	-20.2	9.7	129.4	-16.7	2.9
9-7	304.2	-23.0	11.5	124.1	-20.3	3.2
9-8	305.5	-18.5	9.8	125.6	-20.4	3.1
10-1	304.7	-36.8	9.5	135.1	-19.8	2.8
10-2	300.8	-18.3	9.8*	140.8	-21.4	3.2*
10-3	304.2	-35.2	10.0*	125.5	-18.8	3.7
10-4	300.1	-26.6	9.7	119.6	-20.3	3.1
10-5	326.0	-20.1	10.9	124.8	-18.9	3.0
10-6	305.1	-24.3	9.6	125.3	-14.1	2.6
11-1	270.2	-24.3	7.3*	140.5	-19.4	2.9
11-2	310.4	-46.1	8.2*	137.4	-17.3	3.0
11-3	No measurement			140.1	-26.4	3.2*
11-4	296.4	-31.5	9.1	144.3	-18.1	3.4*
11-5	207.6	-17.8	6.7	141.1	-18.8	3.2
11-6	No measurement			142.1	-21.3	2.8*
11-7	No measurement			144.3	-18.1	3.2*

*Only from one specimen.

TABLE A1.1, continued

Airfield formation

Sample No.	NRM D	NRM I	NRM J x 10^{-5}	350°C D	350°C I	350°C J x 10^{-5}
1-1	357.9	- 6.6	7.3	21.8	-28.5	7.3
1-2	12.9	-17.3	6.9	13.1	-15.3	7.0
1-3	16.8	-13.3	6.0	21.6	-21.8	7.8*
1-4	10.3	-12.6	7.0	18.1	-15.1	7.8
1-5	14.6	-11.6	5.0	21.8	-14.9	7.2
2-1	182.7	-12.5	6.7	183.4	-15.9	7.5
2-2	183.5	-13.8	7.1	182.1	-20.9	7.0
2-3	186.2	-17.0	6.7	173.6	-18.0	5.8
2-4	183.7	-15.0	7.0	190.5	-21.8	6.9*
2-5	183.2	-18.4	6.6	189.2	-16.6	6.8*
2-6	178.7	-15.1	5.0	181.2	-14.3	6.9*
3-1	186.2	-18.1	5.5	181.2	-17.6	6.9*
3-2	180.4	-14.8	6.2	182.6	-31.0	7.3
3-3	173.6	-13.2	6.0	194.3	-17.2	6.6*
4-1	192.3	-14.5	7.0	191.2	-12.8	6.8*
4-2	190.3	-12.3	6.5	191.6	-14.0	8.1
4-3	161.8	-16.5	6.5	171.4	-18.6	6.8*
5-1	342.3	+15.4	4.8	359.6	+19.8	6.2
5-2	1.7	+31.4	4.4	10.6	+14.8	6.2*
5-3	330.4	+16.8	4.4*	No measurement		

*Only from one specimen.

TABLE A1.1, continued

Sample No.	NRM D	NRM I	NRM J x 10^{-5}	350°C D	350°C I	350°C J x 10^{-5}
6-1	345.9	+20.3	5.0	298.1	+20.5	7.1
6-2	331.1	+18.6	4.9*	No measurement		
6-3	359.1	+24.0	4.7	1.6	+32.4	7.1
6-4	21.0	+20.8	4.6*	No measurement		
7-1	345.1	+ 9.4	3.7	329.3	+19.3	5.5
7-2	331.6	+23.8	4.3	319.1	+19.2	4.8
7-3	10.1	+15.5	5.1	14.8	+21.3	7.2*
7-4	351.5	+22.4	5.0	352.4	+18.4	6.0
7-5	25.9	+19.1	4.5	1.1	+32.6	6.7
8-1	31.8	+23.5	5.3	23.3	+18.4	7.3*
8-2	37.7	+22.4	4.8	14.3	+21.4	7.2*
8-3	53.6	+16.5	4.6	32.1	+26.7	7.6
8-4	24.2	+15.6	5.0	8.0	+19.7	7.3
8-5	19.0	+22.5	5.0	24.8	+17.2	7.1*
9-1	25.6	+26.3	5.2	43.6	+21.8	7.2*
9-2	16.4	+10.3	4.6	17.4	+21.4	7.4
9-3	12.5	+19.2	5.7	32.8	+19.5	7.1
9-4	19.7	+19.2	5.2	47.6	+13.1	7.1
10-1	14.6	+32.7	4.6	14.0	+23.8	4.9
10-2	18.2	+23.3	4.8	19.9	+23.2	5.0

*Only from one specimen.

TABLE A1.1, continued

Sample No.	NRM D	NRM I	NRM J x 10^{-5}	350°C D	350°C I	350°C J x 10^{-5}
11-1	36.1	+21.2	5.0	18.8	+39.6	6.1
11-2	15.3	+18.1	4.9	17.3	+22.2	6.1
11-3	19.7	+22.3	4.8	11.7	+30.3	6.1
11-4	19.7	+13.7	5.0	21.5	+23.6	6.1
12-1	16.1	+13.4	5.1	6.1	+21.8	5.2
12-2	24.3	+14.5	4.8	20.8	+29.7	5.0
12-3	28.9	+27.2	4.6	No measurement		
12-4	34.2	+26.0	4.9	26.0	+22.5	5.0
12-5	31.9	+23.7	5.0	20.0	+16.0	5.1
12-6	18.5	+23.3	5.1	No measurement		
13-1	21.0	+19.5	5.0	20.3	+20.6	5.1
13-2	22.4	+25.1	4.7	15.5	+21.3	5.1
13-3	20.3	+18.3	4.5	No measurement		

*Only from one specimen.

TABLE A1.1, continued

Sample No.	600°C D	600°C I	600°C J x 10^{-5}	685°C D	685°C I	685°C J x 10^{-5}
1-1	216.4	-15.3	9.0	112.5	-13.0	4.6
1-2	220.7	-18.3	8.1	117.7	-12.5	3.1
1-3	193.1	-20.2	8.2*	127.4	-15.9	3.1
1-4	205.7	-17.3	8.6	115.2	-16.3	3.2
1-5	202.2	-18.1	9.0	129.8	-21.7	3.1
2-1	239.2	-20.9	7.9	120.4	-19.3	3.3
2-2	222.7	-29.6	7.8	116.4	-18.6	3.1
2-3	223.3	-13.6	7.5	117.5	-14.9	2.8
2-4	245.6	-17.8	7.7*	121.1	-17.7	2.9
2-5	200.1	-17.8	7.4*	119.6	-17.7	2.9
2-6	200.0	-12.7	7.7*	121.0	-14.1	2.7
3-1	211.3	-21.8	7.1*	119.5	-20.9	3.0
3-2	210.1	-27.6	9.0	117.8	-10.7	3.0
3-3	221.2	-21.2	7.2*	121.1	-13.4	3.5
4-1	231.4	-43.6	9.6*	123.5	-13.5	3.6
4-2	229.0	-19.4	9.8	122.2	-17.4	3.4
4-3	193.6	-14.1	7.2*	119.9	-10.4	4.0
5-1	166.0	-15.2	7.6	125.4	-18.8	2.5
5-2	200.6	-16.6	6.6	128.5	-18.4	2.6
5-3	No measurement			120.4	-18.3	2.8*

*Only from one specimen.

TABLE A1.1, continued

Sample No.	600°C D	600°C I	600°C J x 10^{-5}	685°C D	685°C I	685°C J x 10^{-5}
6-1	198.3	-25.3	7.0	123.2	-18.3	2.8
6-2	No measurement			124.6	-30.2	2.8*
6-3	198.0	-27.2	7.0	132.1	-18.8	3.1
6-4	No measurement			132.5	-18.9	3.2*
7-1	208.1	-32.7	14.0	125.4	-16.4	2.3
7-2	255.0	-35.7	11.4	130.0	-18.6	3.6
7-3	233.4	-16.8	8.4*	125.7	-20.3	3.5
7-4	215.3	-18.1	9.3	120.1	-18.2	3.1
7-5	235.3	-19.4	9.7	126.0	-20.0	3.3
8-1	198.9	-21.7	9.9*	131.4	-20.1	3.1
8-2	200.3	-20.0	9.8*	130.3	-18.8	3.1
8-3	221.0	-18.1	10.1	131.7	-15.9	3.1
8-4	204.4	-23.6	10.1	128.1	-18.1	3.0
8-5	193.3	-41.2	10.0*	123.3	-21.3	3.1
9-1	200.8	-37.2	10.8*	126.2	-16.9	3.1
9-2	212.4	-19.0	10.3	117.1	-17.9	3.1
9-3	196.3	-19.0	9.8	129.7	-17.8	3.1
9-4	235.1	-37.1	9.7	121.4	-18.9	3.0
10-1	239.1	-17.4	7.8	113.6	-10.2	2.8
10-2	239.3	-18.2	8.1	115.3	-13.4	2.9

*Only from one specimen.

TABLE AI.1, continued

Sample No.	600°C			685°C		
	D	I	J x 10^{-5}	D	I	J x 10^{-5}
11-1	273.1	-22.6	9.2	117.4	-10.4	2.8
11-2	300.1	-21.6	9.1	123.3	-21.2	3.0
11-3	256.7	-24.6	9.1	118.1	-17.3	3.1
11-4	270.8	-20.7	9.4	130.6	-14.4	2.8
12-1	243.8	-38.2	6.6	121.0	-16.5	3.1
12-2	242.2	-21.4	6.8	117.8	-15.7	3.0
12-3	No measurement			110.2	-16.9	3.2
12-4	255.2	-39.3	5.1	125.8	-18.4	2.9
12-5	249.2	-18.3	6.1	129.6	-19.5	3.1
12-6	No measurement			125.2	-15.2	2.9
13-1	270.3	-33.2	6.1	114.5	-12.8	3.6
13-2	305.2	-19.8	6.1	117.5	-15.7	3.6
13-3	No measurement			106.1	-23.3	3.1

*Only from one specimen.

TABLE A2.1

Comparison of specimen magnetizations after 685°C treatment from three procedures

Wabana formation

Sample[1]	1-step			3-step			10-step		
(Wa)	D[2]	I[3]	J[4]	D	I	J	D	I	J
1-2	114	-18	2.8	122	-19	3.0	129	-19	2.8
2-4	131	-17	2.8	132	-21	2.8	127	-20	3.2
3-4	146	-22	3.2	138	-21	3.1	130	-19	2.9
4-4	130	-19	2.8	130	-17	2.8	130	-15	2.8
5-2	130	-22	2.8	129	-20	2.8	128	-19	2.8
6-1	127	-18	2.4	124	-20	2.7	—	—	—
7-3	121	- 8	3.0	121	- 8	3.0	—	—	—
8-8	115	-31	2.2	129	-23	2.5	141	-14	2.8
9-1	121	-12	3.1	126	-15	3.2	131	-18	3.4
10-4	129	-19	3.2	120	-20	3.1	129	-21	3.2
11-5	141	-20	3.5	141	-19	3.2	141	-20	3.5

[1] Different specimens from the same sample are used in three procedures of demagnetization.

[2] D = declination, degrees.

[3] I = inclination, degrees.

[4] J = intensity of magnetization in emu/cm^3 x 10^{-5}.

TABLE A2.1, continued

Comparison of specimen magnetizations after 685°C treatment from three procedures

Airfield formation

Sample[1]	1-step			3-step			10-step		
(Wa)	D[2]	I[3]	J[4]	D	I	J	D	I	J
1-2	121	-12	3.0	118	-13	3.1	125	-10	3.2
2-3	121	-16	2.8	118	-15	2.8	125	-19	3.1
3-3	121	-12	3.8	121	-13	3.5	131	-22	2.9
4-3	119	-12	4.1	120	-10	4.0	121	-15	3.8
5-1	120	-18	2.8	125	-19	2.8	127	-21	3.0
6-2	125	-21	2.9	125	-30	2.8	132	-19	3.2
7-1	120	-22	3.8	125	-16	2.3	121	-14	2.4
8-2	131	-22	3.3	130	-19	3.1	130	-19	3.3
9-1	121	-19	3.0	126	-17	3.1	122	-19	3.2
10.2	118	-13	2.9	115	-13	2.9	132	-14	2.9
11-3	122	-15	3.3	118	-17	3.1	131	-10	3.3
12-6	120	-22	3.2	125	-15	2.9	132	-15	3.1
13-1	114	-15	3.1	115	-13	3.6	125	-20	3.1

See footnotes, previous page.

ACKNOWLEDGEMENTS

The author wishes to acknowledge with thanks the assistance received from the following members of the Physics faculty and staff at Memorial University of Newfoundland:

Professor Ernst Deutsch under whose supervision the present investigations were carried out and who painstakingly guided the author throughout the course of the present work.

Dr. S. W. Breckon, Head of the Department, who offered generous use of facilities and equipment and gave much help.

Dr. J. A. Wright, Assistant Professor, who helped in the measurement of magnetic gradients in the thermal demagnetization unit.

Dr. G. S. Murthy, Post-doctoral Fellow in geophysics, who gave valuable assistance in carrying out alternating field demagnetization experiments.

Mr. Leo Kristjansson, graduate student in geophysics, for the measurements with the Curie point balance designed by him and for making the polished sections and for valuable discussions throughout the work.

Mr. Gary Haardeng-Pedersen, graduate student in geophysics, for much assistance with programs for the Hewlett-Packard Calculator.

Mr. Carl Alcock, graduate student in geophysics, for the orientation measurements with the sun compass during sample collection in the field work.

Mr. W. J. Drodge, geophysical Assistant, for extended help and suggestions in the calibration and measurements with the spinner magnetometer and the equipment in general.

Mr. Robert B. Kennedy for his assistance in the field work and preparation of rock specimens.

At the Geology Department, the author wishes to thank in particular Dr. E. R. W. Neale, Head of the Department, for his generous offer to use the x-ray diffraction unit.

Dr. H. Williams, Associate Professor, for helpful discussions on Appalachian geology.

Mr. Harve Keats for making the x-ray diffraction measurements.

Mr. H. D. Upadhay for the microscope study of polished sections.

The author wishes to thank also Miss D. Janes, who typed and proof-read the thesis; and Messrs. William Higgins and Russ Tucker who carried out the photographic and drafting work.

Finally, the author is much indebted to the Physics Department and Memorial University of Newfoundland for a university fellowship and other financial support since November, 1967, and to the National Research Council of Canada for support during the summers from grant A-1946 to Dr. E. R. Deutsch.

REFERENCES

Amstutz, G. C. and L. Bubenick. in Diagenesis in Sediments: Eds. Larsen, G. and G. V. Chillingar, New York, Elsevier, p. 417-475 (1967)

Bagin, V. I. IZV. Geophy. Ser., p. 1383-1393 (1961)

Banerjee, S. K. J. Geomag. Geoelec., 17, p. 357 (1965)

Black, R. F. Geol. Survey Canada Bull., 83, p. 1-31 (1963)

Black, R. F. Nature, 202, p. 945-948 (1964)

Blackett, P. M. S. Philos. Trans. Roy. Soc. London, A, 245, p. 309-370 (1952)

Blackett, P. M. S. J. Geomag. Geoelec., 13, p. 127-132 (1961)

Blackett, P. M. S. Lectures on Rock magnetism: Jerusalem, Weezmann Science Press of Israel, 131p (1956)

Blackett, P. M. S., et al., Eds. A symposium on continental drift: Philos. Trans. Roy. Soc. London, A, 258, p. 1 (1965)

Briden, J. C. J. Geophy. Res., 70, p. 5205-5221 (1965)

Briden, J. C. Nature, 215, p. 1334-1339 (1967)

Bullard, E. C., et al. Philos. Trans. Roy. Soc. London, A, 258, p. 41-51 (1965)

Carey, S. W. Proc. Roy. Soc. Tasmania, 89, p. 255-288 (1955)

Carey, S. W., Ed. The tectonic approach to continental drift: Hobart, University of Tasmania, p. 177-358 (1956)

Castaño, J. and R. M. Garrels. Econ. Geol., 45, p. 755-770 (1950)

Chamalaun, F. H. and K. M. Creer. J. Geophy. Res., 69, p. 1607-1616 (1964)

Chevallier, R. J. Phys. Radium, 12, p. 172 (1951)

Clegg, J. A., et al. Philos. Mag., 45, p. 583-598 (1954)

Collinson, D. W. and S. K. Runcorn. Geol. Soc. America Bull., 71, p. 915-918 (1960)

Collinson, D. W. Geophy. J., 9, p. 203 (1965)

Collinson, D. W. Nature, 210, p. 516 (1966)

Collinson, D. W. Geophy. J., 11, p. 337 (1966)

Collinson, D. W., et al., Eds. Methods in Paleomagnetism: Amsterdam, Elsevier, 690p (1967)

Collinson, D. W. Geophy. J., 16, p. 531 (1968)

Collinson, D. W. Geophy. J., 18, p. 211-222 (1969)

Cox, A. and R. R. Doell. Geol. Soc. America Bull., 71, p. 645-768 (1960)

Cox, A. and R. R. Doel. Nature, 189, p. 45-47 (1961)

Cox, A. J. Geomag. Geoelec., 13, p. 101-112 (1962)

Cox, A., et al. Sci. American, 216, p. 44-54 (1967)

Creer, K. M., et al. J. Geomag. Geoelec., 6, p. 163-168 (1954)

Creer, K. M. Philos. Trans. Roy. Soc. London, A, 250, p. 130-143 (1957)

Creer, K. M. Geophy. J., 2, p. 261-275 (1959)

Creer, K. M. Geophy. J., 5, p. 16 (1961)

Creer, K. M. J. Geomag. Geoelec., 13, p. 86-100 (1962)

Creer, K. M. J. Geophy. Res., 67, p. 3461-3476 (1962)

Creer, K. M. Philos. Trans. Roy. Soc. London, A, 258, p. 27 (1965)

Creer, K. M. in Magnetism and Cosmos: Eds. Hindmarsh, W. R., et al., New York, Elsevier, p. 45-59 (1965)

Creer, K. M. Nature, 219, p. 246-250 (1968)

Deutsch, E. R. in Roy. Soc. Canada, Special Publications, 9, p. 28-52 (1966)

Deutsch, E. R. in North Atlantic - Geology and Continental Drift: Memoir 12, Amer. Assoc. of Petroleum Geologists, p. 931-954 (1969)

Deutsch, E. R. and C. Somayajulu. Earth Planet. Sci. Lett., 7, p.337-345 (1970)

Deutsch, E. R., et al. in Press (1970)

Dietz, R. S. Amer. J. Science, 264, p. 177-193 (1966)

Doell, R. R. Trans. Amer. Geophys. Union, 37, p. 156-167 (1956)

Donahue, J. J. Sed. Petrology, 39, p. 1399-1411 (1969)

Du Bois, P. M. Nature, 184 (4688), p. 63-64 (1959)

Du Toit, A. L. Our Wandering Continents: Edinburgh, Oliver and Boyd, 336p (1937)

Egyed, L. Acad. Sci. Hungaricae Acta Geol., 5, p. 43-83 (1956)

Fairbridge, R. W. in Diagenesis in Sediments: Eds. Larsen, G. and G. V. Chillingar, p. 19-89 (1967)

Fersmann, A. E. The Geochemistry of Russia: Leningrad, I. Groskhimizdat (1922)

Fisher, R. A. Proc. Roy. Soc. London., A, 217, p. 295-305 (1953)

Fuller, M. D. and S. Uyeda. in Proc. of the Benedum Earth magnetism symposium: Ed. Nagata, T., University of Pittsburgh Press, p. 117-121 (1962)

Garland, G. D., Ed. Continental drift: Roy. Soc. Canada, Spec. Publ. no. 9 (1966)

Gough, D. I. and N. D. Opdyke. Geophy. J., 7, p. 457-468 (1963)

Gough, D. I. in Methods in Paleomagnetism: Eds. Collinson, D. W., et al., p. 119-130 (1967)

Graham, J. W. J. Geophy. Res., 54, p. 131-167 (1949)

Graham, J. W. in Methods in Paleomagnetism: Eds. Collinson, D. W., et al., p. 409-424 (1967)

Griffiths, D. H., et al. Sedimentology, 1, p. 134-144 (1962)

Gross, G. A. Geol. Survey, Canada, Econ. Geol. Rept. 22, I, p. 1-181 (1965)

Gross, G. A. Geol. Survey, Canada, Econ. Geol. Rept. 22, II, p. 1-111 (1967)

Haigh, G. Phil. Mag., 3, p. 267-286 (1958)

Hayes, A. O. Geol. Survey, Canada, Dept. of Mines, 78, p. 1-163 (1915)

Heezen, B. C. Sci. American, 203, p. 98-110 (1960)

Heirtzler, J. R., et al. J. Geophy. Res., 73, p. 2119-2136 (1968)

Hess, H. H. in Petrological studies: New York, Geol. Soc. America, p. 599 (1962)

Hide, R. Science, 157, p. 55-56 (1967)

Hospers, J. and S. I. Van Andel. Tectonophysics, 5, p. 5-24 (1967)

Hospers, J. and S. I. Van Andel. Tectonophysics, 6, p. 475-490 (1968)

Hospers, J. and S. I. Van Andel. Earth-Sci. Revs., 5, p. 5-44 (1969)

Howell, L. G. Amer. J. Science, 260, p. 539-549 (1962)

Irving, E. Phil. Trans. Roy. Soc. London, A, 250, p. 100-110 (1957)

Irving, E. Adv. in Physics, 6, p. 194-218 (1957)

Irving, E., et al. Geophy. Res., 66, p. 1927-1933 (1961)

Irving, E. Paleomagnetism: New York, John Wiley, 399p (1964)

Irving, E. and N. D. Opdyke. Geophy. J., 9, p. 153-167 (1965)

Irving, E. J. Geophy. Res., 71, p. 6025-6051 (1966)

Irving, E. Nature, 213, p. 483-484 (1967)

Irving, E. and L. G. Parry. Geophy. J., 7, p. 395-411 (1963)

Isacks, B., et al. J. Geophy. Res., 73, p. 5855 (1968)

Kay, Marshall. Amer. Assoc. Petroleum Geologists Bull., 51, p. 579-600 (1967)

Kay, Marshall, Ed. North Atlantic - Geology and Continental Drift: Memoir 12, Amer. Assoc. Petroleum Geologists, 1082p (1969)

Kelly, W. C. Amer. Minerologist, 41, p. 353-355 (1956)

Khramov, A. N. Paleomagnetism and stratigraphic correlation: Canberra, Australian National University, 218p (1958)

Khramov, A. N., et al. Defence Research Board, Canada, T460R , p. 1-8 (1966)

Khramov, A. N. IZV. Earth Physics, 1, p. 86-108 (1967)

Knowles, R. R. and N. D. Opdyke. J. Geophy. Res., 73, p. 6515-6526 (1968)

Kobayashi, K. J. Geomag. Geoelec., 10, p. 99-117 (1959)

Kobayashi, K. and E. J. Schwarz. J. Geophy. Res., 71, p. 5357-5364 (1966)

Krs, M. Geophy. J., 12, p. 313-317 (1967)

Larochelle, A. Geol. Survey , Canada, 62-2, p. 44-47 (1964)

Larochelle, A. Geol. Survey, Canada, 67-18, p. 1-15 (1967)

Larsen, G. and G. V. Chillingar, Eds. Diagenesis in Sediments: New York, Elsevier, 551p (1967)

Larson, E., et al. Geophy. J., 17, p. 263-292 (1969)

Leng, J. in Irving (1964)

Lyons, J. C. in Structural Geology of Canadian ore deposits: Common-Wealth Min and Met Congress, p. 503 (1957)

Markowitz, W. M. and B. Guinot, Eds. Continental drift, secular motion of the pole and rotation of the earth: New York, Springer-Verlag, 107p (1968)

McElhinny, M. W. Proc. Int. Union Geol. Sci., UNESCO, Montevideo (1967)

McElhinny, M. W. in Methods in Paleomagnetism: Eds. Collinson, D. W., et al., p. 313-321 (1967)

McElhinny, M. W. and N. D. Opdyke. J. Geophy. Res., 73, p. 689-696 (1968)

Mercanton, P. L. Terr. Magn. Atmos. Elec., 31, p. 187-190 (1926)

Michel, A. and G. Chaudron. C. R. Acad. Sci., Paris, 20, p. 1191 (1935)

Michel, A. Nouveau Traite de Chimie Minerale, 17, p. 653-663 (1963)

Morley, L. W. and A. Larochelle. Roy. Soc. Canada, Special Publication 9, p. 40-51 (1964)

Murthy, G. S. Design and calibration of an astatic magnetometer and the study of remanent magnetization of some Newfoundland rocks: M.Sc. thesis, Memorial University of Newfoundland, 177p (1967)

Nagata, T. Rock magnetism: Tokyo, Meruzen, 350p (1961)

Nagata, T. Hand Buch der Physik, X, p. 248 (1964)

Nairn, A. E. M., et al. Nature, 183, p. 596-597 (1959)

Nairn, A. E. M., Ed. Descriptive Paleoclimatology: New York, Wiley-Interscience (1961)

Nairn, A. E. M., Ed. Problems in Paleoclimatology: New York, Wiley-Interscience (1964)

Nautiyal, A. C. The Cambro-Ordovician sequence in the Southeastern part of the Conception Bay Area, Eastern Newfoundland: M.Sc. thesis, Memorial University of Newfoundland, 334p (1967)

Néel, L. Adv. in Phys., 4, p. 191 (1955)

Nicholls, G. D. Adv. in Phys., 4, p. 113 (1955)

Opdyke, N. D. J. Geophy. Res., 66, p. 1941-1949 (1961)

Opdyke, N. D., et al. Science, 154, p. 349-357 (1966)

Opdyke, N. D. and K. W. Henry. Earth Planet. Sci. Lett., 6, p. 139-151 (1969)

O'Reilly, W. O. J. Geomag. Geoelec., 20, p. 381-386 (1968)

Pearce, G. W. Design and calibration of apparatus for the alternating field demagnetization of rocks: M.Sc. thesis, Memorial University of Newfoundland, 134p (1967)

Petranek, J. in Deltaic and shallow marine deposits: Ed. Van Streaten, L. M. J. U., New York, Elsevier, P. 319-322 (1966)

Pettijohn, F. J. Sedimentary rocks: Calcutta, Oxford Book Company, 718p (1957)

Phinney, R. A., Ed. The History of the earth's crust: Princeton, Princeton University Press, 244p (1968)

Poole, W. H. in Geology of the Atlantic Region: Geol. Assoc. Canada, Special Paper, no. 4, p. 9-51 (1967)

Porath, H. J. Geophy. Res., 73, p. 5959-5965 (1968)

Robertson, W. A., et al. Can. J. Earth Sci., 5, p. 1175-1181 (1968)

Robertson, W. A. Geol. Survey Canada Bull., 167, p. 1-51 (1969)

Rodionov, V. P. Defence Research Board, Canada, T460R, p. 9-13 (1966)

Roquet, J. Ann. Geophys., 10, p. 226-247 and 282-325 (1954)

Rose, E. R. Geol. Survey, Canada, Mem. 265, p. 1-64 (1952)

Rowland, R. A. and E. C. Jonas. Amer. Minerologist, 34, p. 550-558 (1949)

Roy, J. L. Can. J. Earth Sci., 3, p. 139-161 (1966)

Roy, J. L., et al. Geophy. J., 72, p. 1-12 (1967)

Roy, J. L., et al. J. Geophy. Res., 72, p. 5075-5086 (1967)

Roy, J. L. and W. A. Robertson. Can. J. Earth Sci., 5, p. 275-285 (1968)

Roy, J. L., et al. J. Geophy. Res., 73, p. 697-702 (1968)

Roy, J. L. and J. K. Park. J. Geophy. Res., 74, p. 594-604 (1969)

Roy, J. L. Can. J. Earth Sci., 6, p. 663-669 (1969)

Runcorn, S. K. Geol. Assoc. Canada Proc., 8, p. 77-85 (1956)

Runcorn, S. K., Ed. Continental drift: New York, Academic Press, 338p (1962)

Schwarz, E. J. Earth Planet. Sci. Lett., 5, p. 333-338 (1969)

Sheridan, R. E. and C. L. Drake. Can. J. Earth Sci., 5, p. 337-374 (1968)

Smith, E. J. Geophy. J., 12, p. 321 (1967)

Somayajulu, C. R. Paleomagnetic studies of volcanic rocks in Ireland, Newfoundland and Labrador: M.Sc. thesis, Memorial University of Newfoundland, 197p (1969)

Stacey, F. D. Adv. in Phys., 12, p. 45 (1963)

Stacey, F. D. in International dictionary of geophysics: Eds. Runcorn, S. K., et al., p. 1141 (1967)

Stacey, F. D. Physics of the Earth: New York, John Wiley & Sons, Inc., 324p (1969)

Stephens, M. A. J. Amer. Statistical Assoc., 59, p. 160 (1964)

Stephenson, A. Geophy. J., 13, p. 425-440 (1967)

Storetvedt, K. M., et al. Tectonophysics, 5(5), p. 413-426 (1967)

Storetvedt, K. M. Earth Planet. Sci. Lett., 4, p. 107-112 (1968)

Storetvedt, K. M. Earth Planet. Sci. Lett., 3, p. 444-448 (1968)

Strakhov, N. M., et al. Formation of sediments in recent basins: IZV. Akad. Nauk S.S.S.R., Moscow, 791p (1954)

Strangway, D. W., et al. Geophy. J., 15, p. 345-359 (1968)

Strangway, D. W. in Methods in Paleomagnetism: Eds. Collinson, D. W., et al., p. 200-216 (1967)

Tarling, D. H. in Methods in Paleomagnetism: Eds. Collinson, D. W., et al., p. 347-349 (1967)

Taylor, F. B. in Principles of physical geology: by A. Holmes, Don Mills, Nelson, 1288p (1969)

Thellier, E. in Irving (1964)

Uyeda, S. Japan, J. Geophy., 2, p. 1-123 (1958)

Van Andel, S. I. and J. Hospers. Nature, 212, p. 891-893 (1966)

Van der Marel, H. W. J. Sed. Petrology, 21, p. 12-21 (1951)

Van Houten, F. B. Jour. Sed. Petrology, 6, p. 296-300 (1961)

Van Houten, F. B. Geol. Soc. America Bull., 79, p. 399-416 (1968)

Van Ingen, G. Geol. Soc. America Bull., 25 (1914)

Vine, F. J. and D. H. Matthews. Nature, 199, p. 947-949 (1963)

Ward, M. A. Geophy. J., 8, p. 217-225 (1963)

Wasilewski, P. J. J. Geomag. Geoelec., 21, p. 655-667 (1969)

Watson, G. S. Monthly notices, Roy. Astron. Soc., Geophy. Supp., 7, p. 153 (1956)

Watson, G. S. and E. Irving. Monthly notices, Roy. Astron. Soc., Geophy. Supp., 7, p. 289 (1957)

Wegener, A. The origin of continents and oceans: New York, Dover Publications Inc. (Transl), 246p (1966)

Wells, J. M. and J. Verhoogen. Jour. Geophy. Res., 72, p. 1777-1781 (1967)

Williams, H. in North Atlantic - Geology and Continental Drift: Ed. Kay, M., Amer. Assoc. of Petroleum Geologists, Memoir 12, p. 32-58 (1969)

Wilson, J. T. Nature, 195, p. 135-138 (1962)

Wilson, J. T. Nature, 211, p. 676-681 (1966)

Wilson, R. L. Geophy. J., 5, p. 59-69 (1961)

Wilson, R. L. and C. W. F. Everitt. Geophy. J., 8, p. 235-241 (1963)

Wilson, R. L. and N. D. Watkins. Geophy. J., 12, p. 405 (1967)

Wilson, R. L., et al. Geophy. J., 16, p. 79-86 (1968)

Wilson, R. L. and P. J. Smith. J. Geomag. Geoelec., 20, p. 367-380 (1968)